

# Measurement of microcirculation in clinical research

Birkhoff, W.A.J.

# MEASUREMENT OF MICROCIRCULATION IN CLINICAL RESEARCH

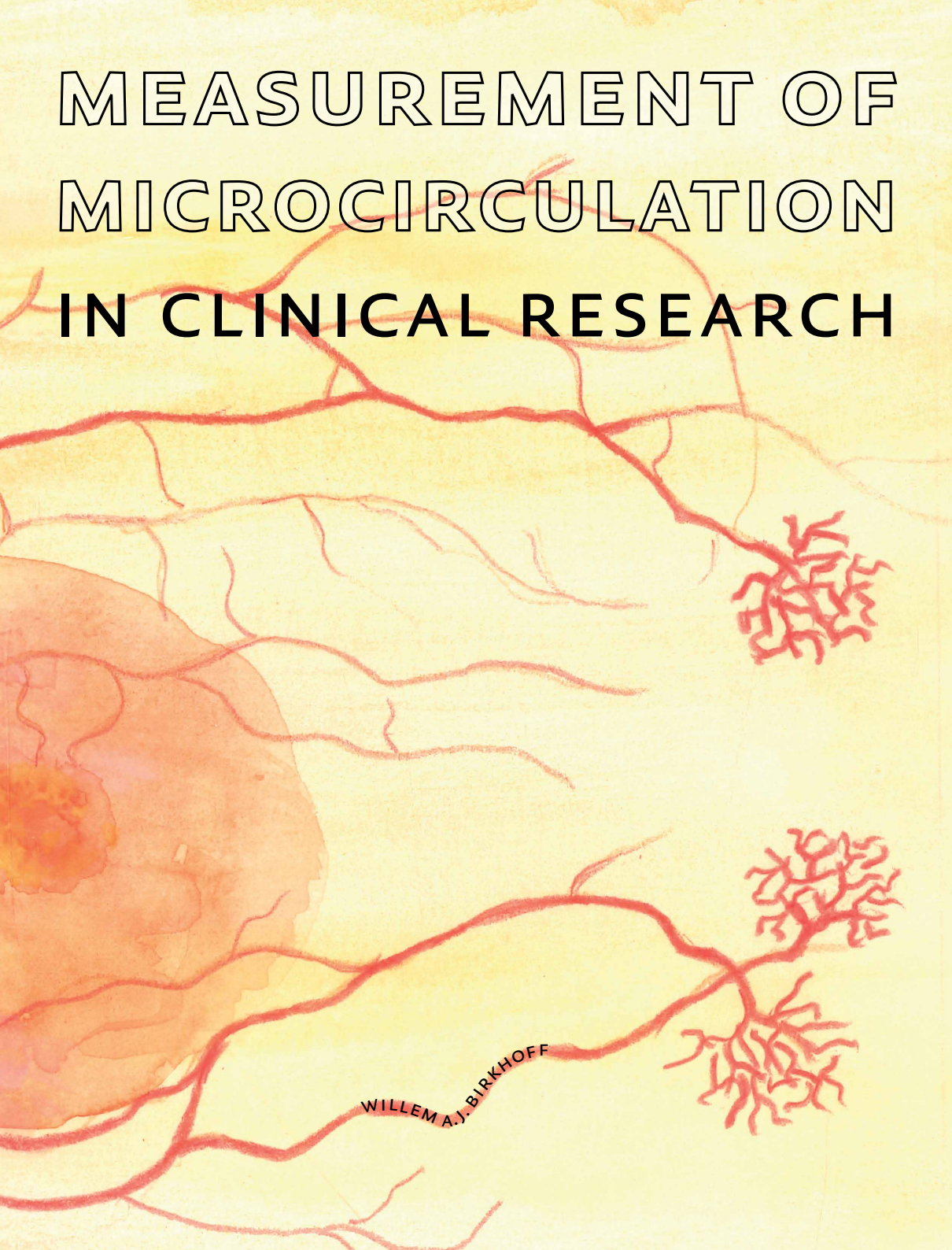

WILLEM A.J. BIRKHOFF

# MEASUREMENT OF MICROCIRCULATION IN CLINICAL RESEARCH

Proefschrift

ter verkrijging van
de graad van doctor aan de Universiteit Leiden,
op gezag van rector magnificus prof.dr.ir. H. Bijl,
volgens besluit van het college voor promoties
te verdedigen op dinsdag 20 juni 2023
klokke 15:00 uur
door
Willem Arnold Jan Birkhoff
geboren te Dordrecht
in 1985

COLOFON
The publication of this thesis was financially supported by the foundation Centre for Human Drug Research in Leiden, the Netherlands

Design: Caroline de Lint, Den Haag (caro@delint.nl)
Cover image: Jacolien Wismeijer, Delft (j.j.wismeijer@gmail.com)

PROMOTORES
Prof. dr. A.F. Cohen
Prof. dr. J.C. van Meurs

COPROMOTOR
Dr. P Gal

PROMOTIECOMMISSIE
Prof.dr. JI Rotmans
Prof.dr. PHA Quax
Dr. L.I. van den Born
(*Het Oogziekenhuis Rotterdam*)
Dr. M.J.B. Kemme
(*Amsterdam UMC*)

## TABLE OF CONTENTS


CHAPTER I
Introduction – **6**

CHAPTER II
Microcirculation measurements in the skin and retina: review of non-invasive tools and their challenges – **11**

CHAPTER III
Retinal microcirculation imaging in sickle cell disease patients – **27**

CHAPTER IV
Skin blood flow functions as potential proxy for cerebral blood flow in adults with Sickle cell disease – **37**

CHAPTER V
Retinal oximetry and fractal analysis of capillary maps in sickle cell disease patients and matched healthy volunteers – **49**

CHAPTER VI
Validation of miniaturized dynamic light scattering in the evaluation of endothelial function, coagulation and rheology – **59**

CHAPTER VII
Recombinant human erythropoietin does not affect several microvascular parameters in well-trained cyclists – **67**

CHAPTER VIII
Detection of cutaneous oxygen saturation using a novel snapshot hyperspectral camera: a feasibility study – **75**

Summary – **87**
Nederlandse samenvatting – **90**
List of publications – **95**
Curriculum vitae – **96**

# INTRODUCTION

### Measurement of microcirculation in clinical research

Cardiovascular disease is still one of the most important causes of death, with 17.7 million deaths in 2015, although this has dropped substantially in the last decades.[1]This was mainly caused by emerging treatment options initially driven by the Framingham studies which identified hypertension and hyperlipidemia as risk factors for cardiovascular disease. This resulted in the development of pharmacological treatments which are still widely used. Currently, a treatment option is available for most macrovascular diseases. However, interventions targeting the microcirculation are few and far between. Evaluation of treatments affecting the microcirculation is difficult because of absence of standardized accepted techniques Moreover, it has only become apparent recently that large macrovascular diseases are preluded by microvascular abnormalities and microvascular measurements were strong predictors of long-term cardiovascular disease and survival.[2–4] Therefore, early intervention targeting the microvascular abnormalities may support preventing later onset of cardiovascular problems thereby reducing the impact on global heath.

### Microcirculation anatomy

The systemic circulation delivers blood to all organs and body tissues, amongst others exchanging oxygen and carbon dioxide during its course. Exchange takes place mostly in the capillaries, which are about 5 to 10 µm in diameter, are lined with endothelial cells, and are one layer thick. Despite their small size, the surface area of the capillaries is the largest of all vessels in the circulation. Together with the arterioles, venules, lymphatic capillaries and collecting ducts, these vessels form the microcirculation.

### Physiology

Blood flow in the (micro)circulation is mainly regulated by the arterioles. The arterioles can adjust their diameter and vascular tone by contracting and relaxing the vascular smooth muscle wall. The endothelial tissue in the vessels responds to various stimuli, including neuropeptides, neurotransmitters, several hormones, and distension of the vessels due to increased blood pressure.[5] These stimuli have an effect on the complex interplay of hormones secreted by the endothelial tissue, the main hormones being nitric oxide (NO) and endothelin-1 (ET-1). NO is a gaseous hormone, which is generated by endothelial nitric oxide synthase (eNOS), which is in its turn activated by acetycholine, bradykinin or serotonin.

NO is secreted from the endothelial layer and then travels to the smooth muscle cells, where the NO triggers membrane-bound - and soluble guanylate cyclases, which in its turn synthesizes cyclic guanylate monophosphate (cGMP), after which cGMP-kinase is activated. By stimulation of K+-channels and thereafter inhibition of the Ca++-channels – this enzyme lowers intracellular Ca++ [6] and subsequently relaxes the smooth muscle cells. However, nitric oxide has various other functions including platelet adherence, leucocyte chemotaxis and smooth muscle cell proliferation.[7,8] Endothelin-1 has the exact opposite effect from NO, although its effects have not been as well described. Predominantly through up- and downregulation of these hormones, the endothelial tissue can regulate wall stress.

### Pathophysiology – Endothelial dysfunction

Endothelial dysfunction is the harmful alteration of endothelial physiology, thereby affecting blood flow and vascular homeostasis. The main mechanism by which these alterations have an effect is by reducing the bioavailability of NO. For example, hypercholesterolemia induces a mild inflammation of the vascular wall and generates $O_2$ radicals. These $O_2$ radicals react with NO to form peroxynitrie ($ONOO^-$), reducing the vascular relaxation effects of NO. Peroxynitrite in itself modulates the NO generation by inactivating eNOS, through modification of the $Zn^{2+}$sulfur motifs in the eNOS protein,[9] even further reducing the bioavailability of NO.[10] Endothelial dysfunction is of pathophysiologic importance in atherosclerosis and has been shown to be a strong predictor of atherosclerotic cardiovascular disease. In several studies, endothelial dysfunction, measured by flow mediated dilation, was observed before any other indication of atherosclerosis.[11] This has led to various research initiatives on improving endothelial function and thereby alleviating atherosclerosis. Endothelial dysfunction is associated with cardiovascular risk factors for atherosclerosis, such as diabetes, dyslipidemia, hypertension, smoking and aging. In the clinic, early detection and correction of endothelial dysfunction may therefore play an important role in preventing these (irreversible) conditions.





### Interventions

Clinical studies have observed that endothelial function can be improved by treatment with angiotensin converting enzyme (ACE) inhibitors,[12] antioxidant agents,[13,14] beta blockers,[15] calcium channel blockers,[16] phosphodiesterase (PDE) 5 inhibitors[17] and statins.[18]

These interventions cause indirect antioxidant effects (e.g. prevention of eNOS uncoupling) and through their anti-inflammatory improve the functioning of the endothelium. This exact mechanism is extensively described.[12] Briefly, the antioxidant effects consists of three components:

1 ACE inhibitors and and angiotensin-II receptor antagonist increase the NO bioavailability by decreased bradykinin breakdown
2 hydrogen peroxide, cellular superoxide, and peroxynitrite levels are decreased by avoiding the activation of the Nox2 enzyme
3 ACE inhibitors inhibit the development of diacylglycerol, a induction of NADPH-oxidase activity. The anti-inflammatory effect is caused by interruption of monocyte adhesion to the endothelium.[12]

Most studies regarding these mechanisms have been performed in knockout mice, or by measuring FMD in patients, although more recently microvascular measurements have been implemented.[19]

Although these treatments are widely available and have been shown to reduce cardiovascular complications, there is a need for evaluation of the effect of these and new pharmacological therapies on microvascular endothelial dysfunction. There is increasing evidence that microvascular dysfunction is not only a consequence of atherosclerosis but also an independent risk factor for vascular events

### Interest into evaluation

The microvasculature is considered sensitive to various stimuli, from vascular, immunological, metabolic and neurologic origins, making the microvasculature a final common pathway for many (pharmacological) interventions. Combined with its excellent accessibility and relatively non-invasive measuring tools, since microvascular evaluation can be performed on lower forearm skin or in the eyes, further evaluation to identify the possible applications for microvasculature models is warranted. In particular interest for this thesis is the application of microvascular models to evaluate novel compounds in healthy volunteers.

### Validation

The overall aim of this thesis is to perform the first steps into validating multiple tools to identify pharmacological or disease effects on the microvasculature. To do this, the CHDR model for validation is applied. The CHDR algorithm is an algorithm which novel devices must complete before they can be implemented in routine clinical care or clinical studies. The algorithm consists of the following steps:

1 Analytical validation (EG intra/inter subject/measurement repeatability)
2 Clinical validation: demonstrating an association between the device output and disease activity, disease severity, or another area of interest; which is divided in the following substeps:
   - Can devices discriminate between clinical and healthy populations?
   - Can devices detect various event types, like known (negative) rigorous interventions (i.e. admission vs recovery)?
   - Can you correlate validated or traditional outcomes with the device parameters?
   - Performance qualification: Does a (known) effective health care intervention provide a comparable output with the device's parameters?
   - Practical usability in clinical practice.

After the device completes all steps successfully, the device is ready to be used in clinical care or studies, but only for the purpose that was identified in step 1.

**FIGURE 1 Schematic representation of the endothelium and pharmacological targets. The image highlights potential sites for drug intervention.**

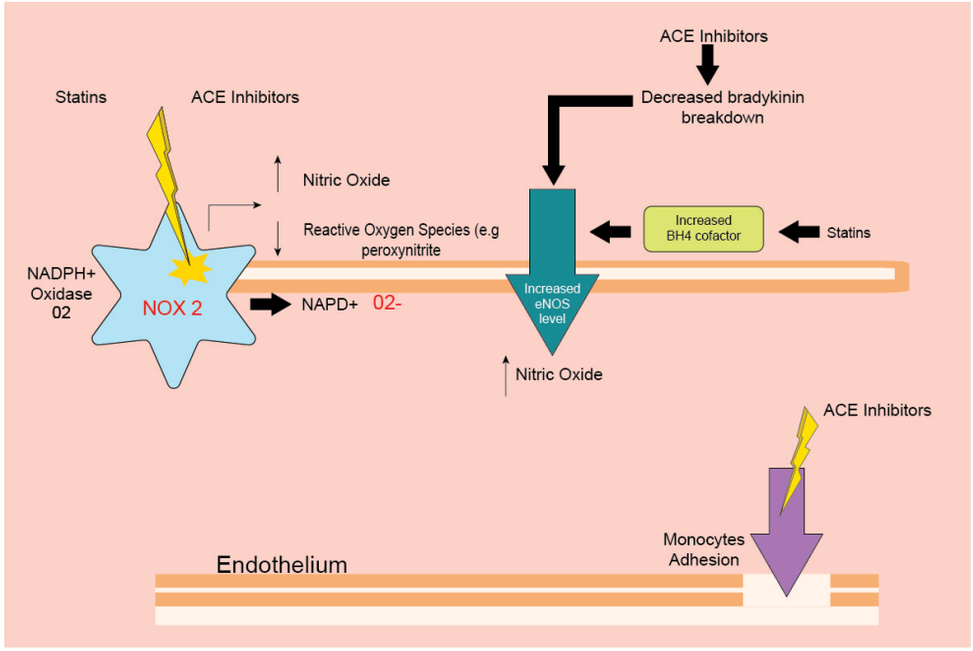


## This thesis

The present thesis investigates multiple novel devices that can perform measurements of microvascular function. We have investigated several new devices that have been developed or are that are currently under development and we investigated the applicability of several novel microcirculation measurement devices for their utility in the clinic or in a clinical research setting. These techniques are more extensively described in the next chapter.

For early phase drug development, studies are performed in healthy volunteers. Therefore, non-invasive access to evaluate the microvascular function is key, and therefore we have chosen to validate devices that are able to measure the microcirculation in either the skin or in the eye. As these organs are relatively accessible and the measurements non-invasive, but nevertheless can potentially be very informative about general microcirculation without harming the study subject. Most measurements in these organs can be performed with relative comfort for the patient and as such are suitable for frequent application in the clinic or in clinical studies.

**Chapter 3** focuses on validating the ability of the devices to distinguish between sickle cell patients and healthy volunteers, given that they were relatively new at the time. Sickle cell disease is a genetic disorder in which a single point mutation leads to abnormal synthesis of hB (HBS). This HBS can lead to abnormal folding of hB chains and subsequently formation of sickle cells. Besides painful and invalidating sickle cell crises, sickle cell patients have severe vascular and rheological abnormalities, leading also to an impaired endothelial function. [20]

In **chapter 4,** cutaneous microvascular measurements were compared to cerebral flow measurements in sickle cell patients, with the aim of validating the device to measure cerebral flow. Next to applications in early phase drug development, for example for drugs that aim to increase cerebral blood flow, the device has potential to be an alternative for expensive and time-consuming MRI measurements.





In **chapter 5**, new techniques and analyzing methods were evaluated for retinal microvascular measurement, including fractal analysis which can be used to measure microvascular function in retinal vascular beds and multispectral imaging in the retina. Also, in **chapter 8**, multispectral imaging was evaluated in the skin in heathy volunteers, aiming to validate the technique for further use. In **chapter 6**, Micro Dynamic light scattering was evaluated for the applicability in clinical and research use, by evaluating the robustness of the MDLS by benchmarking it against other microvascular imaging techniques.

Finally, in **chapter 7**, we evaluated if the microvascular techniques can be used to evaluate the effects of a pharmacological intervention affecting the blood's rheological characteristics before and after exercise.

## *REFERENCES*


1 Mendis S. Global status report on noncommunicable diseases 2014: World health organization; 2014.

2 Desouza CV, Bolli GB, Fonseca V. Hypoglycemia, diabetes, and cardiovascular events. Diabetes care. 2010;33(6):1389-94.

3 Brownrigg JR, Hughes CO, Burleigh D, Karthikesalingam A, Patterson BO, Holt PJ, et al. Microvascular disease and risk of cardiovascular events among individuals with type 2 diabetes: a population-level cohort study. The Lancet Diabetes & Endocrinology. 2016;4(7):588-97.

4 Rosenson R, Fioretto P, Dodson P. Does microvascular disease predict macrovascular events in type 2 diabetes? Atherosclerosis. 2011;218(1):13-8.

5 Tuma RF, Durán WN, Ley K. Microcirculation: Academic Press; 2011.

6 Ghofrani HA, Pepke-Zaba J, Barbera JA, Channick R, Keogh AM, Gomez-Sanchez MA, et al. Nitric oxide pathway and phosphodiesterase inhibitors in pulmonary arterial hypertension. Journal of the American College of Cardiology. 2004;43(12 Supplement):S68-S72.

7 Lowenstein CJ, Dinerman JL, Snyder SH. Nitric oxide: a physiologic messenger. Annals of internal medicine. 1994;120(3):227-37.

8 Bogdan C. Nitric oxide and the immune response. Nature immunology. 2001;2(10):907-16.

9 Pacher P, Beckman JS, Liaudet L. Nitric oxide and peroxynitrite in health and disease. Physiological reviews. 2007;87(1):315-424.

10 Kuzkaya N, Weissmann N, Harrison DG, Dikalov S. Interactions of peroxynitrite, tetrahydrobiopterin, ascorbic acid, and thiols implications for uncoupling endothelial nitric-oxide synthase. Journal of Biological Chemistry. 2003;278(25):22546-54.

11 Nieuwenhoff MD, Wu Y, Huygen F, Schouten AC, van der Helm F, Niehof S. Reproducibility of axon reflex-related vasodilation assessed by dynamic thermal imaging in healthy subjects. Microvascular research. 2016;106:1-7.

12 Steven S, Münzel T, Daiber A. Exploiting the pleiotropic antioxidant effects of established drugs in cardiovascular disease. International journal of molecular sciences. 2015;16(8):18185-223.

13 Engler MM, Engler MB, Malloy MJ, Chiu EY, Schloetter MC, Paul SM, et al. Antioxidant vitamins C and E improve endothelial function in children with hyperlipidemia: Endothelial Assessment of Risk from Lipids in Youth (EARLY) Trial. Circulation. 2003;108(9):1059-63.

14 Grebe M, Eisele HJ, Weissmann N, Schaefer C, Tillmanns H, Seeger W, et al. Antioxidant vitamin C improves endothelial function in obstructive sleep apnea. American journal of respiratory and critical care medicine. 2006;173(8):897-901.

15 Peller M, Ozierański K, Balsam P, Grabowski M, Filipiak KJ, Opolski G. Influence of beta-blockers on endothelial function: a meta-analysis of randomized controlled trials. Cardiology journal. 2015;22(6):708-16.

16 Taddei S, Virdis A, Ghiadoni L, Magagna A, Pasini AF, Garbin U, et al. Effect of calcium antagonist or beta blockade treatment on nitric oxide-dependent vasodilation and oxidative stress in essential hypertensive patients. Journal of hypertension. 2001;19(8):1379-86.

17 Rosano GM, Aversa A, Vitale C, Fabbri A, Fini M, Spera G. Chronic treatment with tadalafil improves endothelial function in men with increased cardiovascular risk. European urology. 2005;47(2):214-22.

18 Blum A, Shamburek R. The pleiotropic effects of statins on endothelial function, vascular inflammation, immunomodulation and thrombogenesis. Atherosclerosis. 2009;203(2):325-30.

19 Jekell A, Kalani M, Kahan T. The effects of alpha 1-adrenoceptor blockade and angiotensin converting enzyme inhibition on central and brachial blood pressure and vascular reactivity: the doxazosin–ramipril study. Heart and vessels. 2017;32(6):674-84.

20 Belhassen L, Pelle G, Sediame S, Bachir D, Carville C, Bucherer C, et al. Endothelial dysfunction in patients with sickle cell disease is related to selective impairment of shear stress–mediated vasodilation. Blood, The Journal of the American Society of Hematology. 2001;97(6):1584-9.

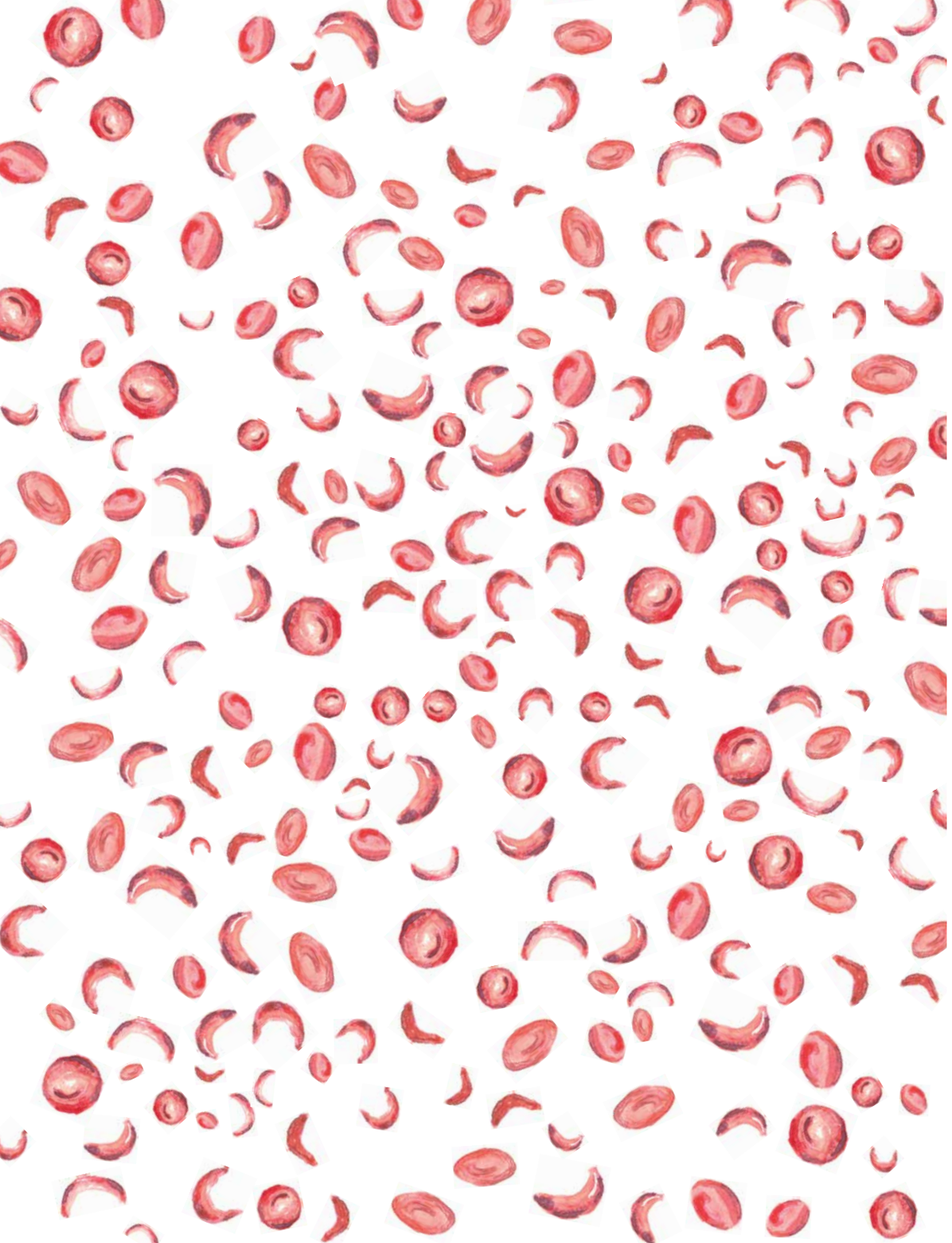

CHAPTER II

# Microcirculation measurements in the skin and retina: review of non-invasive tools and their challenges

*Willem A.J. Birkhoff [1,2], Sebastiaan J.W. van Kraaij [1,2], Matthijs Moerland [1], Karen Broekhuizen [1], Adam F Cohen [1,2], Pim Gal [1,2]*

*1. Centre for Human Drug Research, Leiden, the Netherlands / 2. Leiden Universitair Medisch Centrum, Leiden, the Netherlands / Corresponding author: Prof. Dr. A.F. Cohen*

**In the last decade new and more advanced microvascular imaging techniques have become available for use in clinical research. As it became more evident that microvascular dysfunction might prelude (cardio) vascular events, microvascular measurements have gained increasing interest for their applicability in the clinic and research. In this narrative review we aim to provide an updated oversight of microvascular measurement techniques. We have made an outline of the most common and latest techniques for microvascular cutaneous and retinal measurements and included the most frequently used challenges used together with these measurements. Furthermore this review includes an updated evaluation of the mechanistic background of microcirculatory dysfunction. Hereby this narrative literature review aims to assist with the identification of the most adequate microvascular imaging technique(s) for clinical application and research**

**The microcirculation plays a major role in tissue perfusion, the exchange of nutrients, oxygen and carbon dioxide between blood and interstitial fluid and in vascular homeostasis.** Endothelial tissue is a key regulator of the microcirculation. Abnormalities in the microcirculation are considered to be strong predictors of major adverse cardiovascular events and one of the first signs of atherosclerosis.[1] Adequate physiological measurement of the microcirculation is challenging because the vessel structure is spatially heterogeneous in most locations and perfusion shows high variability over time and in different environmental conditions, such as temperature.[2] Recently however, new devices have become available, such as dynamic optical coherence tomography (d-OCT) and laser speckle flowgraphy (LSFG). Moreover, image processing from existing devices improved due to technological advancements, for instance better lenses, higher resolution cameras and more sensitive sensors with improved noise performance.

There are several ways to evaluate the microcirculation, and, although the influence of different endothelial-derived factors, such as nitric oxide

(NO) and endothelium-derived hyperpolarizing factors, is variable in vascular beds of different organs, the pathological alterations in these signaling pathways are remarkably similar.[3] Due to the easy accessibility, the skin is an excellent location to investigate pharmacological effects on the microcirculation. In particular for healthy volunteer studies, challenge models have been developed that can be applied in healthy volunteers so that pharmacodynamic effects can be monitored in first into man studies. Another easily accessible site is the retina, where the microcirculation can be visualized and monitored repeatedly over time. Retinal microvascular abnormalities have been linked to several cerebrovascular, [4,5] cardiovascular, [5] renal [6] and metabolic outcomes. [7]

Few reviews on the applicability of microvascular measurements have been published, and these frequently focused on a limited number of imaging techniques or on measurements in a single organ system.[8–11] The most comprehensive technical review on cutaneous non-invasive methods for imaging of the microcirculation was published in 2014.[10] However, there have been new developments and as such, there is a need to provide an updated oversight of microvascular measurement techniques. This narrative literature review aims to assist with the identification of the most adequate microvascular imaging technique(s) for clinical application and research. In contrast to previous reviews on this subject, this review puts emphasis on the clinical utility of the non-invasive microvascular imaging techniques that are currently commercially available for skin and retinal microcirculation assessments. In this review we have made an outline of the most common and latest techniques for microvascular cutaneous and retinal measurements. Most microcirculation measurements are indirect and tend to give little information about microcirculatory function over the full range of adaptive response possible. Therefore, these measurements are usually combined with challenges to drive the regulatory system to a more extreme state. Over the years various challenges techniques have been developed which can give inside in different aspects of the microcirculatory function. However, most of them focus on the endothelial microcirculation function. In this review we also provide an overview of the most applied challenges with these techniques.

## MECHANISTIC BACKGROUND OF MICROCIRCULATORY DYSFUNCTION

Endothelial dysfunction (ED) and abnormalities in the microcirculation are considered to be prelude development of atherosclerosis and are correlated with various cardiovascular risk factors as well as cardiovascular outcomes. Endothelial dysfunction is a vascular phenotype characterized by an imbalance between endothelial-derived contracting factors (EDCF), such as endothelin-1 and angiotensin II and endothelial-derived relaxing factors (EDRF), such as nitric oxide (NO), prostacyclin and bradykinin.

The ED phenotype can be induced in endothelial cells by a variety of stimuli, such as disturbed blood flow, bacterial lipopolysaccharides (LPS), pro-inflammatory cytokines and chemokines, pathogen- or damage associated molecular patterns and oxidized low-density lipoproteins (OXLDL).[12] These stimuli activate transcription factors such as NF-KB through various cell adhesion molecules (CAMs). This results in increased expression of these adhesion molecules, such as VCAM-1, ICAM-1, p- and e-selectin.[13] Additionally, monocytes, neutrophils and various types of T-cells are recruited to the vascular wall by these adhesion molecules, enhancing the inflammatory process by secreting various pro-inflammatory cytokines. The amount of reactive oxygen species (ROS) increases in this pro-inflammatory environment, leading to a reduction in availability of NO, one of the main EDRFs,[14] and increased pro-inflammatory signaling to the recruited leukocytes. This cellular environment also promotes the formation of OXLDL, creating an additional feedback loop of pro-inflammatory signaling through NF-KB in endothelial cells.[12,15] Production of EDCF is increased, while pro-dilatory signaling is reduced. All these processes combined lead to ED, promoting the development of atherosclerosis before any macroscopic atherosclerotic changes in vasculature can be detected.

### *Nitric Oxide as a main actor*

One of the main and early indicators of the presence of the ED phenotype is the reduction in bioavailability of NO.[13,16] NO is a highly reactive soluble gas with an extravascular half-life of 0.09 to >2 seconds, decreasing with rising NO concentration.[17]





Since NO decays quickly, it has to be produced continuously in the vascular endothelium. Endothelial produced NO is a potent vasodilator responsible for endothelium-dependent vasodilation. NO reverses the constrictive effects of acetylcholine (ACH) on smooth muscle cells, mediating the potent endothelium-dependent vasodilatory effects of ACH. Similarly, endothelial NO release can reverse the vasoconstrictive effects of various vasoactive agents such as serotonin and norepinephrine.[18,19] Moreover, endothelial NO signaling inhibits inflammation, platelet activation, leukocyte adhesion and vascular smooth muscle cell proliferation, processes that are essential in the development of atherosclerosis.[12,20,21]

### *NO biosynthesis*

Under physiological circumstances, NO is produced in endothelial tissue by endothelial nitric oxide synthase (ENOS) by metabolizing L-arginine, creating L-citrulline as a byproduct. It is also synthesized in various tissues by inducible nitric oxide synthase (INOS) and neuronal nitric oxide synthase (NNOS). In their monomeric (uncoupled) state ENOS, INOS and NNOS are incapable of binding L-arginine, instead producing the ROS $O_2^{\cdot-}$.[22] In the presence of calmodulin (CaM), heme and tetrahydrobiopterin (BH4) NOS proteins become coupled and produce NO. ENOS and NNOS are dependent on the presence of $Ca^{2+}$ activated CaM to form dimers [23], whereas INOS is calcium-independent. Activity of ENOS in endothelial cells is thus increased significantly by raised intracellular $Ca^{2+}$levels, although various other cellular signals increase the activity of ENOS, including shear stress, bradykinin and insulin.[24]

### *Effects of endothelial NO*

The effects of endothelial derived NO are mainly mediated through activation of soluble guanylate cyclase, which promotes the conversion of guanosine triphosphate to cyclic guanosine monophosphate (CGMP). CGMP then activates CGMP-dependent protein kinase (protein kinase G), which induces vasodilation in vascular smooth muscle cells[25] and inhibits platelet activation.[18] Additionally, S-nitrosylation, the addition of NO to a cysteine thiol, modifies the function of various cellular proteins, including inhibition of NF-KB,[26,27] producing the anti-inflammatory and anti-proliferative effects of NO. These effects are crucial to maintaining vascular homeostasis, since NF-KB itself upregulates ENOS in addition to its pro-inflammatory effects,

**FIGURE 1** **Schematic overview of NO biosynthesis**

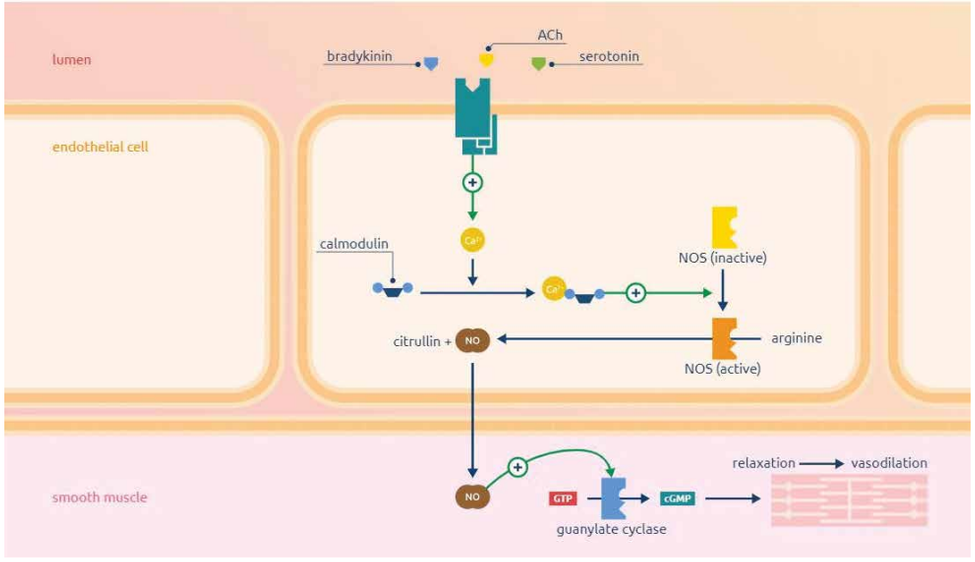

acting as its own inhibitor. Dysfunction of eNOS or reduction in NO availability can lead to unopposed NF-kB activation and vascular inflammation.[27]

*NO in endothelial dysfunction*

During the development of ED, production of NO is decreased, while consumption of NO is increased. ROS, in particular $O_{2-}$, react with NO to produce $ONOO^-$, an inactivating agent of NO itself, as well as a powerful oxidant inducing oxidative stress in the endothelium. $ONOO^-$ also oxidizes BH4 [28], inactivating it, leading to the uncoupling of eNOS dimers. eNOS in its uncoupled state produces more $O_{2-}$, creating a vicious feedback loop. The subsequent reduction of NO bioavailability and disappearance of its anti-inflammatory, anti-proliferative and vasodilatory effects creates imbalance between EDCF and EDRF and exacerbates the inflammatory environment and recruitment of leukocytes, ultimately causing the development of atherosclerotic plaques.[29]

*Measurement of NO in pathophysiological conditions*

In vivo, inhibition of NO synthesis raises baseline blood pressure in rats, increases coronary vascular resistance in dogs and promotes aortic atherosclerosis in rabbit hypercholesterolemia models. In healthy humans, inhibition of NO synthesis increases fore-arm vascular tone, decreases coronary artery diameter and blunts the response to ACH infusion.[18] Diminished NO synthesis is also associated with various pathological conditions promoting atherosclerosis, such as diabetes, hypertension, hypercholesterolemia, smoking and heart failure. Since reduction of NO bioavailability plays a pivotal role in the development of ED [25], measurement of NO bioavailability is an important diagnostic and investigative goal in the assessment of ED.

However, due to the instability of NO, direct measurement of eNOS activity in vivo has proven challenging. Nitrite and nitrate are stable metabolites produced by oxidation of NO, so their levels were considered surrogate levels of NO production and eNOS activation. However, nitrite and nitrate are commonly present in the human diet, and nitrite and nitrate are also endogenously reduced to form NO independently of eNOS activity.[24,30] Nitrite and nitrate are thus more reflective of an equilibrium between NO oxidation and reduction and dietary effects rather than in vivo eNOS activation. Most measurements of endothelial (dys) function and NO bioavailability therefore rely on measuring the physiological effects of local NO production, chiefly vasodilation.[21] By inducing NO production with challenges or inhibiting it with antagonists while simultaneously non-invasively measuring its effects on vasculature, a relatively accurate picture of eNOS activity and endothelial function can be acquired.

*Evaluation of the endothelial system in man*

The importance of measuring endothelial dysfunction as an early marker of atherosclerosis and cardiovascular risk is shown by its correlation to various proven cardiovascular risk factors, such as hypercholesterolemia, smoking, hypertension, obesity and diabetes.[31] Endothelial dysfunction is consistently documented in patients with established cardiovascular disease using a variety of methods.[32] Moreover, endothelial dysfunction, measured by flow-mediated dilation (FMD) or reactive hyperemia-peripheral arterial tonometry is significantly predictive of CV events, with a 1 SD decrease in endothelial function associated with double risk of CV events, and FMD itself being a significant predictor of myocardial infarction, angina, coronary revascularization, stroke, resuscitated cardiac arrest and CV related death.[33,34] Accurate assessment of endothelial function is therefore a promising method for early CV risk stratification and risk prevention.

## MICROVASCULAR CUTAENEOUS IMAGING TECHNIQUES

*Doppler flowmetry*

Doppler flowmetry is a technique measuring the Doppler shift in ultrasonic waves induced by the movement of blood through arteries to quantify the velocity of flow through that artery. This, multiplied with the measured cross-sectional area of that artery results in a measurement of flow volume. Determination of flow by itself does not provide much information about the functional status of the vascular bed. However, once combined with a challenge like the passive leg movement (PLM), changes in flow before and after PLM can provide





insight in endothelial function. During PLM, the flow volume through the common femoral artery (CFA) is measured before and after passive 90 degree flexion of the knee.[35] This passive movement produces an increase in CFA blood flow thought to be due to vasodilation and hyperemia downstream from the CFA.[36] The hyperemic response measured in the CFA after PLM is shown to be 80-90% NO-dependent [37,38] and correlates with the established gold standard of endothelial functional measurements, flow-mediated dilation (FMD). Moreover, measurement of the PLM hyperemic response correlates strongly with an established invasive method of assessing NO-dependent vasodilation: intra-arterial ACH infusion.[38] Disadvantages of the technique include the requirement of a trained operator maintaining a constant angle of insonation, including during movement of the leg, familiarization of subjects with the technique before measurements and the relatively high cost of equipment needed.[39] Advantages include that the technique is relatively easy to master compared to FMD and minimally invasive. Moreover, changes in PLM response due to age or vascular dysfunction far exceed the intra subject variability (within-day and day-to-day coefficient of variation 15-20%), making it a reliable technique to detect inter-subject differences in vascular function.[39]

*Laser Doppler flowmetry*

Laser Doppler flowmetry (LDF) is based on the principle of measuring the Doppler shift[40] induced by erythrocyte movement, to the illuminating coherent light. LDF output, is in literature often expressed as flux and is close related to the blood flow. In practice, LDF has a reported coefficient of variation of ~35%,[41] mostly related to the spatial variability (variability caused by different measurement sites) of the measurements.[42] However the coefficient of variation of most challenges can be reduced to <10% in a controlled laboratory setting and when executed under the right protocol.[43] As in most microvascular measuring techniques, LDF flux measurements, without using any challenge, have little predictive value for microvascular function, therefore they are usually combined with challenges. LDF measurements, like most other microvascular function techniques, does not correlate well with macrovascular function measurements[44,45] except for post occlusion reactive hyperemia measurements (PORH) which shows a weak correlation with flow-mediated dilation FMD.[46]

*Laser Doppler imaging*

Laser Doppler imaging (LDI) was developed to overcome the spatial variability of LDF. LDI follows the same mechanism as LDF, also measuring the doppler shift of the movement of erythrocytes. However, the laser light scans over the skin surface, rather than measuring one single point, thereby measuring the flux over an area. Contrary to LDF, LDI is a non-contact measurement method and has been used with the same challenges as LDF.[47] Furthermore LDI can be used to make perfusion maps of the skin, to obtain information about wound healing, burn wounds, skin flap surgery and to evaluate pharmacological responses[48,49] LDI has an intra-subject variability of ±20%.[47] LDI has an image acquisition frequency ~1 Hz frequency (depending on the size of the measurement area) which makes it less suitable to measure acute microvascular changes such as obtained during PORH as these changes happen within a second.[47]

*Laser speckle contrast imaging*

Laser speckle contrast imaging (LSCI) is able to record the changes in speckle pattern that is returned from the skin (i.e. a flat surface) after illumination with a laser. From the changes in the speckle pattern the microcirculatory erythrocyte flow can be obtained.[50] Similar to LDI and LDF LSCI output is also expressed as flux,[47,51] but flux can be measured at a higher frequency and in a larger area than LDI and LDF. LSCI has an intra-subject variability of 6-12% CV for healthy volunteers [51–53] and patients,[54–57] Since there is a limited number of trials in cardiovascular disease, [56] the available evidence is not sufficient to use LSCI measurements as a diagnostic or prognostic biomarker in the clinic and therefore the method is currently mainly used in (pharmacological) research.[58] Disadvantages of LSCI are a high sensitivity to movement artefacts and indirect and superficial measurements.[59] However new techniques are developed to overcome these disadvantages.[60, 61]

*Infrared thermography*

Infrared thermography measures skin temperature by recording the infrared radiation that is being returned from the skin, from which dermal

blood flow can be estimated through an proprietary algorithm.[62] Besides being of diagnostic value in sSC/Raynaud's phenomenon patients[63,64] and burn wounds[65] it is used in experimental settings in dermatological conditions such as psoriasis[66] or eczema.[67] Reported reproducibility for healthy volunteers was moderate for most measurements ICC ~0.7-[62] and for Raynaud's phenomenon and sSC ICC ~0.55.[68] The predictive value of this methodology remains unknown due to lack of standardization of methods[63] which are currently under development.[69] Disadvantages are the extreme sensitivity to environmental temperature as a drop from three degrees C decreases baseline measurements by about 20%. Therefore measurements should be performed in strictly climate-controlled laboratories.[62] Thermography is a relatively simple measurement, however calibration and maintenance of the device requires experts.

*Video capillaroscopy*

Video capillaroscopy (VC) is the gold standard for morphological measurements of the microcirculation. VC allows for real-time 2D capillary network visualization. The preferred sites of measurement are the nailfolds or the sublingual mucosa, as capillaries at these sites are u-shaped and lie horizontally to the skin surface.[64] VC measures shape (torquation, microaneurysms), density, size (diameter, length), morphology (oedema, microhaemorrhages) and in experimental setting can measure flow dynamics.[70] Of all microvascular imaging techniques, VC is the most frequently applied technique in clinical practice.[71] In rheumatology it can be used to distinguish between primary and secondary Raynaud's phenomenon and is included as a standard assessment in the ACR-EULAR guidelines.[72,73] Several studies show an excellent intra-visit ICC of >0.9 and a moderate inter-visit ICC of ~0.65 distal vessel density.[74,75] Disadvantages of VC are spatial variability which can lead to high intra subject variability,[76] time required for the assessment and the high technical skills needed for the appropriate measurement.[77]

*Optical coherence tomography*

OCT allows visualization of tissue structures in a manner similar to ultrasound but instead uses infrared light. Reconstruction of cross-sectional images to en-face images of tissue can be performed, allowing visualization of the microvasculature. Recent development of dynamic OCT (D-OCT) also allows for the visualization of erythrocyte movement, through combining the speckle variance technique with OCT.[78] In dermatology, OCT is used for morphological assessments for the diagnosis of non-melanoma skin cancer, inflammatory skin disease[79] and burn wounds.[80] Furthermore D-OCT has been used to demonstrate the effect of brimonidine.[81] OCT showed a CV in the range of 5.5 – 8.5%.[82] Disadvantages of OCT are the relatively long time required to perform the scan (+- 3-4 minutes) and the limited area that can be scanned during a single measurement which may lead to variable results due to spatial variability. When performed using the same measurement site, and under the same environmental conditions, OCT measurements can be easily and rapidly performed and show a limited inter- and intra-observer variability of 4.1 and 7.1 (CV%)respectively.[82]

Costs, mechanism, time for assessment, measurement area, variability as well as the major disadvantages of the identified microvascular imaging techniques are summarized in *Table 1*.

## CUTANEOUS CHALLENGES

This section covers different challenges that can be used in cutaneous microcirculation techniques. These challenges change or destabilize the cutaneous microcirculation, thereby allowing an induced (pharmacological) effect to be quantified. (*Table 2* for an overview).

*Transdermal iontophoresis*

Transdermal iontophoresis is the delivery of drugs through the dermal barrier using a weak electrical current. For microcirculation testing, acetylcholine (ACH) and sodium nitroprusside (SNP) are most frequently used. ACH causes a temporal increase in local vasodilation and subsequently increase blood flow through predominantly nitric oxide (NO) and prostaglandin release by the endothelium. Administration of exogenous NO through SNP is used as a control measure for general vasodilatory capacity.[83] Iontophoresis is mainly used to study endothelial NO release and can be used the investigate the effect of pharmacological





**TABLE 1 Overview of skin and retinal microvascular measurements**

| Technique | Cost estimate | Measurements and challenges | Time for assessment | Repeatability |
|---|---|---|---|---|
| Laser Doppler flowmetry | €13.500 | Flux, LTH, PORH, Local cooling, iontepheresis | ± 30 s<br>Challenges: 15-30 min | intra subject CV ~35% [41] |
| Laser Doppler imager | NA | Flux, LTH, PORH, Local cooling | ± 30 s<br>Challenges: 15-30 min | intra subject CV ±20% % [47] |
| LSCI | €60.000 | Flux, LTH, PORH, Local cooling, iontepheresis | ± 30 s<br>Challenges: 15-30 min | intra subject CV 6-12% [51-53] |
| Thermography | €50.000 | Skin temperature, PORH | ± 30 s<br>Chalenges: 15-30 min | Intra class correlation (ICC) 0.7-0.85 [62] [68] |
| Video capilairoscopy | €6.000 | Flux, LTH, PORH, Local cooling | 2 min | intra visit ICC 0.91 – 0.96, inter visit ICC of 0.56- 0.90[74] |
| OCT | €85.000 | Vessel density / morphology. flow | 2/3 minutes | Intra day (CV%) 5.5 – 8.5 [82] |
| OCT | €20.000 | Retinal thickness, retinal vasculature | ± 10 min | Measurements (CV% ≈ 1.8) between observers ICC ≈ 0.99 [100] |
| Laser Doppler flowmetry (ophthalmology) | | Retinal venous and arterial flow | ± 3 min | CV 12.7% - 13.8% [94] |
| LSFG | €85.000 | Retinal venous and arterial flow | | ICC of ≥ 0.937 [95] |
| Retinal function imager | €150.000 | Retinal venous and arterial flow, retinal vasculature, retinal oximetry | ±20 min | Intra subject CV 6-11% [90] |
| Fundus photography | €15.000 | Retinal vasculature | ±10 min | Measurement ICC 0.64-0.69 for, grader ICC 0.79 to 0.83 [110] |

**TABLE 2 Overview of suitable challenges for cutaneous microvascular measurements**

| | Laser Doppler flowmetry | Laser Doppler imaging | Laser speckle contrast imaging | Thermography | Video capilairoscopy | D-OCT |
|---|---|---|---|---|---|---|
| Transdermal iontophoresis | X | X | X | X | | X |
| Local thermal hyperemia | X | X | X | X | X | |
| Local cooling | X | X | X | X | X | |
| Post-occlusive reactive hyperemia (PORH) | X | X | X | X | | |
| Assessment of micro-oscillations | X | | X | | | |

compounds that influence the bioavailability of NO in the endothelium. Furthermore, iontophoresis can be also used to study other effects on the microvascular physiology, such as the effect of histamine on skin blood flow and thermoregulation capacity of the skin. An issue with iontophoresis is the variability which is especially large with laser Doppler imaging (34.4% to 42.0%)[84] and the nonspecific vasodilation caused by the electric current and ions in the vehicle, which is variable in effect. Although this can be minimalized by using deionized water as vehicle and using a control vehicle to estimate this effect, the effect remains substantial.[83] Moreover, there is currently no standard protocol which makes it difficult to compare from different studies.

*Local thermal hyperemia*

The skin is locally heated to a temperature of up to 42°C producing a local vasodilation which induces an increase in skin blood flow within 5 minutes after the start of heating and a prolonged secondary plateau is reached after 20–30 minutes of heating. The initial peak is caused by a sensory nerve axon reflex mainly mediated through endothelium-derived hyperpolarizing factors and transient receptor potential vanilloid type-1 (TRPV1) channels. The secondary peak is mostly mediated through the endothelial tissue, for a large part due to NO release.[85] Alternatively, local heating to 39° is thought to induce an isolated NO-dependent dilation without the sensory axon reflex.[86] Results of this challenge need to be performed in strictly climate controlled laboratory, and have an intermediate variability (CV% 17 for plateau and CV% 39 for peak measurements), however this is dependent on the peak temperature and the heating rate.[87]

*Local cooling*

Rapid local cooling of the skin leads to vasoconstriction and consequent decreased blood flow, which is followed by a transient vasodilation and subsequently a prolonged vasoconstriction. The initial vasoconstriction is mediated through the adrenergic system by upregulation of α-2c-receptors, where the sustained vasoconstriction is mostly mediated by inhibition of NO. The mechanism for the transient vasodilation is unknown.[85] Local cooling is mostly studied in patients with Raynaud phenomena, but can also be used to study endothelial function, however due to the complex and partly not understood physiology of this reaction, other methods are preferable.

*Post-occlusive reactive hyperemia*

PORH measurements are usually performed on the volar forearm, where occlusion is produced by inflating a blood pressure cuff on the upper arm. Releasing the occlusion results in an initial peak in blood flow, which returns to baseline several minutes after the occlusion. The initial peak is mediated by a mixture of sensory nerve involvement[88] and endothelium-derived hyperpolarizing factors, caused by the shear stress ischemia during the occlusion.[88] NO-release does not play a major role in occlusion-induced cutaneous hyperemia.[89] Endpoints of PORH include, time to hyperemia, maximal flow, time to return to baseline and AUC from time of maximal flow to time of return to baseline. PORH is frequently used as a test for microvascular endothelial function, as it is minimal invasive, easy to perform, shows good contrast between populations with different endothelial functions and has an excellent repeatability(CV 8-11%).[47,87,90]

*Assessment of micro-oscillations*

Frequency domain analysis of longitudinal microvascular blood flow measurements such as LDF and LSCI has been performed in various disease models.[91] Oscillations in different frequencies have been linked to vasomotion, neurogenic activity and endothelial function. NO release and EDHF have been attributed the main factors to the vasomotion. However, there is limited evidence for the use as a marker for endothelial or vascular function. Furthermore there is no standardization of this measurement between different studies.[91]

## RETINAL MICROVASCULAR MEASUREMENTS

*Laser Doppler flowmetry*

Doppler/speckle imaging techniques have also been applied to monitor the retinal microcirculation. Through Doppler imaging, the Doppler shift





(i.e., the movement of the erythrocytes in the retina vessels) can be assessed, which is an indirect measurement of retinal blood flow. Measurements are expressed in arbitrary units. Besides the application in ophthalmologic research these measurements can be predictive for microvascular dysfunction and therefore can be applied in research for a wide range of diseases including cardiac and nephrological disease.[92,93] Laser Doppler flowmetry showed good inter session repeatability (CV of 12.7% - 13.8%) and intra observer (CV of 12.6%) in healthy volunteers. [94] Limitations are the use of arbitrary units and the requirement of clear media to obtain images of sufficient quality.

*Laser speckle flowgraphy (LSFG)*

Laser speckle flowgraphy (LSFG) is a relatively new technique and uses the speckle pattern to obtain information about microvascular blood flow and is an indirect measurement of retinal blood flow. Measurements are expressed in arbitrary units.

LSFG has showed excellent reproducibility with an ICC of ≥ 0.93[95] and also LSFG measurements are strongly correlated with age,[95] brachial–ankle pulse-wave velocity and intima–media thickness.[96] Measurements are relatively easy to perform, are non-invasive, and do not require pupil dilation.[97] Limitations are the use of arbitrary units, the requirement of subject fixation and clear ocular media to obtain images of sufficient quality.

*Optical coherence tomography- angiography*

The technology behind ophthalmologic OCT is similar to dermatological OCT and gives information about the retinal nerve fiber layer and retinal micro vasculature using OCT- angiography (OCT-A) measurements. Although experimental set-ups have been used to quantitatively measure retinal blood flow with D-OCT[98,99] currently no commercial OCT devices are available for the assessment of retinal blood flow. Most studies with OCT therefore include static measurements of the retinal vasculature and morphology. OCT has demonstrated an excellent CV of 1.8% between measurements and an excellent intra-observer correlation of 0.99.[100] However, results from devices from different manufacturers are not interchangeable, due to the high inter device variability, and therefore comparisons between these instruments is nearly impossible.[101] Besides its utility in several ocular diseases,[102] OCT has shown to be a useful biomarker measurement in several other specialisms for example neurology[103] Disadvantages of OCT-A are the small measurement area, measurement time (up to 10 minutes per eye) and the complex analysis.

*Retinal function imager*

Retinal function imager (RFI) is a technique that measures retinal blood flow velocity by detecting the movement of individual erythrocytes via stroboscopic illumination and high-speed digital imaging of the retina. With RFI, the velocity is assessed instead of the flow, while theoretically, this can be estimated through vessel diameter. Through an advanced algorithm, detailed capillary maps of the retina can be obtained. RFI has been applied in several patient groups, including sickle cell patients, multiple sclerosis patients, and several ocular diseases.[104–107] RFI has a CV of 6-11% in both patients and healthy volunteers.[90] However further development of the device has been halted. Acquirement of pictures requires well-trained specialists. Other disadvantages are the time required for acquisition and the time required and the complexity of the analysis.

*Fundus photography*

Fundus photography covers the imaging of the retina, fundus photography cannot be used to directly measure the retinal blood flow. Although fundus video with fluorescence agents can provide none quantitively information, such as vasospasm,[108] or venous increased pressure. Outcome measures such as vessel diameters, tortuosity, and fractal dimensions, fovea size and thickness have been intensively studied and related to several systemic diseases.[109] Fundus photography has a repeatability of 0.64 to 0.69 for intra individual variability and 0.79 to 0.83 for the inter-observer variability.[110] Fundus photography has been used for the diagnosis and long-term follow-up of eye disease in several mechanistic and epidemiologic studies, due to its widespread availability.[111] With the usage of deep learning algorithms it is expected that even more outcome measures can be obtained from fundus photography such as cardiovascular risk factors and gender.[112] Furthermore new devices have been developed with a dynamic imaging frequency which can be useful in combination with challenges.

### Retinal challenges

*Hyperoxic measurements*

The breathing of 100% oxygen leads to an increase in $pO_2$ and subsequently vasoconstriction of vessels and a decreased blood flow. The exact mechanism of this vasoconstriction is not understood.[113] Measurements of hyperoxia-induced vasoconstriction are usually performed in the retina, however have been assessed in the skin as well.[114] Disadvantages of the challenge are the differences in results with different measurement techniques,[115] and the cutaneous measurements, showing little effect. To our knowledge, there is no literature available about the variability.

*Retinal Flickering light stimulation*

Stimulation with flickering light leads to an increased neural activity and metabolic activity subsequently leading to vasodilation of the retinal vasculature. This response has been shown to be mediated by the endothelial release of NO.[116] There is a large body of studies that links retinal abnormalities to cardiac and metabolic diseases.[117] Advantages of the technique are that responses are fast, can be measured in real time, show a good reproducibility [118] are noninvasive and the technique is widely available. Although some studies have issues regarding repeatability the intra subject repeatability has been reported up to ICC 0.819.[119]

## CURRENT PRACTICE

For cutaneous functional microvascular assessments, LSCI is becoming the gold standard, due to the low variability, full field imaging and high acquisition speed compared to other methods. Moreover, most challenges can be performed using LSCI, meaning most endothelial effects can be assessed, measurements are relatively simple and therefore can be performed in a clinical setting. However, drawbacks are the high costs and limited mobility.

For morphological and anatomical assessments of the skin, video capilaroscopy is still the primary choice for morphological assessments due to the excellent measurement accuracy and limited variability. Downsides however include relatively complex execution of the measurement. Furthermore, D-OCT has great potential to surpass video capilaroscopy, although standardization between device specifications and homogenization of measurement protocols is necessary in addition to clinical validation.

For ophthalmologic measurements there is no gold standard and several measurements can be used complementary with each other as they measure different outcomes. For LSFG, there is a great potential for functional measurements although larger standardized studies in which the outcomes are related to clinical outcomes are required to further establish this methodology. For morphological assessments, there is a large body of evidence for using fundus photography outcomes as a biomarker.[109] However OCT-A is able to measure the microvasculature in higher detail, but has not been applied in large cross sectional studies.

### Future implications

For wider acceptation and application of these methodologies in the clinical setting, standardized protocols are essential. These standardized protocols should be clinically validated including variability of the measurements and comparison of the microvascular measurements with clinical outcomes.[120]

Future development in microvascular imaging is expected to be heading towards low cost handheld devices which will be easy to apply and with low variability in clinical practice. The recent development of infrared cameras attached to mobile devices is one example. [121] Although these devices might show higher variability, their low costs and high portability will make them more usable in a clinical setting since measurements can be repeated within the same subject frequently. Also this will allow for microvascular home monitoring, which will more closely mimic a real life situation.

Furthermore, work is done for imaging devices to directly measure flow speed, opposed to indirect measurements.[122] For dermal imaging multispectral imaging devices might become commercial available, which will allow outcomes based on different techniques such as oxygenation and microvascular flow to be obtained during a single measurement. Automated analysis of measurements will be of great value for the comparison of results between different studies with different methods as this will decrease inter-observer variability. There





are currently a few devices available that are able to do this such as the periflux. [123] Furthermore analysis with artificial intelligence and deep learning will have a great impact as it might be able to predict events and outcome measurements that we were previously not able to predict by manual analysis. [112]

Microvascular (retinal) abnormalities may be a useful marker for disease in the traditional (cardio) vascular specialisms such as cardiology and nephrology, but intriguingly have also be used as a predictor for events in psychiatry (schizophrenia)[124] and neurology (multiple sclerosis).[125]

Despite the wide-spread use of some of the techniques, there is a lack of measurement standardization between different studies. Therefore, it is difficult to compare variability and sensitivity of different studies and to relate them to physiological or pathological processes. Moreover, it is difficult to compare the results from different methodologies. A few studies have been performed comparing measurements of different techniques, which showed that results from laser based methods are exchangeable,[47] however there is only a weak to none correlation between microvascular and macrovascular measurements for endothelial function.[44,126,127] Although, for clinical application it is useful that outcomes of different methodologies are exchangeable.

These techniques could not only be useful for research but also on a daily basis in clinical practice. VC and OCT are already established tools for the diagnosis of certain diseases and also LDI and thermography are used in the monitoring of wound healing. Intra-operative imaging with LSCI to predict clinical outcome such as flap survival.[128,129] Future larger multicenter studies, might help in validating these methodologies and thereby establishing their clinical use.

## CONCLUSION

In conclusion, various methods for microvascular imaging are currently available and selection of the applied methodology should be based on pathology and clinical setting of the different techniques. LSCI and LSFG show great potential for functional measurements however different challenges cannot be related to particular pathways. The skin and retinal measurements described in this article are an example of how these techniques can be used to assist in research and even clinical monitoring of patients. Validation of all current techniques is at best partial and more work has to be done to perform such standardized validation tests.[120]

## *REFERENCES*


1 Camici, P.G. and F. Crea, *Coronary microvascular dysfunction.* New England Journal of Medicine, 2007. **356**(8): p. 830-840.

2 Allen, J. and K. Howell, *Microvascular imaging: techniques and opportunities for clinical physiological measurements.* Physiol Meas, 2014. **35**(7): p. R91-r141.

3 Holowatz, L., C. Thompson-Torgerson, and W. Kenney, *Viewpoint: The human cutaneous circulation as a model of generalized microvascular function.* J Appl Physiol.

4 Cabrera DeBuc, D., G.M. Somfai, and A. Koller, *Retinal microvascular network alterations: potential biomarkers of cerebrovascular and neural diseases.* American Journal of Physiology-Heart and Circulatory Physiology, 2016. **312**(2): p. H201-H212.

5 Al-Fiadh, A.H., et al., *Usefulness of retinal microvascular endothelial dysfunction as a predictor of coronary artery disease.* The American journal of cardiology, 2015. **115**(5): p. 609-613.

6 Balmforth, C., et al., *Chorioretinal thinning in chronic kidney disease links to inflammation and endothelial dysfunction.* JCI insight, 2016. **1**(20).

7 Williams, R., et al., *Epidemiology of diabetic retinopathy and macular oedema: a systematic review.* Eye, 2004. **18**(10): p. 963.

8 Roustit, M. and J.-L. Cracowski, *Assessment of endothelial and neurovascular function in human skin microcirculation.* Trends in pharmacological sciences, 2013. **34**(7): p. 373-384.

9 Wei, X., et al., *Assessment of flow dynamics in retinal and choroidal microcirculation.* Survey of ophthalmology, 2018.

10 Allen, J. and K. Howell, *Microvascular imaging: techniques and opportunities for clinical physiological measurements.* Physiological measurement, 2014. **35**(7): p. R91.

11 Eriksson, S., J. Nilsson, and C. Sturesson, *Non-invasive imaging of microcirculation: a technology review.* Medical devices (Auckland, NZ), 2014. **7**: p. 445.

12 Gimbrone, M.A., Jr. and G. Garcia-Cardena, *Endothelial Cell Dysfunction and the Pathobiology of Atherosclerosis.* Circ Res, 2016. **118**(4): p. 620-36.

13 Incalza, M.A., et al., *Oxidative stress and reactive*

*oxygen species in endothelial dysfunction associated with cardiovascular and metabolic diseases.* Vascul Pharmacol, 2018. **100**: p. 1-19.
14 Förstermann, U., N. Xia, and H. Li, *Roles of Vascular Oxidative Stress and Nitric Oxide in the Pathogenesis of Atherosclerosis.* Circ Res, 2017. **120**(4): p. 713-735.
15 Gradinaru, D., et al., *Oxidized LDL and NO synthesis--Biomarkers of endothelial dysfunction and ageing.* Mech Ageing Dev, 2015. **151**: p. 101-13.
16 Napoli, C., et al., *Nitric oxide and atherosclerosis: An update.* Nitric Oxide, 2006. **15**(4): p. 265-279.
17 Thomas, D.D., et al., *The biological lifetime of nitric oxide: implications for the perivascular dynamics of NO and O2.* Proc Natl Acad Sci U S A, 2001. **98**(1): p. 355-60.
18 Tousoulis, D., et al., *The role of nitric oxide on endothelial function.* Curr Vasc Pharmacol, 2012. **10**(1): p. 4-18.
19 Shibasaki, M., et al., *Nitric oxide inhibits cutaneous vasoconstriction to exogenous norepinephrine.* J Appl Physiol (1985), 2008. **105**(5): p. 1504-8.
20 Tousoulis, D., et al., *Endothelial dysfunction in conduit arteries and in microcirculation. Novel therapeutic approaches.* Pharmacol Ther, 2014. **144**(3): p. 253-67.
21 Flammer, A.J., et al., *The assessment of endothelial function: from research into clinical practice.* Circulation, 2012. **126**(6): p. 753-67.
22 Stuehr, D., S. Pou, and G.M. Rosen, *Oxygen reduction by nitric-oxide synthases.* J Biol Chem, 2001. **276**(18): p. 14533-6.
23 Förstermann, U. and W.C. Sessa, *Nitric oxide synthases: regulation and function.* European Heart Journal, 2011. **33**(7): p. 829-837.
24 Cyr, A.R., et al., *Nitric Oxide and Endothelial Dysfunction.* Crit Care Clin, 2020. **36**(2): p. 307-321.
25 Mónica, F.Z., K. Bian, and F. Murad, *The Endothelium-Dependent Nitric Oxide-cGMP Pathway.* Adv Pharmacol, 2016. **77**: p. 1-27.
26 Matthews, J.R., et al., *Inhibition of NF-κB DNA Binding by Nitric Oxide.* Nucleic Acids Research, 1996. **24**(12): p. 2236-2242.
27 Grumbach, I.M., et al., *A negative feedback mechanism involving nitric oxide and nuclear factor kappa-B modulates endothelial nitric oxide synthase transcription.* Journal of Molecular and Cellular Cardiology, 2005. **39**(4): p. 595-603.
28 Laursen, J.B., et al., *Endothelial regulation of vasomotion in apoE-deficient mice: implications for interactions between peroxynitrite and tetrahydrobiopterin.* Circulation, 2001. **103**(9): p. 1282-8.
29 Chen, J.Y., et al., *Nitric oxide bioavailability dysfunction involves in atherosclerosis.* Biomed Pharmacother, 2018. **97**: p. 423-428.
30 Carlstrom, M. and M.F. Montenegro, *Therapeutic value of stimulating the nitrate-nitrite-nitric oxide pathway to attenuate oxidative stress and restore nitric oxide bioavailability in cardiorenal disease.* Journal of Internal Medicine, 2019. **285**(1): p. 2-18.
31 Bonetti, P.O., L.O. Lerman, and A. Lerman, *Endothelial Dysfunction: A Marker of Atherosclerotic Risk.* Arteriosclerosis, Thrombosis, and Vascular Biology, 2003. **23**(2): p. 168-175.
32 Polovina, M.M. and T.S. Potpara, *Endothelial Dysfunction in Metabolic and Vascular Disorders.* Postgraduate Medicine, 2014. **126**(2): p. 38-53.
33 Matsuzawa, Y., et al., *Prognostic Value of Flow-Mediated Vasodilation in Brachial Artery and Fingertip Artery for Cardiovascular Events: A Systematic Review and Meta-Analysis.* J Am Heart Assoc, 2015. **4**(11).
34 Yeboah, J., et al., *Predictive value of brachial flow-mediated dilation for incident cardiovascular events in a population-based study: the multi-ethnic study of atherosclerosis.* Circulation, 2009. **120**(6): p. 502-9.
35 Trinity, J.D. and R.S. Richardson, *Physiological Impact and Clinical Relevance of Passive Exercise/Movement.* Sports Med, 2019. **49**(9): p. 1365-1381.
36 Shields, K.L., et al., *The passive leg movement technique for assessing vascular function: defining the distribution of blood flow and the impact of occluding the lower leg.* Exp Physiol, 2019. **104**(10): p. 1575-1584.
37 Trinity, J.D., et al., *Nitric oxide and passive limb movement: a new approach to assess vascular function.* J Physiol, 2012. **590**(6): p. 1413-25.
38 Mortensen, S.P., et al., *The hyperaemic response to passive leg movement is dependent on nitric oxide: a new tool to evaluate endothelial nitric oxide function.* J Physiol, 2012. **590**(17): p. 4391-400.
39 Gifford, J.R. and R.S. Richardson, *CORP: Ultrasound assessment of vascular function with the passive leg movement technique.* J Appl Physiol (1985), 2017. **123**(6): p. 1708-1720.
40 Drain, L.E., *The laser doppler techniques.* Chichester, Sussex, England and New York, Wiley-Interscience, 1980. 250 p., 1980.
41 Roustit, M., et al., *Reproducibility and methodological issues of skin post-occlusive and thermal hyperemia assessed by single-point laser Doppler flowmetry.* Microvascular research, 2010. **79**(2): p. 102-108.
42 Jung, F., et al., *Laser Doppler flux measurement for the assessment of cutaneous microcirculation–critical remarks.* Clinical hemorheology and microcirculation, 2013. **55**(4): p. 411-416.
43 Kubli, S., et al., *Reproducibility of laser Doppler imaging of skin blood flow as a tool to assess endothelial function.* Journal of cardiovascular pharmacology, 2000. **36**(5): p. 640-648.
44 Gori, T., et al., *Correlation analysis between different parameters of conduit artery and microvascular vasodilation.* Clinical hemorheology and microcirculation, 2006. **35**(4): p. 509-515.
45 Shamim-Uzzaman, Q.A., et al., *Altered cutaneous microvascular responses to reactive hyperaemia in coronary artery disease: a comparative study with conduit vessel responses.* Clinical Science, 2002. **103**(3): p. 267-274.
46 Ibrahimi, K., et al., *Reproducibility and agreement of different non-invasive methods of endothelial function assessment.* Microvascular research, 2018. **117**: p. 50-56.
47 Millet, C., et al., *Comparison between laser speckle contrast imaging and laser Doppler imaging to assess skin blood flow in humans.* Microvascular research, 2011. **82**(2): p. 147-151.
48 Van der Schueren, B., et al., *Reproducibility of the capsaicin-induced dermal blood flow response as assessed by laser Doppler perfusion imaging.* British journal of clinical pharmacology, 2007. **64**(5): p. 580-590.
49 van der Kolk, T., et al., *Comprehensive, multi-modal characterization of an imiquimod-induced human skin inflammation model for drug development.* Clinical and translational science, 2018.
50 Briers, J.D., G.J. Richards, and X.-W. He, *Capillary blood flow monitoring using laser speckle contrast analysis (LASCA).* Journal of biomedical optics, 1999. **4**(1): p. 164-176.
51 Puissant, C., et al., *Reproducibility of non-invasive assessment of skin endothelial function using laser Doppler flowmetry and laser speckle contrast imaging.* PLoS One, 2013. **8**(4): p. e61320.
52 Rousseau, P., et al., *Increasing the 'region of interest' and 'time of interest', both reduce the variability of blood flow measurements using laser speckle contrast imaging.* Microvasc Res, 2011. **82**(1): p. 88-91.
53 Millet, C., et al., *Comparison between laser speckle contrast imaging and laser Doppler imaging to assess skin blood flow in humans.* Microvasc Res, 2011. **82**(2): p. 147-51.
54 Birkhoff, W., et al., *Retinal microcirculation imaging in sickle cell disease patients.* Microvasc Res, 2018. **116**: p. 1-5.
55 Matheus, A.S., et al., *Sensibility and specificity of laser speckle contrast imaging according to Endo-PAT index in type 1 diabetes.* Microvascular research, 2018. **117**: p. 10-15.
56 Souza, E.G., et al., *Impairment of systemic microvascular endothelial and smooth muscle function in individuals with early-onset coronary artery disease: studies with laser speckle contrast imaging.* Coronary artery disease, 2014. **25**(1): p. 23-28.
57 Minniti, C.P., et al., *Vasculopathy, inflammation, and blood flow in leg ulcers of patients with sickle cell anemia.* Am J Hematol, 2014. **89**(1): p. 1-6.
58 Hellmann, M., M. Roustit, and J.-L. Cracowski, *Skin microvascular endothelial function as a biomarker in cardiovascular diseases?* Pharmacological Reports, 2015. **67**(4): p. 803-810.
59 Briers, D., et al., *Laser speckle contrast imaging: theoretical and practical limitations.* Journal of biomedical optics, 2013. **18**(6): p. 066018.
60 Zotterman, J., et al., *Methodological concerns with laser speckle contrast imaging in clinical evaluation of microcirculation.* PLoS One, 2017. **12**(3): p. e0174703.
61 Bahadori, S., T. Immins, and T.W. Wainwright, *A Novel Approach to Overcome Movement Artifact When Using a Laser Speckle Contrast Imaging System for Alternating Speeds of Blood Microcirculation.* J Vis Exp, 2017(126).
62 Pauling, J.D., et al., *Comparison of infrared thermography and laser speckle contrast imaging for the dynamic assessment of digital microvascular function.* Microvascular research, 2012. **83**(2): p. 162-167.
63 Pauling, J., et al., *Use of infrared thermography as an endpoint in therapeutic trials of Raynaud's phenomenon and systemic sclerosis.* Clinical and Experimental Rheumatology-Incl Supplements, 2012. **30**(2): p. S103.
64 Herrick, A.L. and A. Murray, *The role of capillaroscopy and thermography in the assessment and management of Raynaud's phenomenon.* Autoimmunity reviews, 2018.
65 Jaspers, M.E., et al., *A systematic review on the quality of measurement techniques for the assessment of burn wound depth or healing potential.* Burns, 2018.
66 Zalewska, A., et al. *Thermography in psoriasis vulgaris evaluation*. in *Engineering in Medicine and Biology Society, 2005. IEEE-EMBS 2005. 27th Annual International Conference of the*. 2006. IEEE.
67 Hornstein, O.P., F. Boissevain, and H. Wittmann, *Non-invasive Measurement of the Vascular Dynamics of Dermographism: Comparative Study in Atopic and Non-atopic Subjects.* The Journal of dermatology, 1991. **18**(2): p. 79-85.
68 Pauling, J.D., et al., *Use of laser speckle contrast imaging to assess digital microvascular function in primary Raynaud phenomenon and systemic sclerosis: A comparison using the Raynaud condition score diary.* The Journal of rheumatology, 2015: p. jrheum. 141437.
69 Wilkinson, J.D., et al., *A Multicenter Study of the Validity and Reliability of Responses to Hand Cold Challenge as Measured by Laser Speckle Contrast Imaging and Thermography: Outcome Measures for Systemic Sclerosis–Related Raynaud's Phenomenon.* Arthritis & Rheumatology, 2018.
70 Berks, M., et al., *Automated structure and flow measurement—a promising tool in nailfold capillaroscopy.* Microvascular research, 2018. **118**: p. 173-177.
71 Lambova, S.N. and U. Muller-Ladner, *Nailfold Capillaroscopy Within and Beyond the Scope of Connective Tissue Diseases.* Current rheumatology reviews, 2018. **14**(1): p. 12-21.
72 van den Hoogen, F., et al., *Classification criteria for systemic sclerosis: An ACR-EULAR Collaborative Initiative.* Arthritis and rheumatism, 2013. **65**(11): p. 2737.
73 Chojnowski, M.M., A. Felis-Giemza, and M. Olesińska, *Capillaroscopy–a role in modern rheumatology.* Reumatologia, 2016. **54**(2): p. 67.
74 Dinsdale, G., et al., *Quantitative outcome measures for systemic sclerosis-related Microangiopathy–Reliability of image acquisition in Nailfold Capillaroscopy.* Microvascular research, 2017. **113**: p. 56-59.
75 Dinsdale, G., et al., *Intra-and inter-observer reliability of nailfold videocapillaroscopy—A possible outcome measure for systemic sclerosis-related microangiopathy.* Microvascular research, 2017. **112**: p. 1-6.
76 Dinsdale, G., et al., *Intra-and inter-observer reliability of nailfold videocapillaroscopy - A possible outcome measure for systemic sclerosis-related microangiopathy.* Microvasc Res, 2017. **112**: p. 1-6.
77 Sekiyama, J.Y., et al., *Reliability of widefield nailfold capillaroscopy and video capillaroscopy in the assessment of patients with Raynaud's phenomenon.* Arthritis Care Res (Hoboken), 2013. **65**(11): p. 1853-61.
78 Ulrich, M., et al., *Dynamic optical coherence tomography of skin blood vessels–proposed terminology and practical guidelines.* Journal of the European Academy of Dermatology and Venereology, 2018. **32**(1): p. 152-155.
79 Fluhr, J.W., T. Zuberbier, and R. Darlenski, *Noninvasive measures in atopic dermatitis.* Current opinion in allergy and clinical immunology, 2018. **18**(5): p. 417-424.

80 Lindert, J., et al., *Optical coherence tomography provides an optical biopsy of burn wounds in children—a pilot study.* Journal of biomedical optics, 2018. **23**(10): p. 106005.

81 Themstrup, L., et al., *In vivo, micro-morphological vascular changes induced by topical brimonidine studied by Dynamic optical coherence tomography.* Journal of the European Academy of Dermatology and Venereology, 2016. **30**(6): p. 974-979.

82 Gambichler, T., et al., *In vivo data of epidermal thickness evaluated by optical coherence tomography: effects of age, gender, skin type, and anatomic site.* Journal of dermatological science, 2006. **44**(3): p. 145-152.

83 Tesselaar, E. and F. Sjöberg, *Transdermal iontophoresis as an in-vivo technique for studying microvascular physiology.* Microvascular research, 2011. **81**(1): p. 88-96.

84 Turner, J., J.J. Belch, and F. Khan, *Current concepts in assessment of microvascular endothelial function using laser Doppler imaging and iontophoresis.* Trends in cardiovascular medicine, 2008. **18**(4): p. 109-116.

85 Johnson, J.M. and D.L. Kellogg Jr, *Local thermal control of the human cutaneous circulation.* Journal of applied physiology, 2010. **109**(4): p. 1229-1238.

86 Choi, P.J., et al., *New approach to measure cutaneous microvascular function: an improved test of NO-mediated vasodilation by thermal hyperemia.* Journal of Applied Physiology, 2014. **117**(3): p. 277-283.

87 Roustit, M. and J.L. Cracowski, *Non-invasive assessment of skin microvascular function in humans: an insight into methods.* Microcirculation, 2012. **19**(1): p. 47-64.

88 Lorenzo, S. and C.T. Minson, *Human cutaneous reactive hyperaemia: role of BKCa channels and sensory nerves.* The Journal of physiology, 2007. **585**(1): p. 295-303.

89 Wong, B.J., et al., *Nitric oxide synthase inhibition does not alter the reactive hyperemic response in the cutaneous circulation.* Journal of Applied Physiology, 2003. **95**(2): p. 504-510.

90 Birkhoff, W., et al., *Retinal microcirculation imaging in sickle cell disease patients.* Microvascular Research, 2017.

91 Rossi, M., et al., *Skin vasomotion investigation: a useful tool for clinical evaluation of microvascular endothelial function?* Biomedicine & Pharmacotherapy, 2008. **62**(8): p. 541-545.

92 Houben, A.J., R.J. Martens, and C.D. Stehouwer, *Assessing Microvascular Function in Humans from a Chronic Disease Perspective.* Journal of the American Society of Nephrology, 2017: p. ASN. 2017020157.

93 Shiba, T., M. Takahashi, and T. Maeno, *Pulse-wave analysis of optic nerve head circulation is significantly correlated with kidney function in patients with and without chronic kidney disease.* Journal of ophthalmology, 2014. **2014**.

94 Yoshida, A., et al., *Reproducibility and clinical application of a newly developed stabilized retinal laser Doppler instrument.* American journal of ophthalmology, 2003. **135**(3): p. 356-361.

95 Luft, N., et al., *Ocular blood flow measurements in healthy white subjects using laser speckle flowgraphy.* PLoS One, 2016. **11**(12): p. e0168190.

96 Shiba, T., et al., *Pulse-wave analysis of optic nerve head circulation is significantly correlated with brachial–ankle pulse-wave velocity, carotid intima–media thickness, and age.* Graefe's Archive for Clinical and Experimental Ophthalmology, 2012. **250**(9): p. 1275-1281.

97 Matsumoto, T., et al., *Reproducibility of neonate ocular circulation measurements using laser speckle flowgraphy.* BioMed research international, 2015. **2015**.

98 Haindl, R., et al., *Total retinal blood flow measurement by three beam Doppler optical coherence tomography.* Biomedical optics express, 2016. **7**(2): p. 287-301.

99 Doblhoff-Dier, V., et al., *Measurement of the total retinal blood flow using dual beam Fourier-domain Doppler optical coherence tomography with orthogonal detection planes.* Biomedical optics express, 2014. **5**(2): p. 630-642.

100 Carpineto, P., et al., *Reproducibility and repeatability of foveal avascular zone measurements in healthy subjects by optical coherence tomography angiography.* Br J Ophthalmol, 2016. **100**(5): p. 671-6.

101 Corvi, F., et al., *Reproducibility of Vessel Density, Fractal Dimension, and Foveal Avascular Zone Using 7 Different Optical Coherence Tomography Angiography Devices.* Am J Ophthalmol, 2018. **186**: p. 25-31.

102 Chen, C.-L. and R.K. Wang, *Optical coherence tomography based angiography.* Biomedical optics express, 2017. **8**(2): p. 1056-1082.

103 Satue, M., et al., *Optical coherence tomography as a biomarker for diagnosis, progression, and prognosis of neurodegenerative diseases.* Journal of ophthalmology, 2016. **2016**.

104 Wang, L., et al., *A Mini Review of Clinical and Research Applications of the Retinal Function Imager.* Curr Eye Res, 2018. **43**(3): p. 273-288.

105 Jiang, H., et al., *Impaired retinal microcirculation in multiple sclerosis.* Mult Scler, 2016. **22**(14): p. 1812-1820.

106 Jiang, H., et al., *Automated segmentation and fractal analysis of high-resolution non-invasive capillary perfusion maps of the human retina.* Microvasc Res, 2013. **89**: p. 172-5.

107 Burgansky-Eliash, Z., et al., *Blood-Flow Velocity in Glaucoma Patients Measured with the Retinal Function Imager.* Curr Eye Res, 2016. **41**(7): p. 965-70.

108 Ota, I., K. Kuroshima, and T. Nagaoka, *Fundus video of retinal migraine.* JAMA ophthalmology, 2013. **131**(11): p. 1481-1482.

109 Wong, T.Y., et al., *Retinal microvascular abnormalities and their relationship with hypertension, cardiovascular disease, and mortality.* Survey of ophthalmology, 2001. **46**(1): p. 59-80.

110 Couper, D.J., et al., *Reliability of retinal photography in the assessment of retinal microvascular characteristics: the Atherosclerosis Risk in Communities Study.* American journal of ophthalmology, 2002. **133**(1): p. 78-88.

111 Pries, A.R., T.W. Secomb, and P. Gaehtgens, *Structural autoregulation of terminal vascular beds: vascular adaptation and development of hypertension.* Hypertension, 1999. **33**(1): p. 153-161.

112 Poplin, R., et al., *Prediction of cardiovascular risk factors from retinal fundus photographs via deep learning.* Nature Biomedical Engineering, 2018. **2**(3): p. 158.

113 Dean, J.B., et al., *Hyperoxia, reactive oxygen species, and hyperventilation: oxygen sensitivity of brain stem neurons.* Journal of Applied Physiology, 2004. **96**(2): p. 784-791.







114 Rousseau, A., et al., *Hyperoxia decreases cutaneous blood flow in high-perfusion areas.* Microvascular research, 2007. **74**(1): p. 15-22.

115 Kiss, B., et al., *Retinal blood flow during hyperoxia in humans revisited: concerted results using different measurement techniques.* Microvascular research, 2002. **64**(1): p. 75-85.

116 Dorner, G.T., et al., *Nitric oxide regulates retinal vascular tone in humans.* American Journal of Physiology-Heart and Circulatory Physiology, 2003. **285**(2): p. H631-H636.

117 Houben, A.J., R.J. Martens, and C.D. Stehouwer, *Assessing Microvascular Function in Humans from a Chronic Disease Perspective.* Journal of the American Society of Nephrology, 2017. **28**(12): p. 3461-3472.

118 Kotliar, K.E., et al., *Retinal vessel reaction in response to chromatic flickering light.* Graefe's Archive for Clinical and Experimental Ophthalmology, 2004. **242**(5): p. 377-392.

119 Rauschel, V., et al., *Test-retest reliability of visual-evoked potential habituation.* Cephalalgia, 2016. **36**(9): p. 831-839.

120 Kruizinga, M.D., et al., *Development of Novel, Value-Based, Digital Endpoints for Clinical Trials: A Structured Approach Toward Fit-for-Purpose Validation.* Pharmacological Reviews, 2020. **72**(4): p. 899-909.

121 *Integrated thermal imaging | Cat Phones*. Available from: https://www.catphones.com/en-us/features/integrated-thermal-imaging/.

122 Li, H., et al., *Directly measuring absolute flow speed by frequency-domain laser speckle imaging.* Optics express, 2014. **22**(17): p. 21079-21087.

123 Bakker, J. *Transcutaneous tissue oxygen pressure monitor PeriFlux 6000*. Available from: https://www.perimed-instruments.com/products/periflux-6000-toe-pressure-ABI-tcpO2.

124 Appaji, A., et al., *Retinal vascular abnormalities in schizophrenia and bipolar disorder: A window to the brain.* Bipolar disorders, 2019. **21**(7): p. 634-641.

125 Sepulcre, J., et al., *Diagnostic accuracy of retinal abnormalities in predicting disease activity in MS.* Neurology, 2007. **68**(18): p. 1488-1494.

126 Hansell, J., et al., *Non-invasive assessment of endothelial function–relation between vasodilatory responses in skin microcirculation and brachial artery.* Clinical physiology and functional imaging, 2004. **24**(6): p. 317-322.

127 Jekell, A., M. Kalani, and T. Kahan, *The interrelation of endothelial function and microvascular reactivity in different vascular beds, and risk assessment in hypertension: results from the Doxazosin–ramipril study.* Heart and vessels, 2018: p. 1-12.

128 Zötterman, J., E. Tesselaar, and S. Farnebo, *The use of laser speckle contrast imaging to predict flap necrosis: An experimental study in a porcine flap model.* Journal of Plastic, Reconstructive & Aesthetic Surgery, 2019. **72**(5): p. 771-777.

129 Nguyen, C.D., et al., *Blood perfusion in human eyelid skin flaps examined by laser speckle contrast imaging—Importance of flap length and the use of diathermy.* Ophthalmic Plastic & Reconstructive Surgery, 2018. **34**(4): p. 361-365.

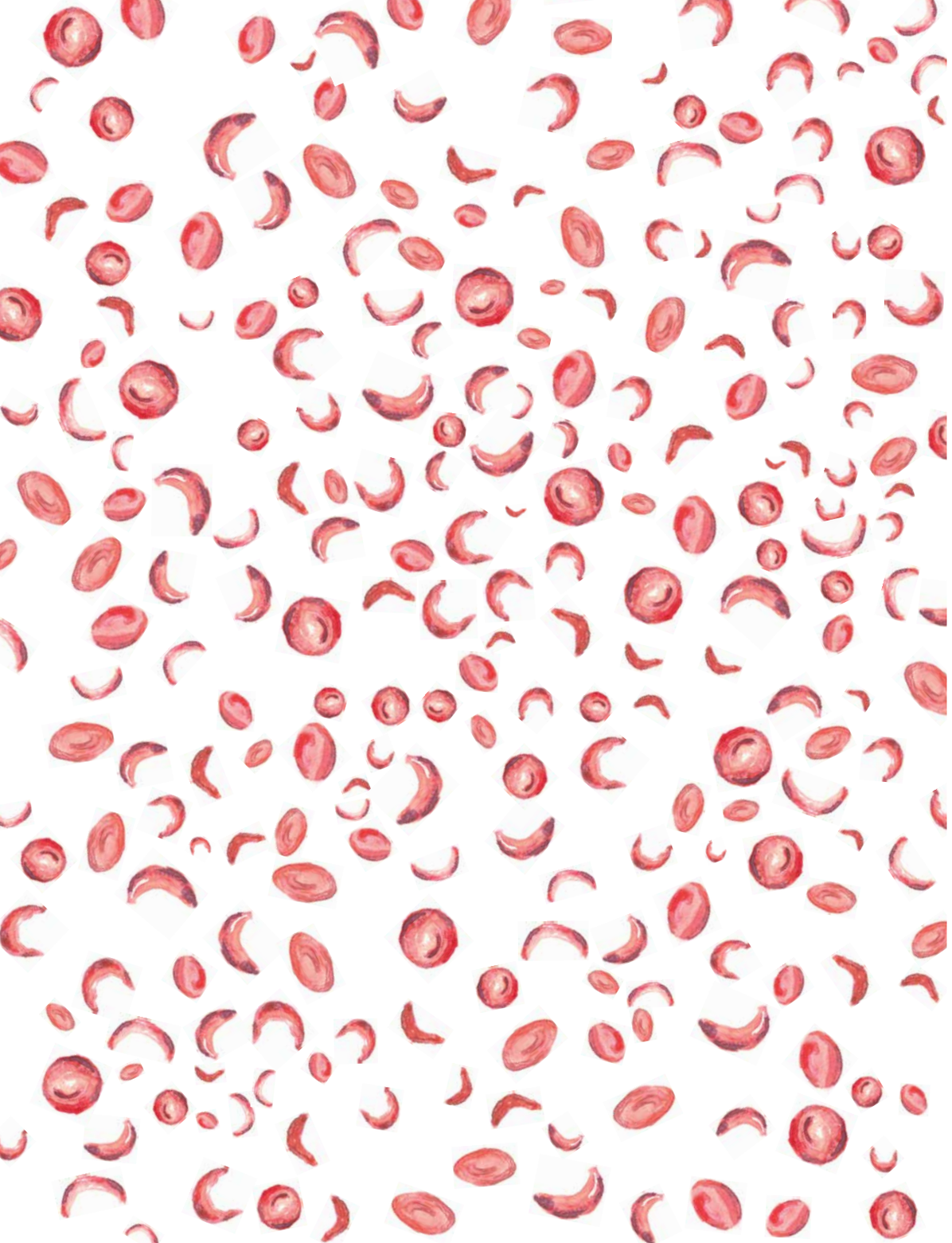

CHAPTER III

# Retinal microcirculation imaging in sickle cell disease patients

*W. Birkhoff [1], J. de Vries [1], G. Dent [2], A. Verma[2] J.L. Kerkhoffs [3], A.H.F. van Meurs [3], M. de Kam [1], M. Moerland [1], J. Burggraaf [1]*

*1 Centre for Human Drug Research, Leiden, The Netherlands / 2 Biogen, Cambridge, Massachusetts, United States / 3 HAGA hospital, Den Haag, The Netherlands / Corresponding author: Prof. Dr. J. Burggraaf*

**OBJECTIVES: To explore the feasibility of a new quantitative method for microvascular function: noninvasive retinal function imaging (RFI). in sickle cell disease (SCD) patients and healthy controls and have it benchmarked against Laser Speckle Contrast Imaging (LSCI) measurements. METHODS: The variability of Microvascular measurements was assessed in 8 SCD patients and 8 healthy matched controls. Measurements were conducted twice on two different study days. RFI was performed for assessment of arterial and venous retinal blood flow. LSCI measurements included post occlusive reactive hyperemia and IBH challenges. Measured variables included basal flow, flow upon occlusion-reperfusion and flow during an IBH. RESULTS: RFI arterial flow and venous flow and LSCI basal flow and peak flow showed excellent intra subject repeatability between days (CVC of 8.5% 9.5%, 7.6% and 7.7% respectively) and between measurements on one day (CVC of 7.0%, 7.7%, 7.6% and 4.7% respectively). RFI arterial flow (P<0.002), and RFI venous flow (P=0.007) differed significantly between SCD patients and controls in as did LSCI basal flow, maximal flow and delta flow during IBH (P <0.0001) CONCLUSIONS: RFI showed low variability for all readout measures, comparable with most microvascular measures from LSCI. The discriminating power of the RFI between SCD patients and controls demonstrate the feasibility of this device for quantitative assessment of the microcirculation in clinical research.**

**Sickle cell disease (SCD) is an inherited genetic disorder that affects approximately 100.000 people in the United States of America.** One out of 500 African American newborns is affected by this disease and in some western European countries SCD is the most common hereditary disorder.[1–3] The disease is caused by a single amino acid substitution in the hemoglobin molecule,[3] which leads to a rigid, sickle-like shape of red blood cells which polymerize when deoxygenated.[4] The polymerized sickle cells form heterocellular aggregates that alters blood flow and tissue perfusion. These acute vascular obstructions results clinically in severe painful episodes known as vaso-occlusive crisis, which often requires hospitalization and are a hallmark of SCD.[5]

Hydroxyurea (HU) is the only approved drug for SCD. It increases the expression of fetal hemoglobin

in the erythrocyte, which inhibits the polymerization of hemoglobin S.[6] HU may also exhibit nitric oxide (NO) donor properties and induce NO-synthase activity and production in endothelial cells [7]. Several studies show that HU reduces the occurrence of SCD-related acute complications as well as survival.[8–11] However, not all SCD patients respond to HU, and the exact individual factors contributing to treatment success are unclear.[12] Moreover, HU therapy has side effects such as constipation, nausea, drowsiness, hair loss, and inflammation of the mouth, or even more severely neutropenia or thrombocytopenia. Hence, for some patients the risks of untreated SCD may outweigh the risks of HU's side effects.[10] Thus, there is a need for alternative pharmacological therapies for SCD.[13]

Drug development in SCD often uses clinical measures such as vaso-occlusive crises, which are not practical for proof-of-pharmacology experiments and drug development in general. The availability of quantitative biomarkers, which report on the underlying pathophysiology leading to clinical insults, could be of great assistance. Since vaso-occlusive phenomena in SCD originate from the impact of sickled cells on the integrity and functionality of the microvasculature,[14–16] validated quantitative measures of microvascular function in SCD patients may provide useful pharmacodynamics biomarkers. Abnormal hemodynamics in SCD patients has been reported for several organs.[17–23] Because of easy accessibility, earlier studies examined cutaneous and conjunctival microcirculation as a surrogate to investigate microvascular mechanisms in SCD. These studies demonstrated an abnormal cutaneous microvascular blood flow with periodic oscillations and a prolonged reactive hyperemic response compared to control subjects.[17] Conjunctival red blood cell velocity is also slower in SCD patients than in control subjects.[18,19,23,24]

New methodologies may allow more precise and quantitative assessments in SCD microcirculation. An interesting new non-invasive technique for quantitative assessment of microvascular function is retinal function imaging (RFI).[25,26] RFI measures retinal blood flow velocity by detecting the movement of individual erythrocytes via stroboscopic illumination and high-speed digital imaging of the retina. By calculating the distance that an erythrocyte moves over a series of pictures, blood velocity is quantified.[27] Using RFI, early changes in retinal blood flow in diabetes,[28] MS patients,[29] age-related macular degeneration and retinitis pigmentosa[30,31] have been demonstrated. As such, RFI could be a valuable technique for quantification of the effects of drugs targeting endothelial integrity in sickle cell disease. However, data on retinal function in sickle cell disease patients are not available. Moreover, performance of RFI in healthy volunteers or patient populations in terms of measurement variability over day and over a longer period of time is lacking. Since these factors are crucial for rational clinical application of the technique, a series of clinical experiments was performed to assess the performance of the RFI in sickle cell disease. The variability of the measurements was assessed in SCD patients and matched controls, and retinal function was compared between moderate to severe sickle cell disease patients and healthy age-, ethnicity-, skin tone- and gender-matched controls. As reference, laser speckle contrast imaging (LSCI)[32,33] measurements were included. LSCI measures cutaneous microvascular blood flow by detecting the movement of laser-illuminated circulating red blood cells in dermal capillaries. Although LSCI has not been used for assessment of vascular function in SCD patients before, it has been shown to be superior to laser Doppler flowmetry in terms of reduced variability and higher discriminating power when assessing microvascular function.[34,35] Laser Doppler has been commonly used in studies with SCD patients.[36,37] LSCI measurements included acute microvascular changes in response to a physiological challenge (post-occlusive reactive hyperemia and inspiratory breath holding).

## MATERIALS AND METHODS

### Study population

Variability in microvascular measures was assessed in SCD patients, aged 18-65 (n=8), and healthy controls matched for age, ethnicity, gender, and body mass index (n=8). SCD patients had a minimum of 4 vaso-occlusive crises in the past, and at least one vaso-occlusive crisis in the last year. SCD patients who underwent transfusion therapy within 3 weeks





prior to the measurements and experienced a vaso-occlusive crisis within 1 week prior to the measurements were excluded. SCD patients continued their usual medication, including, but not limited to, hydroxyurea, vitamin D, folic acid and (prophylactic) antibiotics. For all study participants, the incidental use of acetaminophen (up to 4 g/day) was allowed.

### Study design

This was an observational study, carried out at the Centre of Human Drug Research (CHDR) in Leiden, the Netherlands. Sequential RFI and LSCI were conducted twice on two study days separated by one week. On both study days, subjects arrived at the clinical unit fasted for at least 4 hours. Subjects were asked to abstain from the use of alcohol from 12 hours prior to each study visit, and from tobacco-or nicotine-containing products for at least 2 hours prior to the each study visit, until discharge from the clinical unit. Upon arrival at the clinical unit, the subjects received a standardised breakfast. Two hours after arrival, the first block of RFI and LSCI measurements was started. The second block measurements started two hours after start of the first measurements. All measurements were performed in climate-controlled rooms, at 20–24°C, after a 30minute acclimatization period with the subject in supine position. During the study days, subjects were encouraged to drink sufficient water to avoid dehydration (which is was especially relevant for SCD patients).

The study protocol was approved by the ethics committee of Leiden University and performed according the Dutch law on medical research.

#### RFI

The retinal microcirculation was quantified using the Retinal Function Imager 3005 (Optical Imaging, Rehovot, Israel). Measurements were performed as described previously.[38] In brief, one pupil was dilated using tropicamide. The subject remained seated quietly with the head in a headrest, which allowed collection of 10-15 series of 8 retinal images over a period of 25 minutes. The images were analyzed using Odian browse software (Optical Imaging, Rehovot, Israel). RFI endpoints included average arterial and average venous retinal blood flow velocity (mm/sec).

#### LSCI

LSCI (PSI; Perimed, Järfälla, Sweden) was performed on the ventral side of the upper forearm, on a surface of 3 x 10 centimeters. The laser head was placed 20 cm above the skin. The frame was positioned more than 5 cm from the elbow and beginning of the wrist, avoiding visible veins. A vacuum pillow was used to limit arm movements. The cutaneous blood flow was measured continuously. After the basal flow was recorded for at least 5 min, the brachial artery was occluded by inflating a pressure cuff placed around the upper arm to 200 mm/Hg for 5 min. Subsequently, the cuff was deflated, inducing a hyperemic reaction. Six minutes after the occlusion, subjects were asked to hold their breath for at least 20 seconds. This was repeated two more times, with inspiratory breath holding (IBH) periods separated by three minutes.

Obtained data were analyzed using PIMSOFT oftware (Perimed, Järfälla, Sweden). LSCI endpoints included basal flow (arbitrary units (AU)), peak flow after occlusion (AU), ratio peak flow/basal flow (%),time to return to basal flow (seconds), post-occlusive index as previously described [39] (AUC peak flow/basal flow; %), time to recovery after IBH (seconds), and the delta flow before - during IBH (arbitrary units).

### Statistical analysis

For repeatedly assessed endpoints, contrasts between groups were estimated with a mixed model analysis of variance with fixed factors group (SCD versus controls), day (day 1 and day 8), measurement (0 and 2 hour), group by day, group by measurement and group by day by measurement, and subject, subject by day and subject by time as random factors. LSCI time to maximum flow (sec), LSCI time to return to basal flow (sec) and LSCI time to recovery after IBH (sec) were log- transformed before analysis. For both groups, the estimated intra-subject variability within one day and between days, defined as the short- and long-term repeatability, was calculated. For all endpoints the minimal detectable effect size (MDES) was calculated as a combined measure of the effect size and the estimated variability, assuming a parallel comparison of two groups of 8 subjects. All calculations were performed using SAS for windows V9.4 (SAS Institute, Inc., Cary, NC, USA).

## RESULTS

### Study population

Microvascular function was assessed in SCD patients (n=8), and healthy controls matched for age, BMI, and ethnicity (n=8). Subject demographics are provided in *Table 1*. All included subjects were female and had normal resting blood pressure and heart rate. There was 1 light smoker in the SCD group, and no smokers in the matched control volunteer group.

Six sickle cell patients had a self-reported SCD type HbSS, one subject had HbSE, and one subject was uncertain about the SCD subtype. Medication included folic acid, hydroxycarbamide, vitamin D, deferasirox, deferiprone, and acetaminophen. One SCD patient was on hydroxyurea therapy. Most SCD patients and healthy controls had a Fitzpatrick skin tone of VI (black or African-American).

**TABLE 1 Demographics**

| | SCD patients | Controls |
|---|---|---|
| Age (years) | 34 ± 7.5 | 31 ± 7.6 |
| BMI kg/m² | 25.4 ± 4.8 | 26.4 ± 4.2 |
| Male:female | 0:8 | 0:8 |
| Systolic blood pressure (mmHg) | 109 ± 8 | 116 ± 18 |
| Diastolic blood pressure(mmHg) | 65 ± 6 | 73 ± 12 |

### Variability

Sequential RFI and LSCI were conducted twice on two study days separated by one week. Measurements blocks performed on one study day were separated by 2 hours.

The variability for retinal blood flow velocity by RFI was limited between days (coefficient of variation (CV) 8.5% for arterial flow and 9.5% for venous flow) and between measurements on one day (CV: 7.0% for arterial flow and 7.7% for venous flow). Also LSCI parameters showed limited variability for basal flow and peak flow after occlusion between days (CV 7.6% and 7.7%, respectively) and between measurements on one day (CV: 7.6% and 4.7%, respectively). The variability for the time to recovery after IBH was larger (CV: 23.9% between days and 22.7% within day). *Table 2* provides the variability of microvascular parameters for the two groups separately.

Based on the calculated variances, MDES were assessed for the main microvascular measures, assuming a parallel study design with 2 groups of 8 subjects. The MDES for arterial blood flow velocity was 0.91 mm/sec, for venous blood flow velocity 0.66 mm/sec. The MDES for LSCI basal flow was 8.04 AU, for peak flow after occlusion 21.31 AU, and for the effect of inspiratory breath holding (as assessed by the difference between LSCI blood flow before and during breath holding) 4.51 AU.

### Microvascular parameters and the effect of brachial artery occlusion and IBH

In SCD patients, arterial and venous blood flow velocity, quantified by RFI, were estimated to be 3.87 (95%CI 3.51, 4.23) mm/sec and 3.00 (95%CI 2.73, 3.26) mm/sec. The basal flow assessed by LSCI was 33.4 (95%CI 29.9-36.9) AU. Blood flow increased during the hyperemic reaction following occlusion of the brachial artery, with a peak flow of 93.1 (95%CI 83.9-102.3) AU, returning to basal flow in 129 (95%CI 117, 142) seconds after release of the occlusion. LSCI was also able to detect changes in blood flow upon inspiratory breath holding. This physiological challenge resulted in a temporary reduction in blood flow: delta flow before versus during IBH was estimated to be 9.8 (95%CI 7.8, 11.9) AU in SCD patients. Return to basal flow after IBH occurred within 54 (95%CI 48, 61) seconds. In controls comparable effects of brachial artery occlusion and IBH, quantified by LSCI were observed.

### Contrasts between populations

Statistically significant differences were observed between SCD patients and controls in microvascular function as assessed by the RFI: retinal arterial blood flow velocity 3.87 vs 3.42 mm/sec, p=0.002; retinal venous blood flow velocity 3.00 vs 2.68 mm/sec, p=0.007. Also microvascular function as assessed by the LSCI was significantly different between SCD patients and matched healthy controls: basal flow 33.4 vs 24.5 AU, p<0.0001; peak flow after occlusion 93.1 vs 76.8 AU, p<0.0001; and ratio peak flow/basal flow 286.3 vs 318.6 %, p=0.002. No statistically significant differences were observed between both populations in time to peak flow or





**TABLE 2 CV for LSCI and RFI parameters per population**

| Parameter | Group | Intra-subject cv (between days) | Intra-subject cv (within day) | Inter-subject cv |
|---|---|---|---|---|
| LSCI basal flow (AU) | Sickle cell patients | 9.9% | 6.4% | 21.4% |
| | Controls | 8.1% | 8.1% | 17.2% |
| LSCI peak flow after occlusion (AU) | Sickle cell patients | 7.3% | 4.5% | 16.0% |
| | Controls | 8.8% | 5.8% | 17.1% |
| LSCI ratio peak flow/basal flow (%) | Sickle cell patients | 9.5% | 6.9% | 14.8% |
| | Controls | 6.1% | 11.1% | 13.0% |
| LSCI time to return to basal flow (sec) | Sickle cell patients | 14.4% | 8.6% | 12.8% |
| | Controls | 10.8% | 7.9% | 15.7% |
| LSCI delta flow before- during IBH (AU) | Sickle cell patients | 31.1% | 25.8% | 27.8% |
| | Controls | 24.7% | 35.0% | 54.5% |
| RFI average arterial blood flow velocity (mm/sec) | Sickle cell patients | 5.9% | 5.9% | 22.4% |
| | Controls | 10.9% | 6.8% | 13.1% |
| RFI average venous blood flow velocity (mm/sec) | Sickle cell patients | 7.2% | 6.8% | 22.3% |
| | Controls | 7.5% | 7.5% | 7.3% |

**TABLE 3 LSCI and RFI parameters per population (least square means with 95% CI) and contrasts between populations**

| parameter | SCD patients | Controls | SCD patients versus controls |
|---|---|---|---|
| LSCI basal flow (AU) | 33.4 (29.9 - 36.9) | 24.5 (21.0 - 28.0) | 8.9 (6.7, 11.1) p=<.0001 |
| LSCI peak flow after occlusion (AU) | 93.1 (83.9 - 102.3) | 76.8 (67.6 - 86.0) | 16.3 (10.2, 22.3) p=<.0001 |
| LSCI ratio peak flow/basal flow (%) | 286.3 (257.4 - 315.2) | 318.6 (289.6 - 347.6) | -32.3 (-52.7, -11.8) p=0.002 |
| LSCI time to return to basal flow (sec) | 129 (117 - 142) | 122 (111 - 134) | 5.7% (-1.6%,13.7%) p=0.13 |
| LSCI post-occlusive index (%) | 213.1 (192.2 - 234.0) | 210.6 (189.7 - 231.5) | 2.5 (-10.5, 15.4) p=0.7 |
| LSCI time to recovery after IBH (sec) | 54 (48-61) | 45 (41-51) | 18.9% (9.5%, 29.2%) p=<.0001 |
| LSCI delta flow before-during IBH (AU) | 9.8 (7.8 - 11.9) | 4.7 (2.7 - 6.3) | 5.1 (3.8, 6.4) p=<.0001 |
| RFI average arterial blood flow velocity (mm/sec) | 3.87 (3.51 - 4.23) | 3.42 (3.06 - 3.78) | 0.45 (0.17, 0.73) p=0.002 |
| RFI average venous blood flow velocity (mm/sec) | 3.00 (2.73 - 3.26) | 2.68 (2.42 - 2.95) | 0.31 (0.09, 0.54) p=0.007 |

time to return to basal flow, or in post-occlusive index. The effect of inspiratory breath holding, as assessed by LSCI as the difference between blood flow before and during breath holding, differed significantly between both populations: 9.8 vs 4.7 AU, p<0.0001. Whereas the time to return to basal flow after occlusion of the brachial artery did not discriminate between populations, the time to recover after IBH did, 54 vs 45 sec p<0.0001. *Table 3* provides the point estimates of all microvascular parameters (least square means with 95%CI) and contrasts for both populations (SCD patients and controls).

## DISCUSSION

We explored the performance of RFI in SCD patients, in comparison with a group of age- ethnicity- and gender-matched controls. Hereby, we aimed to qualify RFI-derived measures for microvascular function as biomarkers of vascular dysfunction in SCD. As reference, LSCI measurements were performed, also for quantification of acute microvascular changes in response to a physiological challenge. Sequential measurements were performed twice on two study days, separated by one week.

RFI and LSCI showed comparable limited variability for the various microvascular measures (coefficient of variation in the range of 4-10%), both between study days and between measurements performed on one day for all groups. The observed variability for RFI-derived measures is well comparable with the variability reported for retinal blood flow when assessed by trans-cranial colour Doppler[40] and the variability observed for LSCI-derived measures are in line with the variability and reproducibility of LSCI reported in literature.[13,25,33] Using the LSCI as a benchmark, these data suggest that in terms of variability RFI is equivalent to standard microvascular measurement methods in clinical research. A recent studied showed that there is a strong correlation between laser speckle flowgraphy measurements and RFI measurements for retinal blood flow, suggesting that the results are valid for use in clinical research.[41]

Microvascular function as assessed by RFI differed significantly between SCD patients and matched controls. SCD patients had an elevated arterial and venous blood flow velocity. Statistically significant differences were also observed between SCD patients and matched controls for LSCI-assessed microvascular function measures: SCD patients had an increased basal and peak flow after occlusion, and reduced ratio peak flow/basal flow. An increased cutaneous microvascular flow has been demonstrated previously in SCD by other techniques.[37,42,43] This increased flow is believed to compensate the effects of anaemia and insufficient tissue oxygenation, and may relate to low haematocrit levels and reduced erythrocyte aggregation.[44,45] The reduced ratio peak flow/basal flow in SCD patients is also in line with reports in literature, and may be explained by a reduced capacity of hyper-activated endothelial cells to secrete vasodilatory substances in response to shear stress.[46,47]

RFI assesses the blood flow velocity in the smallest arterioles and venules in the retina, whereas LSCI assesses the blood flow in the capillaries of the skin. It is unknown how the microvascular function in the two different vascular beds relate to each other, and how the estimated blood flow or blood flow velocity relate to clinical outcomes. Previous studies have shown that the cutaneous microvascular function could mirror the microvascular function in other organs.[48]

Visual loss has been observed in 10% to 20% of eyes of SCD patients, strongly associated with proliferative retinopathy.[49] Symptoms include vitreous hemorrhages, neovascularization, retinal detachment and anastomoses.[50] The observed increased retinal blood velocity in SCD patients may relate to these symptoms. Abnormalities in the retinal microvasculature may also relate to cerebral diseases such as dementia and decreased cognitive function, and retinopathy and brain abnormalities as shown by MRI or CT.[51] Although the RFI technique in this study allowed visualization of capillary maps without contrast agents, quantification of retinopathy was not possible since automated and validated software is not available yet. Another limitation of RFI is the fact that image acquisition requires highly experienced operators, since the technique is from an operational point-of-view more difficult than LSCI. As such, the introduction of operator-related measurement variability may be a risk for RFI. Also, a drawback of RFI is that is not possible yet to assess the effects of a physiological challenge on microvascular function (e.g. IBH), whereas LSCI does allow such interventions.





One limitation of our study is the fact that mainly female subjects were enrolled. We cannot exclude the possibility that gender is a factor of influence on microvascular function in SCD patients. Gender differences in NO availability have been reported for SCD patients, possibly related to the effects of oestrogens.[47] However, since all SCD patients in our study were matched to a healthy control subject, this does not affect our main conclusions.

In summary, RFI is a robust technique to assess microvascular dysfunction in SCD, even though the correlation between RFI-derived measures and clinical outcome is unknown. We showed that arterial and venous blood flow velocity by RFI are highly stable measures over time, and differentiate between SCD patients and controls.

## *REFERENCES*


1 Hansell J, Henareh L, Agewall S, Norman M. Non-invasive assessment of endothelial function–relation between vasodilatory responses in skin microcirculation and brachial artery. Clinical physiology and functional imaging. 2004;24(6):317-22.

2 Elguero E, Délicat-Loembet LM, Rougeron V, Arnathau C, Roche B, Becquart P, et al. Malaria continues to select for sickle cell trait in Central Africa. Proceedings of the National Academy of Sciences. 2015;112(22):7051-4.

3 Ingram VM. Gene mutations in human haemoglobin: the chemical difference between normal and sickle cell haemoglobin. Nature. 1957;180(4581):326-8.

4 Bookchin RM, Balazs T, Nagel RL, Tellez I. Polymerisation of haemoglobin SA hybrid tetramers. Nature. 1977;269(5628):526-7.

5 Platt OS, Brambilla DJ, Rosse WF, Milner PF, Castro O, Steinberg MH, et al. Mortality in sickle cell disease – life expectancy and risk factors for early death. New England Journal of Medicine. 1994;330(23):1639-44.

6 Platt OS, Orkin SH, Dover G, Beardsley GP, Miller B, Nathan DG. Hydroxyurea enhances fetal hemoglobin production in sickle cell anemia. Journal of Clinical Investigation. 1984;74(2):652.

7 Gladwin MT, Shelhamer JH, Ognibene FP, Pease-Fye ME, Nichols JS, Link B, et al. Nitric oxide donor properties of hydroxyurea in patients with sickle cell disease. British journal of haematology. 2002;116(2):436-44.

8 Charache S, Terrin ML, Moore RD, Dover GJ, Barton FB, Eckert SV, et al. Effect of hydroxyurea on the frequency of painful crises in sickle cell anemia. New England Journal of Medicine. 1995;332(20):1317-22.

9 Ferster A, Vermylen C, Cornu G, Buyse M, Corazza F, Devalck C, et al. Hydroxyurea for treatment of severe sickle cell anemia: a pediatric clinical trial. Blood. 1996;88(6):1960-4.

10 Steinberg MH, Barton F, Castro O, Pegelow CH, Ballas SK, Kutlar A, et al. Effect of hydroxyurea on mortality and morbidity in adult sickle cell anemia: risks and benefits up to 9 years of treatment. JAMA. 2003;289(13):1645-51.

11 Jones AP, Davies SC, Olujohungbe A. Hydroxyurea for sickle cell disease. The Cochrane Library. 2001.

12 Ware RE, Eggleston B, Redding-Lallinger R, Wang WC, Smith-Whitley K, Daeschner C, et al. Predictors of fetal hemoglobin response in children with sickle cell anemia receiving hydroxyurea therapy. Blood. 2002;99(1):10-4.

13 Yawn BP, Buchanan GR, Afenyi-Annan AN, Ballas SK, Hassell KL, James AH, et al. Management of sickle cell disease: summary of the 2014 evidence-based report by expert panel members. JAMA. 2014;312(10):1033-48.

14 Barabino GA, Platt MO, Kaul DK. Sickle cell biomechanics. Annual review of biomedical engineering. 2010;12:345-67.

15 Epstein FH, Bunn HF. Pathogenesis and treatment of sickle cell disease. New England Journal of Medicine. 1997;337(11):762-9.

16 Stuart MJ, Nagel RL. Sickle-cell disease. The Lancet. 2004;364(9442):1343-60.

17 Rodgers GP, Schechter AN, Noguchi CT, Klein HG, Nienhuis AW, Bonner RF. Periodic microcirculatory flow in patients with sickle-cell disease. New England Journal of Medicine. 1984;311(24):1534-8.

18 Cheung AT, Chan MS, Ramanujam S, Rangaswami A, Curl K, Franklin P, et al. Effects of poloxamer 188 treatment on sickle cell vaso-occlusive crisis: computer-assisted intravital microscopy study. Journal of investigative medicine. 2004;52(6):402-6.

19 Cheung AT, Chen PC, Larkin EC, Duong PL, Ramanujam S, Tablin F, et al. Microvascular abnormalities in sickle cell disease: a computer-assisted intravital microscopy study. Blood. 2002;99(11):3999-4005.

20 Waltz X, Hedreville M, Sinnapah Sp, Lamarre Y, Soter Vr, Lemonne N, et al. Delayed beneficial effect of acute exercise on red blood cell aggregate strength in patients with sickle cell anemia. Clinical hemorheology and microcirculation. 2012;52(1):15.

21 Arogundade FA, Sanusi AA, Hassan MO, Salawu L, Durosinmi MA, Akinsola A. An appraisal of kidney dysfunction and its risk factors in patients with sickle cell disease. Nephron Clinical Practice. 2011;118(3):c225-c31.

22 Ausavarungnirun P, Sabio H, Kim J, Tegeler CH. Dynamic vascular analysis shows a hyperemic flow pattern in sickle cell disease. Journal of Neuroimaging. 2006;16(4):311-7.

23 Gevers S, Nederveen AJ, Fijnvandraat K, van den Berg SM, van Ooij P, Heijtel DF, et al. Arterial spin labeling measurement of cerebral perfusion in children with sickle cell disease. Journal of Magnetic Resonance Imaging.

2012;35(4):779-87.
24 Oguz KK, Golay X, Pizzini FB, Freer CA, Winrow N, Ichord R, et al. Sickle Cell Disease: Continuous Arterial Spin-labeling Perfusion MR Imaging in Children 1. Radiology. 2003;227(2):567-74.
25 Ganekal S. Retinal functional imager (RFI): Non-invasive functional imaging of the retina. Nepalese Journal of Ophthalmology. 2013;5(2):250-7.
26 Landa G, Rosen RB. New patterns of retinal collateral circulation are exposed by a retinal functional imager (RFI). British Journal of Ophthalmology. 2010;94(1):54-8.
27 Tian J, Somfai GM, Campagnoli TR, Smiddy WE, Debuc DC. Interactive retinal blood flow analysis of the macular region. Microvascular research. 2016;104:1-10.
28 Burgansky-Eliash Z, Nelson DA, Bar-Tal OP, Lowenstein A, Grinvald A, Barak A. Reduced retinal blood flow velocity in diabetic retinopathy. Retina. 2010;30(5):765-73.
29 Jiang H, Delgado S, Tan J, Liu C, Rammohan KW, DeBuc DC, et al. Impaired retinal microcirculation in multiple sclerosis. Multiple sclerosis (Houndmills, Basingstoke, England). 2016;22(14):1812-20.
30 Beutelspacher SC, Serbecic N, Barash H, Burgansky-Eliash Z, Grinvald A, Krastel H, et al. Retinal blood flow velocity measured by retinal function imaging in retinitis pigmentosa. Graefe's archive for clinical and experimental ophthalmology. 2011;249(12):1855-8.
31 Barak A, Burgansky-Eliash Z, Barash H, Nelson DA, Grinvald A, Loewenstein A. The effect of intravitreal bevacizumab (Avastin) injection on retinal blood flow velocity in patients with choroidal neovascularization. European journal of ophthalmology. 2012;22(3):423.
32 Briers JD, Richards GJ, He X-W. Capillary blood flow monitoring using laser speckle contrast analysis (LASCA). Journal of biomedical optics. 1999;4(1):164-76.
33 Roustit M, Millet C, Blaise S, Dufournet B, Cracowski JL. Excellent reproducibility of laser speckle contrast imaging to assess skin microvascular reactivity. Microvascular research. 2010;80(3):505-11.
34 Millet C, Roustit M, Blaise S, Cracowski J. Comparison between laser speckle contrast imaging and laser Doppler imaging to assess skin blood flow in humans. Microvascular research. 2011;82(2):147-51.
35 Stewart C, Frank R, Forrester K, Tulip J, Lindsay R, Bray R. A comparison of two laser-based methods for determination of burn scar perfusion: laser Doppler versus laser speckle imaging. Burns. 2005;31(6):744-52.
36 Shi PA, Manwani D, Olowokure O, Nandi V. Serial assessment of laser Doppler flow during acute pain crises in sickle cell disease. Blood Cells, Molecules, and Diseases. 2014;53(4):277-82.
37 L'Esperance VS, Cox SE, Simpson D, Gill C, Makani J, Soka D, et al. Peripheral vascular response to inspiratory breath hold in paediatric homozygous sickle cell disease. Experimental physiology. 2013;98(1):49-56.
38 Vanzetta I, Deneux T, Grinvald A. High-Resolution Wide-Field Optical Imaging of Microvascular Characteristics: From the Neocortex to the Eye. Neurovascular Coupling Methods: Springer; 2014. p. 123-59.
39 Yamamoto-Suganuma R, Aso Y. Relationship between post-occlusive forearm skin reactive hyperaemia and vascular disease in patients with Type 2 diabetes-a novel index for detecting micro-and macrovascular dysfunction using laser Doppler flowmetry. Diabetic Medicine. 2009;26(1):83-8.
40 Krejza J, Mariak Z, Walecki J, Szydlik P, Lewko J, Ustymowicz A. Transcranial color Doppler sonography of basal cerebral arteries in 182 healthy subjects: age and sex variability and normal reference values for blood flow parameters. AJRAmerican journal of roentgenology. 1999;172(1):213-8.
41 Yuda K, Ishida A, Yuda K. Comparison of the retinal blood flow velocity between laser speckle flowgraphy and the retinal function imager. Retina. 2017;37(7):1393-9.
42 Minniti CP, Delaney KM, Gorbach AM, Xu D, Lee CC, Malik N, et al. Vasculopathy, inflammation, and blood flow in leg ulcers of patients with sickle cell anemia. American journal of hematology. 2014;89(1):1-6.
43 Mohan JS, Marshall JM, Reid HL, Thomas PW, Hambleton I, Serjeant GR. Comparison of responses evoked by mild indirect cooling and by sound in the forearm vasculature in patients with homozygous sickle cell disease and in normal subjects. Clinical Autonomic Research. 1998;8(1):25-30.
44 Connes P, Lamarre Y, Hardy-Dessources MD, Lemonne N, Waltz X, Mougenel Dl, et al. Decreased hematocrit-to-viscosity ratio and increased lactate dehydrogenase level in patients with sickle cell anemia and recurrent leg ulcers. 2013.
45 Vent-Schmidt J, Waltz X, Romana M, Hardy-Dessources MD, Lemonne N, Billaud M, et al. Blood thixotropy in patients with sickle cell anaemia: role of haematocrit and red blood cell rheological properties. PloS one. 2014;9(12):e114412.
46 Belhassen L, Pelle G, Sediame S-ê, Bachir D, Carville C, Bucherer C, et al. Endothelial dysfunction in patients with sickle cell disease is related to selective impairment of shear stress-mediated vasodilation. Blood. 2001;97(6):1584-9.
47 Gladwin MT, Schechter AN, Ognibene FP, Coles WA, Reiter CD, Schenke WH, et al. Divergent nitric oxide bioavailability in men and women with sickle cell disease. Circulation. 2003;107(2):271-8.
48 Shamim-Uzzaman QA, Pfenninger D, Kehrer C, Chakrabarti A, Kacirotti N, Rubenfire M, et al. Altered cutaneous microvascular responses to reactive hyperaemia in coronary artery disease: a comparative study with conduit vessel responses. Clinical Science. 2002;103(3):267-74.
49 Moriarty BJ, Acheson RW, Condon PI, Serjeant GR. Patterns of visual loss in untreated sickle cell retinopathy. Eye. 1988;2(Pt 3):330-5.
50 Clarkson JG. The ocular manifestations of sickle-cell disease: a prevalence and natural history study. Transactions of the American Ophthalmological Society. 1992;90:481.
51 Heringa SM, Bouvy WH, van den Berg E, Moll AC, Kappelle LJ, Biessels GJ. Associations between retinal microvascular changes and dementia, cognitive functioning, and brain imaging abnormalities: a systematic review. Journal of Cerebral Blood Flow & Metabolism. 2013;33(7):983-95.



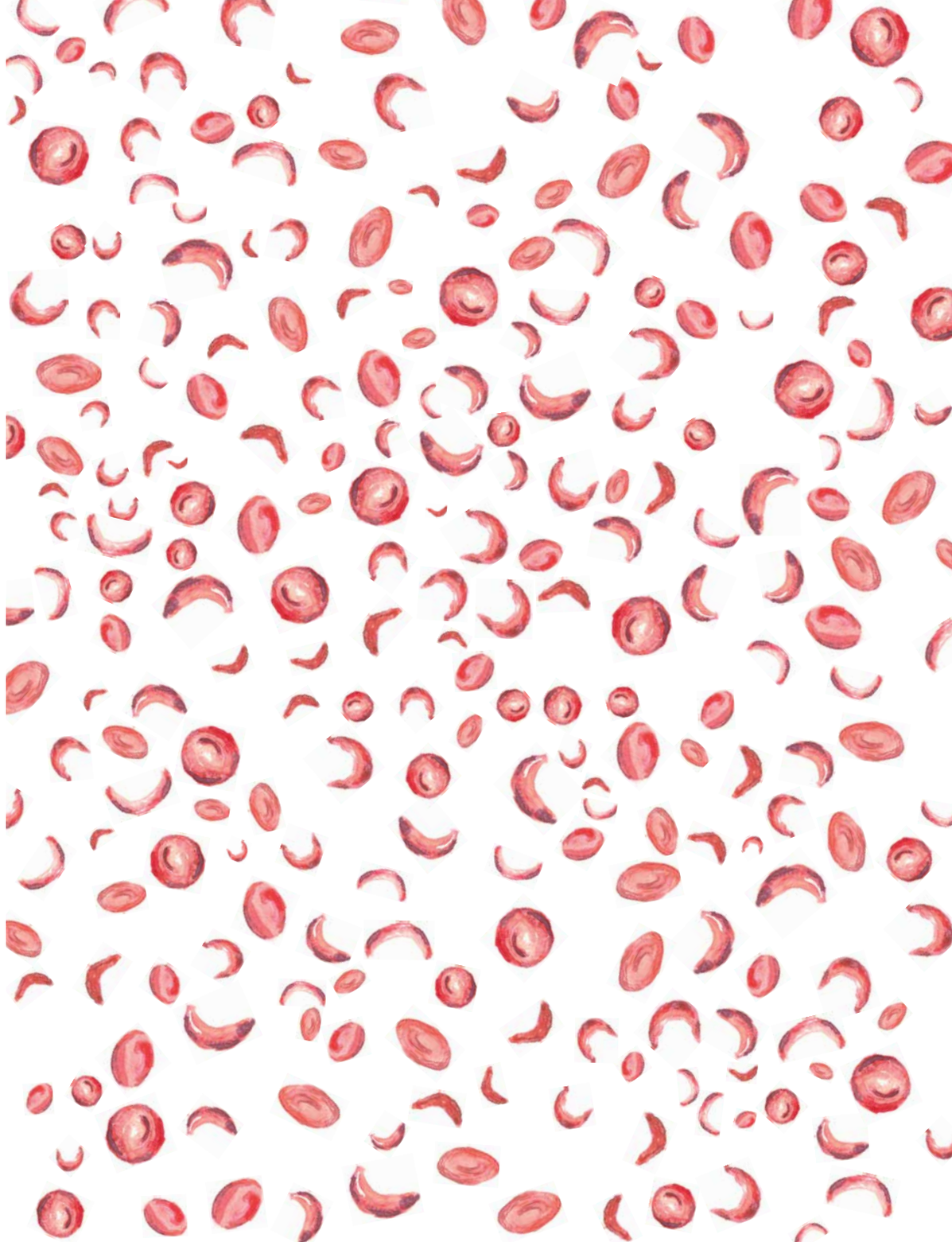

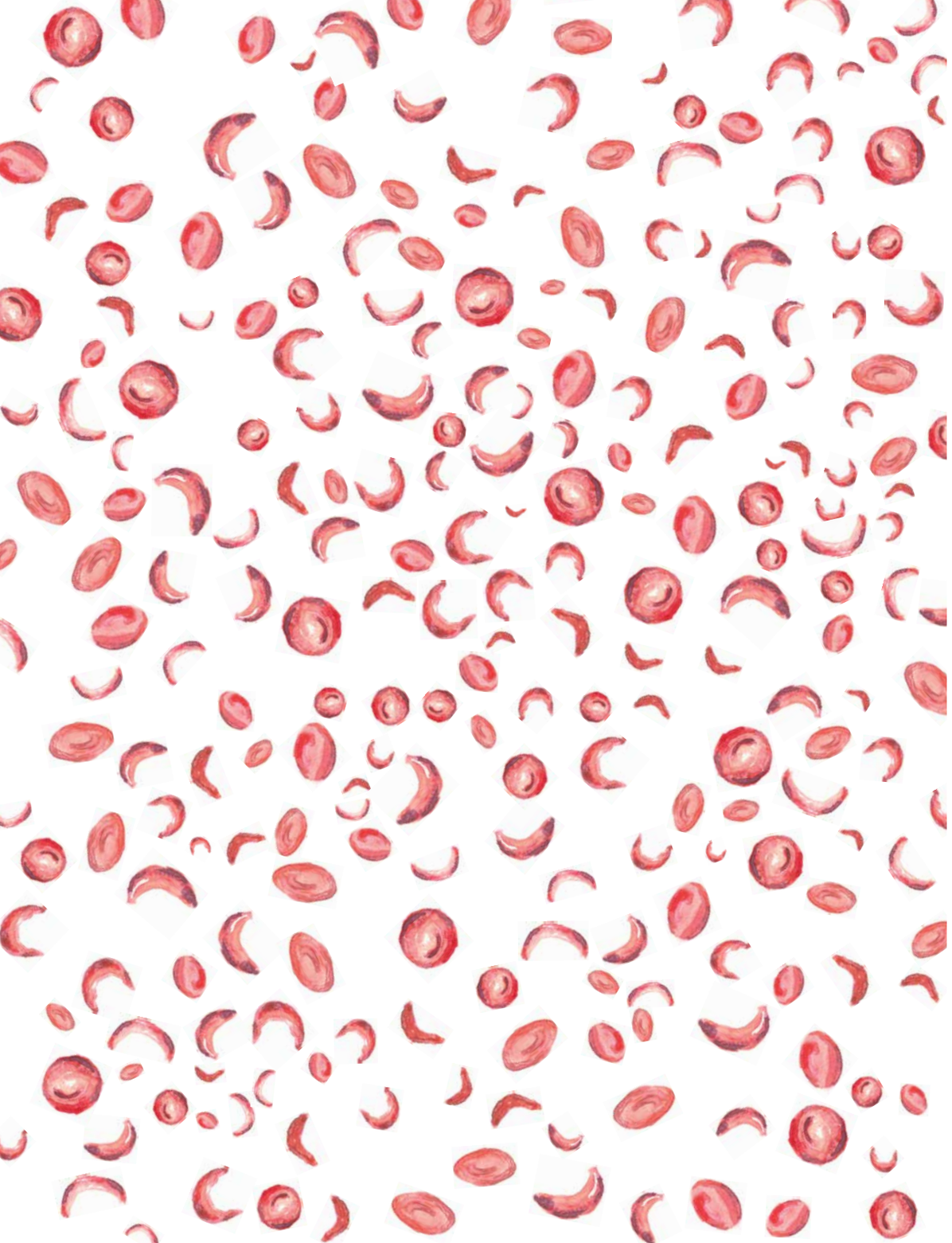

CHAPTER IV

# Skin blood flow functions as potential proxy for cerebral blood flow in adults with Sickle cell disease

*Brijesh Yadav[1,2], Nicolas Currier[3]*, Willem Birkhoff[4], Gersham Dent[3], Paul. S. Swerdlow[5], Sean Sethi6, Kiarash Ghassaban[6], Jacobus Burggraaf[4], Jaspert de Vries[4], Jaladhar Neelavalli[1],William E. Hobbs[7], E. Mark Haacke[1,2,5], Ajay Verma[3]*

*1. Department of Radiology, Wayne State University School of Medicine, Detroit, Michigan, USA / 2. Department of Biomedical Engineering, Wayne State University College of Engineering, Detroit, Michigan, USA / 3. Biogen Inc., Cambridge, Massachusetts, USA / 4. Centre for Human Drug Research, Netherlands / 5. Department of Hematology-Oncology, Wayne State University School of Medicine, Detroit, Michigan, USA / 6. MR Innovations, Detroit, Michigan, USA; 7Bioverativ Inc., Cambridge, Massachusetts, USA*

**Stroke is one of the major causes of morbidity and mortality in patients with Sickle cell disease (SCD). It is caused by vaso-occlusion of major arteries feeding the brain, and experience with life-saving temporal artery ultrasonography in children emphasizes the necessity of knowing the cerebral blood flow (CBF) to assess stroke risk. Less information is available around the CBF in adults with SCD and most of our knowledge is limited to expensive and time consuming magnetic resonance imaging (MRI) analysis. However, based on the pediatric experience it is suspected that it may be highly desirable to ascertain biomarkers of the CBF in adults with SCD. Therefore, in this study, we investigated CBF in adults with SCD using 2 MRI techniques: arterial spin labeling and phase contrast. Additionally we measured skin blood flow using Laser speckle contrast imaging (LSCI) and assessed it as surrogate biomarker of CBF. We enrolled SCD patients (n=17) not undergoing blood transfusion and healthy controls (n=6) in this study. Reliability of blood flow measurements was also studied through test, re-test. In conclusion, we found elevated skin and cerebral blood flow velocity in the adult SCD population compared to matched healthy controls and all measured values exhibited significant longitudinal stability across visits. Furthermore, excellent correlation was found between CBF and skin blood flow in the SCD cohort suggesting skin blood flow measurement using LSCI may be a potential proxy to MRI in routine hemodynamic evaluation in this population.**

**Sickle cell disease (SCD) is a genetic disorder caused by a point mutation in the β-globin gene of hemoglobin, forming a mutant form known as hemoglobin S.** Under deoxygenated conditions, hemoglobin S is abnormally susceptible to polymerization, distorting red blood cells (RBCs) into 'sickled' RBCs (SS-RBCs) and changing their adhesive, rheological, and oxidative properties. SS-RBCs are capable of promoting the formation of heterocellular aggregates that alter blood flow and interrupt normal tissue perfusion. In addition, SCD is associated with aberrant vasomotor responses including impaired vasodilation and vasoconstriction.[1]

Continuous tissue perfusion is crucial for vitality of most organs. Obstructed or inadequate blood flow can lead to ischemic tissue injury, followed by reperfusion injury upon flow restoration. Ischemia and reperfusion injury are major causes of morbidity and mortality in the SCD population. Acute vascular obstruction results clinically in severe painful episodes known as vaso-occlusive crises (VOCs), which often require hospitalization and are a hallmark of SCD. The heterogeneous clinical manifestations of SCD, which in addition to VOC include chronic hemolytic anemia, stroke, and multi-organ dysfunction, likely reflect altered tissue perfusion patterns caused by abnormal SS-RBC associated rheology.[2–5]

Under stable physiological conditions, most tissues can autoregulate and maintain appropriate blood flow to adequately support tissue perfusion needs. Due to chronic anemia, the cardiac output is significantly elevated, resulting in increased perfusion to certain organs (i.e., brain, kidney, and muscle).[6] Hyper-perfusion is also likely to represent compensatory reactive responses to the slower blood flow rates in occluded microvessels, with increased blood volume diverted around occlusions necessitating increased blood flow through 'detour' vessels. Further effects on blood flow in SCD result from impaired vasomotor responses: flow velocity can increase as a function of abnormally narrowed vessels (as from abnormal vasoconstriction) or if increased flow volume exceeds autoregulatory relaxation (as from impaired vasodilation).

SCD impacts the cerebral hemodynamics and therefore, characterized by high cerebral blood flow (CBF). The brain is particularly susceptible to end organ damage (stroke, silent infarcts) in SCD. Due to the reduction in hematocrit and increase in blood viscosity, adaptive vasodilation tries to maintain the cerebral oxygen supply by increasing the CBF and correspondingly the CBV in SCD.[7] When all the available vessels and collaterals reach their maximal compensatory/vasodilation state, the risk of cerebral stroke is significantly elevated. Most of our knowledge to identify the risk of stroke in SCD patients comes from pediatric population. The prevalence of stroke in adults with SCD is higher compared to children.[8] However, no accepted screening measures are present for identifying adults with SCD at high risk for strokes.[9] Therefore, a robust and accurate assessment of CBF in adults with SCD is highly needed.

Magnetic resonance imaging (MRI) is the optimal imaging modality to assess the cerebral hemodynamics due to high soft-tissue contrast, high resolution, no use of ionizing radiations and less operator dependence. MRI techniques namely, arterial spin labeling (ASL) and phase-contrast MRI (PC-MRI), are commonly used to measure CBF. These techniques have been applied previously in adults and children with SCD and showed an elevated level of CBF in the SCD population compared to controls.[9–12]

In line with the increased CBF, the microvascular blood flow in the skin was also found higher in the SCD patients compared to healthy group.[13–15] Vasodilation of micro-vessels as a result of sickling of the RBCs or impaired endothelial layer, might

**FIGURE 1 Schematic study design followed in the work is shown. Following the screening, eligible subjects underwent two imagingvisits which over the course of 10 days. Individuals were followed-up on phone within a week window.**

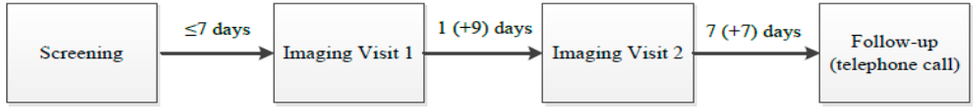






be the reason of elevated blood flow in the skin in SCD. While MRI is suitable for estimating CBF, Laser speckle contrast imaging (LSCI) offers the possibility to measure the entire physiologic range of blood flow velocities in real time at microvascular level to a depth of approximately 300 μm. These measurements reflect blood flow in capillaries, arterioles, venoles and dermal vascular plexuses.[16] Recent LSCI studies have successfully demonstrated the elevated baseline level of blood flow in the skin of adults with SCD compared to healthy individuals.[13–15]

Despite of being an optimal imaging technique, high scan cost of MRI makes it uneconomical for the screening of high risk SCD patients for stroke. Therefore, we explore the possibility of using LSCI as an economical alternative and to examine the skin blood flow as a peripheral surrogate biomarker of the CBF. In this study, we measure blood flow in the skin and brain of adults with SCD and healthy subjects. For each subject and each technique, the test-retest variability in blood flow was also assessed in the brain and skin.

## MATERIALS AND METHODS

### Study Design

This was a single-center, non-randomized study of subjects with SCD and healthy subjects. A written informed consent was obtained from each subject prior to any measurement was performed Following a screening visit, patients underwent two imaging visits over the course of 10 days, to establish test-retest reliability. Imaging visit 2 was followed by a telephone follow-up over a week period (*Figure 1*). No drug treatment was administered as part of this study.

### Study Population

Clinical hematology and blood chemistry laboratory samples were collected at Screening in SCD patients (n=17) and healthy controls (n=7). Diagnosis of SCD (homozygous for HbS or heterozygous for HbS and β0 thalassemia [HbS-β0]) was confirmed by hemoglobin analysis. SCD patients who had a history of clinical strokes or of other major illness such as diabetes mellitus, renal dysfunction were excluded. Also SCD patients who had an acute pain crisis requiring hospitalization, within ≤4 weeks prior to the first imaging or recent (≤3 months) treatment with hydroxyurea, were excluded.

### Imaging

#### *Magnetic resonance imaging*

All MRI scans were performed at 3.0 Tesla (T) Siemens Verio (Erlangen, Germany) and a 32-channel head coil was used for acquiring brain and neck images. CBF was estimated using ASL and PC-MRI. No contrast was administered in the scanning.

#### *Arterial spin labeling*

Images are acquired with and without labeling and their difference provides the perfusion maps. A pseudo-continuous arterial spin labeling (PCASL) sequence was used to analyze the direct perfusion. A reference series along with thirty measurements from both control and tagged ASL images were acquired separately in order to increase the signal-to-noise (SNR) and make the averaging more efficient. The imaging parameters used are as follows: repetition time (TR) = 3500 ms, echo time (TE) = 22.76 ms, flip angle (FA) =180°, turbo spin-echo (TSE) factor = 17, echo-planar imaging (EPI) factor = 31, pixel bandwidth (BW) = 2003 Hz/pixel, in-plane resolution = 3.5 x 3.5 $mm^2$, slice thickness (TH) = 3.5 mm and 32 slices per measurement were acquired. Total scan duration was about 4 mins. The CBF maps of individual subjects were generated using the technique from Wang et al., [17] in the units of ml/100g/min. With the purpose of extracting the average CBF information, a region-of-interest (ROI) encompassing the whole brain was manually drawn on each slice of the CBF maps. The mean CBF map for individual subjects was then calculated by taking the average of all the voxels within the ROI and all the slices. Finally, the mean CBF and associated standard error across all the subjects was estimated.

#### *Phase-contrast MRI*

PC-MRI estimates the blood flow using the phase shift property of the moving water molecules in the blood to encode the blood flow information. PC-MRI sequence was run with the slice positioned perpendicular to the major vessels at two neck levels: C2-C3 and C5-C6. The data were collected with the following parameters: TE=5.17 ms, TR=66.85 ms, FA = 20°, FOV= 256×256, Matrix size= 448×448, TH=

2.5 mm, velocity encoding (VENC) = 100 cm/sec. All the data was reviewed for quality and any cases that had artifacts or inadequate SNR were removed from the analysis.

Using the tissue similarity mapping algorithm[18] (SPIN, Magnetic Resonance Innovations, Inc, Detroit, MI) the target vessels were demarcated. Two experienced image analysts reviewed the vessel segmentation and adjusted manually if necessary. SPIN software was used for quantifying blood flow rate (ml/sec) from differences in phase-contrast over time through major arteries and veins, including internal carotid arteries (ICA) and vertebral arteries (VA) for in-flow and the internal jugular veins (IJV) for outflow. A robust automatic unwrapping algorithm was implemented where phase aliasing in the vessels occurred due to rapid arterial flow in SCD patients.[18] Non-flow regions were drawn on static tissue to compensate for any phase shifts. Individual vessel flow, as well as bilateral total flow, venous total flow (sum of IJVs) and arterial total flow was calculated (CCA+VA for C5/C6 neck level, and ICA+VA for C2/C3 neck level). C2/C3 arterial total (CBF) was used for PC-MR perfusion calculations.

*Laser speckle contrast imaging*

Following MRI participants underwent LSCI measurements in a temperature- and light-controlled room. LSCI measurements were performed as previously described,[13] using Pericam PSI (Perimed, PSI-NR). Briefly an area of 3×10 cm² of the ventral forearm was chosen as measurement site. Following 5 mins of baseline perfusion recording, brachial artery blood flow was occluded for 3-5 minutes after occlusion, the reperfusion peak and the return of baseline was recorded for another 5 minutes. LSCI endpoints included basal flow (arbitrary units (AU)), peak flow after occlusion (AU), time to return to basal flow (seconds) (see *Figure 4*) Obtained data were analyzed using PIMSOFT software (Perimed, Järfälla, Sweden).

*Statistical analysis*

The mean and standard deviation of the CBF and the skin blood flow measurements were calculated. The intraclass correlation coefficient (ICC) were estimated for assessing test-retest reliability. A linear regression analysis was used to investigate the correlation between CBF and skin blood flow measured using MRI and LSCI, respectively.

**TABLE 1 Demographic information and basic laboratory report of the healthy subjects and SCD patients are presented.**

| | Healthy Subjects | SCD Patients |
|---|---|---|
| DEMOGRAPHY | | |
| N | 6 | 17 |
| Age (years) | 27 (± 5) | 34.4 (± 8.7) |
| Height (cm) | 175.1 (± 8.5) | 168.8 (± 10.2) |
| Weight (Kg) | 78.9 (± 26.8) | 74.2 (± 19.3) |
| Male (%) | 67 | 47 |
| VITAL SIGNS | | |
| Systolic blood pressure (mmHg) | 115.2 (± 10.5) | 114.9 (± 12.7) |
| Diastolic blood pressure (mmHg) | 71.7 (± 9.6) | 69.4 (± 8) |
| Pulse (beats/min) | 75.3 (± 7.1) | 83.8 (± 17.3) |

## RESULTS

### Patient information

A total of 17 adults with SCD and 6 healthy subjects completed the study. Demographics and ethnicity of healthy subjects and SCD patients were similar. Demographics, vital signs and lab measurements are presented in *Table 1*.

#### CBF

CBF maps from ASL and PC-MRI images are shown in *Figure 2* and *Figure 3*, respectively. The average CBF measured from ASL was 77.4 21.9) ml/100g/min in SCD population and 48.0 5.3) ml/100g/min in healthy subjects (P = 0.0042). The mean CBF measured using PC-MRI was 68.4 19.9) ml/100g/min (in the SCD population and 43.9 4.3) ml/100g/min in controls (P = 0.0077). The mean CBF was significantly higher in the aduls with SCD compared to the healthy individuals (ASL: *Figure 5*; PC-MRI: *Figure 6*). The test-retest reliability of ASL and PC-MRI measurements of the average CBF showed moderate to high agreement in subjects with SCD (ASL: ICC = 0.66; PC-MRI: ICC = 0.72) and in healthy subjects (ASL: ICC = 0.84; PC-MRI: ICC = 0.75).

### Microvascular skin blood flow

Baseline microvascular blood flow measured by LSCI was significant higher in patients with SCD compared to healthy controls (40.2 7.5) vs. 24.2 4.6) (AU)) (P = 0.0001 ) (*Figure 7*). However, no differences were observed in peak blood flow, time to peak and in time to return to baseline (see *Table 2*).





**FIGURE 2 ASL based perfusion mean CBF maps are shown in A) a 28-year-old healthy control with an average CBF of 57.15 ml/100gin and B) a 44-year-old SCD patient with an average CBF of 116.36 ml/100g/min. The blue line represents the ROIs on six slices from different brain regions.**

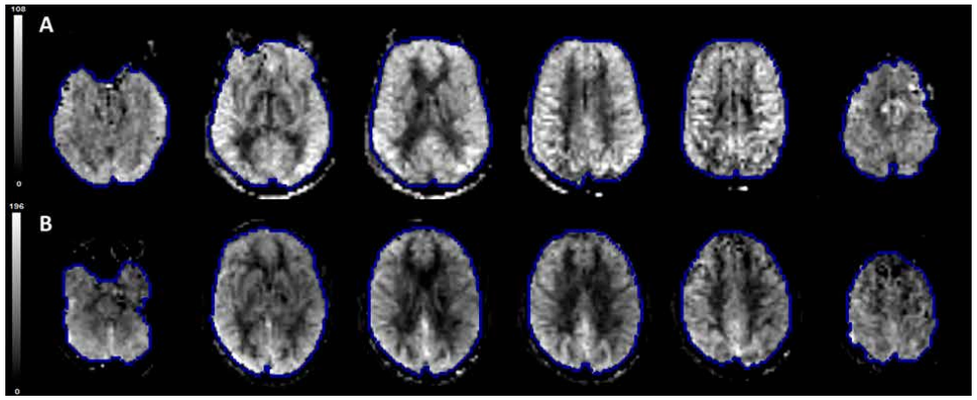


### Correlation between cerebral and skin blood flow

A strong correlation was found between the CBF quantified using ASL or PC-MRI and the baseline blood flow in the skin as measured using LSCI in the population including healthy volunteers and subjects with SCD (ASL vs. LSCI: r = 0.70; PC-MRI vs. LSCI: r = 0.75) (*Figure 8* and *Figure 9*).

## DISCUSSION

In this study, we measured CBF and skin blood flow in SCD patients and healthy subjects. In agreement with previous studies, MRI and LSCI measurements of brain and skin blood flow, were higher in SCD patients compared to healthy controls.[9–15] Furthermore CBF measurements showed a high correlation with LSCI measurements.

The increase in blood flow is attributed to the vasodilation of the major vessels and microvascular beds to compensate the oxygen demand of the brain and skin. While high CBF is a well-described phenomenon in children with SCD, less data is available for adults. Elevated CBF in adults with SCD may be a key consideration for stroke risk, as seen in children.[19] Very few studies have been performed with test-retest assessments with ASL and PC-MRI in SCD. Our test-retest reliability showed moderate to high agreement. In addition, ASL and PC-MRI showed no significant difference in the CBF measurements, indicating the comparability of these two MRI techniques for measuring CBF.

Differences in baseline skin blood flow between SCD patients and healthy controls, were in agreement with recent literature.[13] The baseline blood flow in the skin as measured using LSCI was found to be a strong predictor of the average CBF in both SCD patients and controls. Furthermore this correlation was highly reproducible. We hypothesize that the change in rheological properties of RBCs and increasing viscosity might affect the hemodynamic properties of the CNS and peripheral system proportionally, which is captured in the

**TABLE 2 LSCI measurements-, for healthy individuals and SCD adult patients with means and SD.**

| | Healthy Subject | SCD Patients | |
|---|---|---|---|
| N | 6 | 17 | |
| Baseline flow (AU) | 24.2 (±4.58) | 40.2 (±7.48) | P = 0.0001 |
| Peak flow (AU) | 76.7 (±13.06) | 80.5 (±14.15) | P = 0.5709 |
| Time to peak (sec) | 5.8 (±3.7) | 13.1 (±9.9) | P = 0.0962 |
| Time to return to baseline (sec) | 97.7 (±44.7) | 132.9 (±33.4) | P = 0.054 |

strong and reproducible correlation between CBF and skin blood flow in SCD patients. Furthermore a high blood flow is also observed in the central retinal vessels which share the same vascular anatomical origin as the CNS vasculature.[13] LSCI might be an inexpensive way to indirectly assess critical hemodynamic changes in the brain. With additional independent validation LSCI may be able to spare SCD subjects from undergoing costly and time intensive MRI scans. Finally, based on these and other available data, MRI and LSCI measurements could be implemented as exploratory endpoints in future sickle cell intervention trials.

There are some limitations of this study. The ASL images are known to be affected by susceptibility and motion artifacts and generally have low SNR, low spatial and temporal resolution.[20] In order to reduce the effect of low SNR, a voxel-wise averaging of 30 individual measurements was implemented using tagged and control ASL data. The CBF measurements using PC-MRI contains error mostly due to partial voluming and noise. Error in the vessel demarcation is controlled largely by the robustness of the segmentation algorithm used. Therefore, manual segmentation of the vessel has been shown to be reliable, particularly where vessels are having faster flow and larger diameters.[21] In addition, VENC value also affects the flow measurements. In this study, we used a larger VENC value of 100 cm/sec, which may have lower overall SNR compared to a lower VENC and might be introducing higher errors in slow venous flow. This was a trade-off in order to mitigate phase aliasing effects and preserve the quality of the rapid arterial flow which is present in SCD.

LSCI is highly sensitive to motion, which was overcome by averaging the measurements over a longer period of time.[22] Although, we found a strong correlation between the CSF and skin blood flow, our sample size is small in this study. Further validation of these findings with larger groups is therefore needed.

In conclusion, this study showed that CNS macrovascular blood flow measured by ASL and PC-MRI was elevated in SCD patients compared to controls. Additionally, microvascular skin blood flow, measured using LSCI, was also elevated and could potentially be used as surrogate biomarker for blood flow measurements in the brain. This could potentially provide an affordable solution to screen critical CNS hemodynamics and possible stroke risk in adult sickle cell patients and will open new avenues to find more sensitive biomarkers in this disease.

**FIGURE 3** **PC-MRI based flow estimation is shown. Major vessels are demarcated at C2/C3 neck level in magnitude (left) and complex-divided phase image (right).**
*R: right, L: left, IJV: internal jugular vein, ICA: internal carotid artery, VA: vertebral artery.*

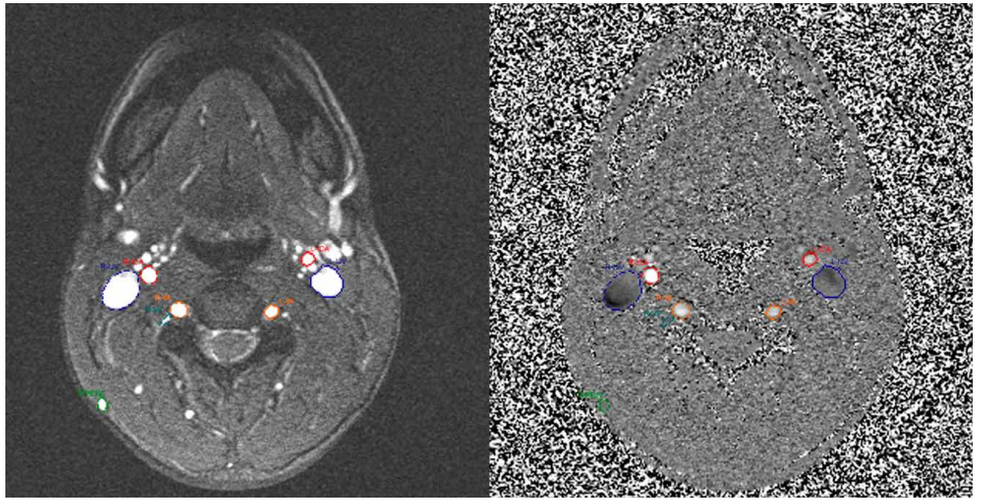





**FIGURE 4** **Graphical rendering of LSCI blood flux measurements and the different parameters included in this research. The flux measurements were measured in AU and the time measurements in seconds.**

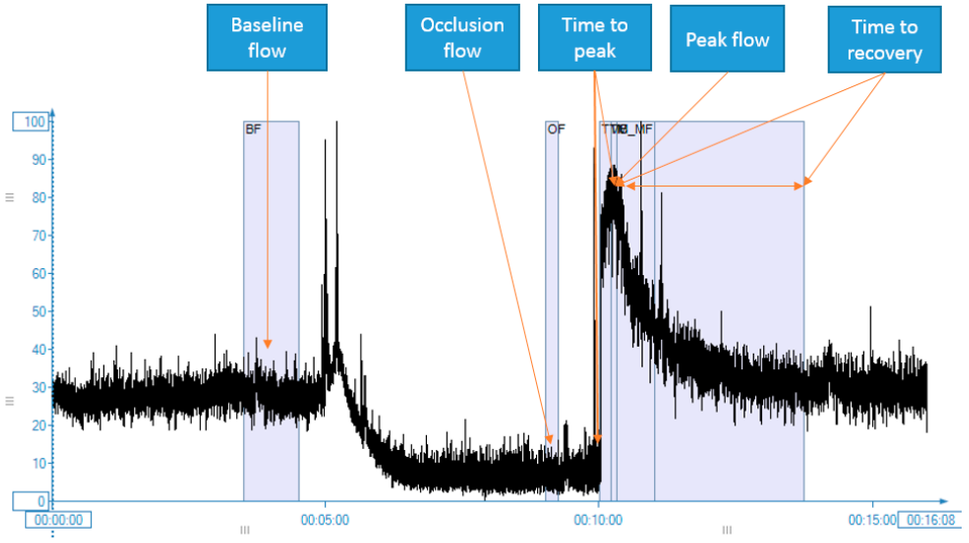


**FIGURE 5** **Cerebral blood flow measured using ASL-MRI was found to be significantly higher in the sickle cell patients compared to the healthy group. The test-retest showed high reliability.**

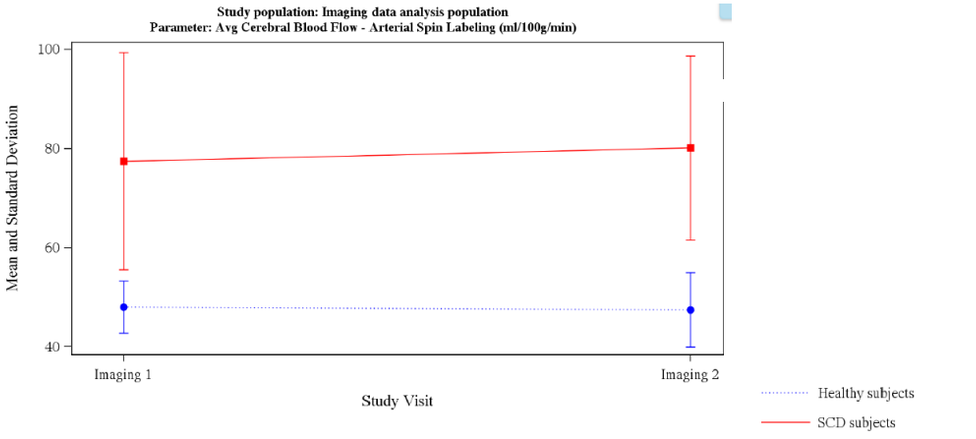

**FIGURE 6** Cerebral blood flow measured using PC-MRI was found to be significantly higher in the sickle cell patients compared to the healthy group. The test-retest was also reliable in both the groups.

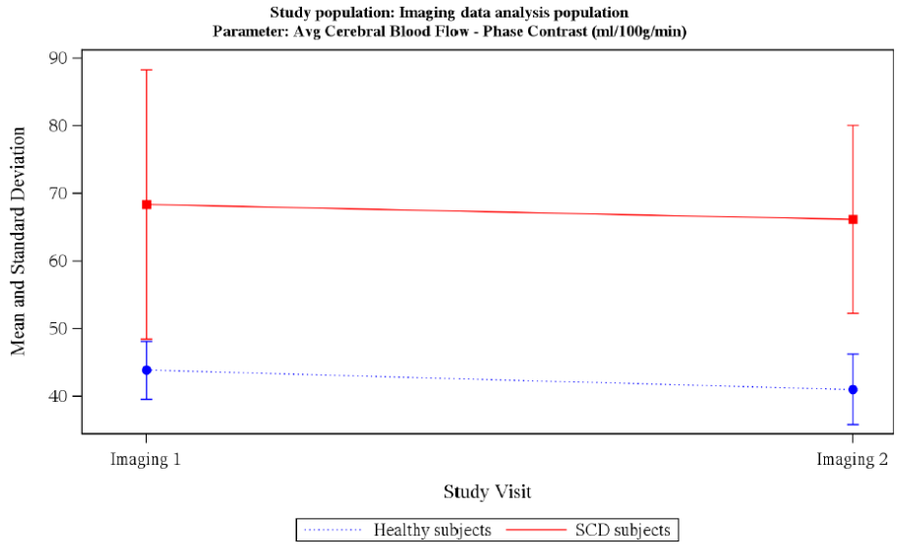


**FIGURE 7** The baseline skin blood flow measured using LSCI was found to be significantly higher in the sickle cell patients compared to the healthy group. Higher test retest reliability was found in both the groups.

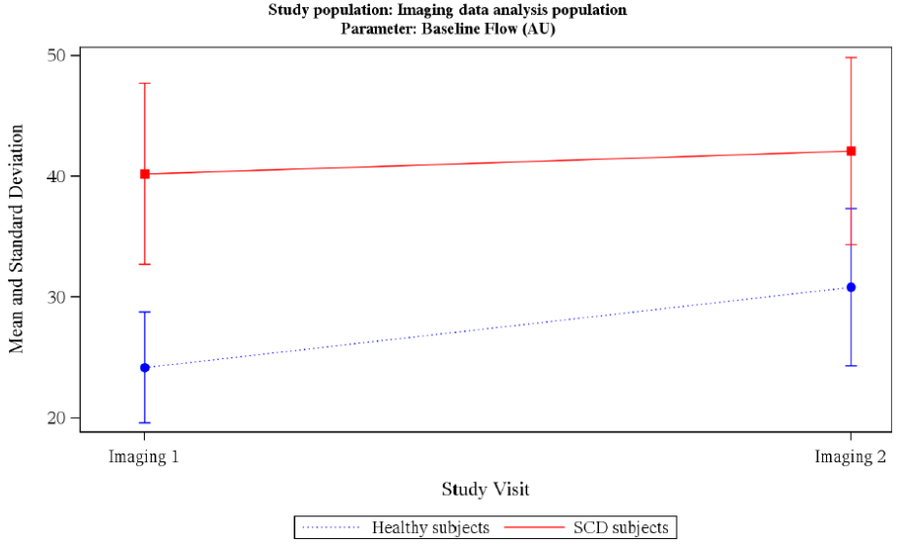






**FIGURE 8** Correlation between average CBF using ASL-MRI and baseline flow using LSCI was shown in healthy and sickle cell patients for in imaging visits. A significant correlation was observed in the measurements of two imaging modalities and it remained consistent in the test-retest.

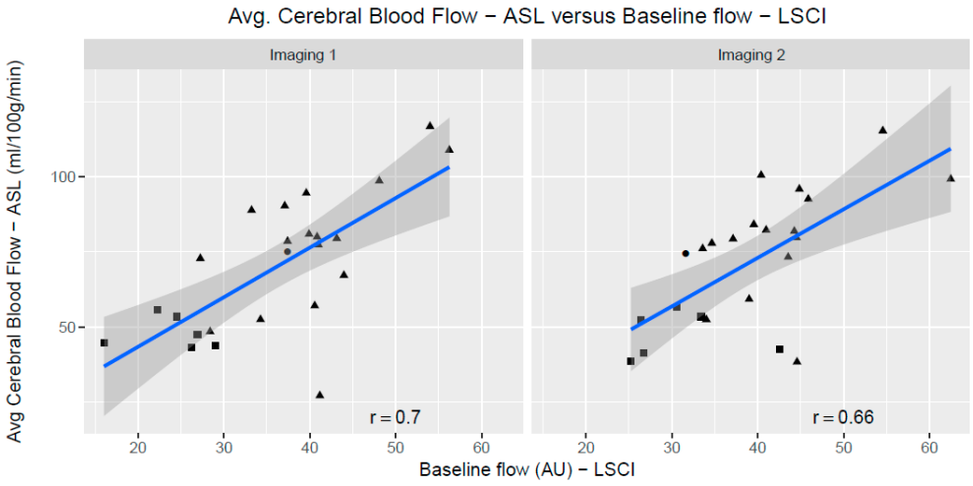


**FIGURE 9** Correlation between average CBF using PC-MRI and baseline flow using LSCI was shown in healthy and sickle cell patients for in imaging visits. A significant correlation was observed in the measurements of two imaging modalities which was consistent in both visits.

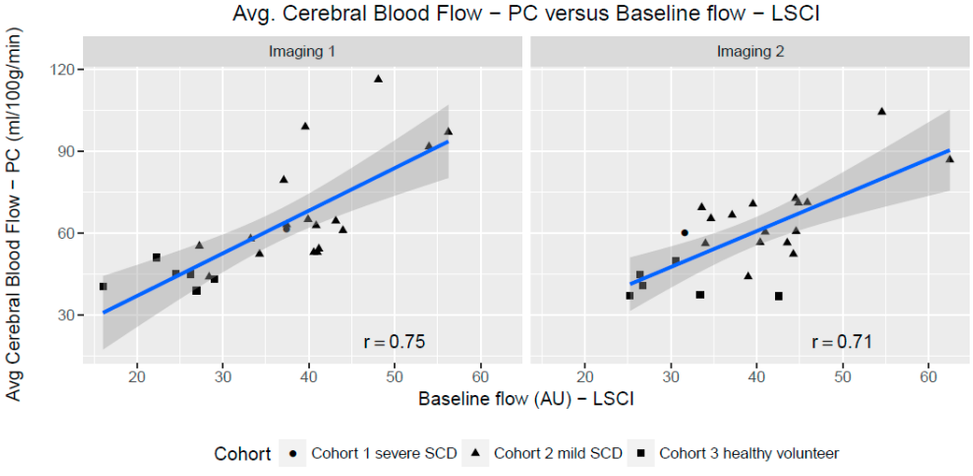

## *REFERENCES*


1 Wood, K.C., L.L. Hsu, and M.T. Gladwin, Sickle cell disease vasculopathy: a state of nitric oxide resistance. Free Radical Biology and Medicine, 2008. 44(8): p. 1506-1528.

2 Alexy, T., et al., Sickle cell disease: selected aspects of pathophysiology. Clinical hemorheology and microcirculation, 2010. 44(3): p. 155-166.

3 Ballas, S.K. and N. Mohandas, Pathophysiology of vaso-occlusion. Hematology/oncology clinics of North America, 1996. 10(6): p. 1221-1239.

4 Hebbel, R.P., G.M. Vercellotti, and K.A. Nath, A systems biology consideration of the vasculopathy of sickle cell anemia: the need for multi-modality chemo-prophylaxis. Cardiovascular & Haematological Disorders-Drug Targets (Formerly Current Drug Targets-Cardiovascular & Hematological Disorders), 2009. 9(4): p. 271-292.

5 Steinberg, M.H., Sickle cell anemia, the first molecular disease: overview of molecular etiology, pathophysiology, and therapeutic approaches. The Scientific World Journal, 2008. 8: p. 1295-1324.

6 Nath, K.A., Z.S. Katusic, and M.T. Gladwin, The perfusion paradox and vascular instability in sickle cell disease. Microcirculation, 2004. 11(2): p. 179-193.

7 Francis, R.J. and C. Johnson, Vascular occlusion in sickle cell disease: current concepts and unanswered questions. Blood, 1991. 77(7): p. 1405-1414.

8 Jordan, L.C. and M.R. DeBaun, Cerebral hemodynamic assessment and neuroimaging across the lifespan in sickle cell disease. Journal of Cerebral Blood Flow & Metabolism, 2017: p. 0271678X17701763.

9 Jordan, L.C., et al., Non-invasive imaging of oxygen extraction fraction in adults with sickle cell anaemia. Brain, 2016. 139(3): p. 738-750.

10 Gevers, S., et al., Arterial spin labeling measurement of cerebral perfusion in children with sickle cell disease. Journal of Magnetic Resonance Imaging, 2012. 35(4): p. 779-787.

11 Helton, K.J., et al., Arterial spin-labeled perfusion combined with segmentation techniques to evaluate cerebral blood flow in white and gray matter of children with sickle cell anemia. Pediatric blood & cancer, 2009. 52(1): p. 85-91.

12 Pegelow, C.H., et al., Longitudinal changes in brain magnetic resonance imaging findings in children with sickle cell disease. Blood, 2002. 99(8): p. 3014-3018.

13 Birkhoff, W., et al., Retinal microcirculation imaging in sickle cell disease patients. Microvasc Res, 2018. 116: p. 1-5.

14 Currier, N.V., et al., Skin Blood Flow Measured By LSCI Demonstrates Treatment Effect of Chronic Transfusion Protocol in Sickle Cell Disease. 2016, Am Soc Hematology.

15 Ikeda, A.K., et al., Laser Speckle Contrast Imaging Characterizes Delayed Reperfusion After Transient Brachial Artery Occlusion in Patients with Sickle Cell Diseas. 2012, Am Soc Hematology.

16 Minniti, C.P., et al., Vasculopathy, inflammation, and blood flow in leg ulcers of patients with sickle cell anemia. American journal of hematology, 2014. 89(1): p. 1-6.

17 Alsop, D.C., et al., Recommended implementation of arterial spin-labeled perfusion MRI for clinical applications: A consensus of the ISMRM perfusion study group and the European consortium for ASL in dementia. Magnetic resonance in medicine, 2015. 73(1): p. 102-116.

18 Jiang, J., et al., Quantifying errors in flow measurement using phase contrast magnetic resonance imaging: comparison of several boundary detection methods. Magnetic resonance imaging, 2015. 33(2): p. 185-193.

19 Adams, R., et al., The use of transcranial ultrasonography to predict stroke in sickle cell disease. New England Journal of Medicine, 1992. 326(9): p. 605-610.

20 Borogovac, A. and I. ASLIani, Arterial spin labeling (ASL) fMRI: advantages, theoretical constrains and experimental challenges in neurosciences. International journal of biomedical imaging, 2012. 2012.

21 Sethi, S.K., et al., Jugular venous flow abnormalities in multiple sclerosis patients compared to normal controls. Journal of Neuroimaging, 2015. 25(4): p. 600-607.

22 Rousseau, P., et al., Increasing the 'region of interest' and 'time of interest', both reduce the variability of blood flow measurements using laser speckle contrast imaging. Microvascular research, 2011. 82(1): p. 88-91.




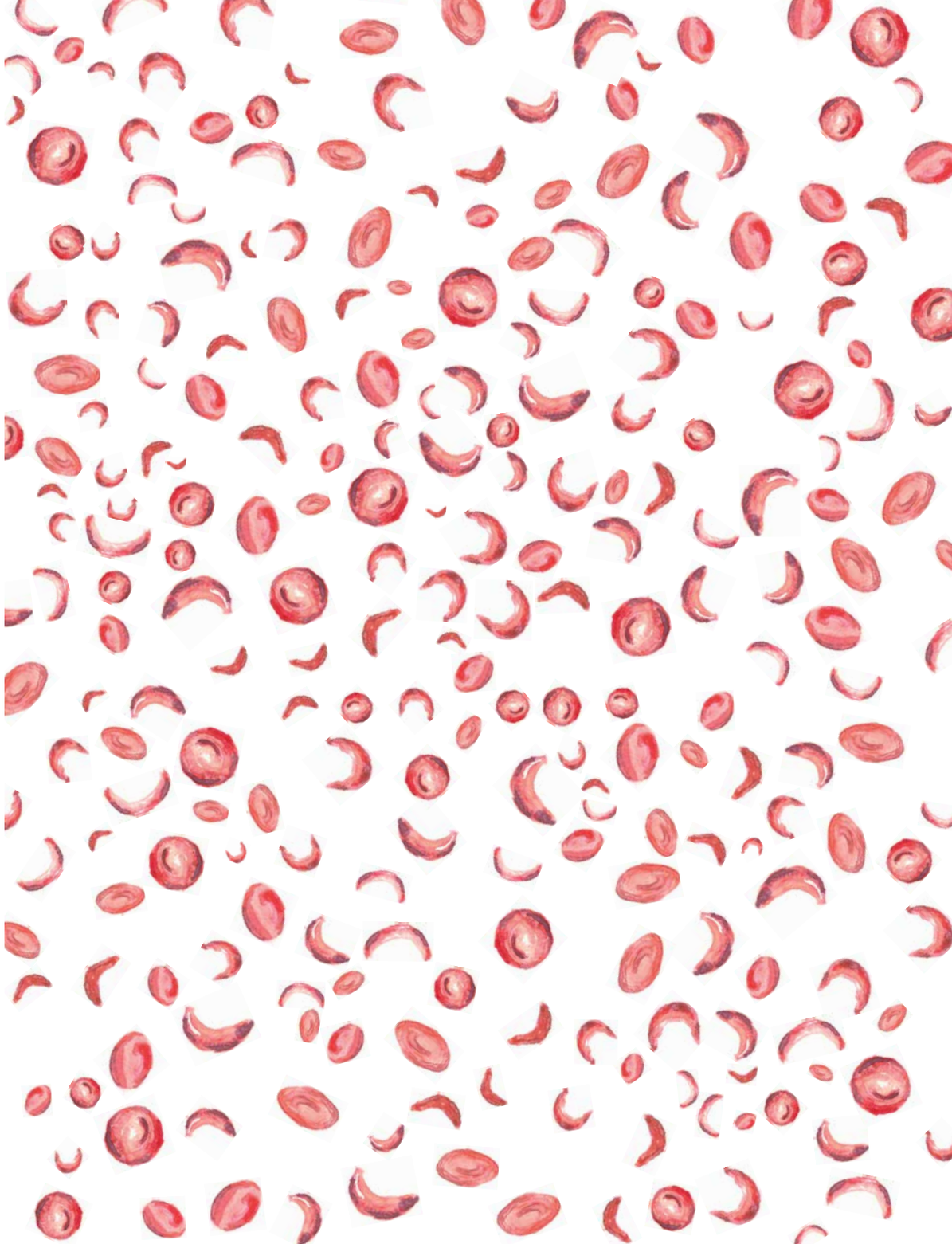

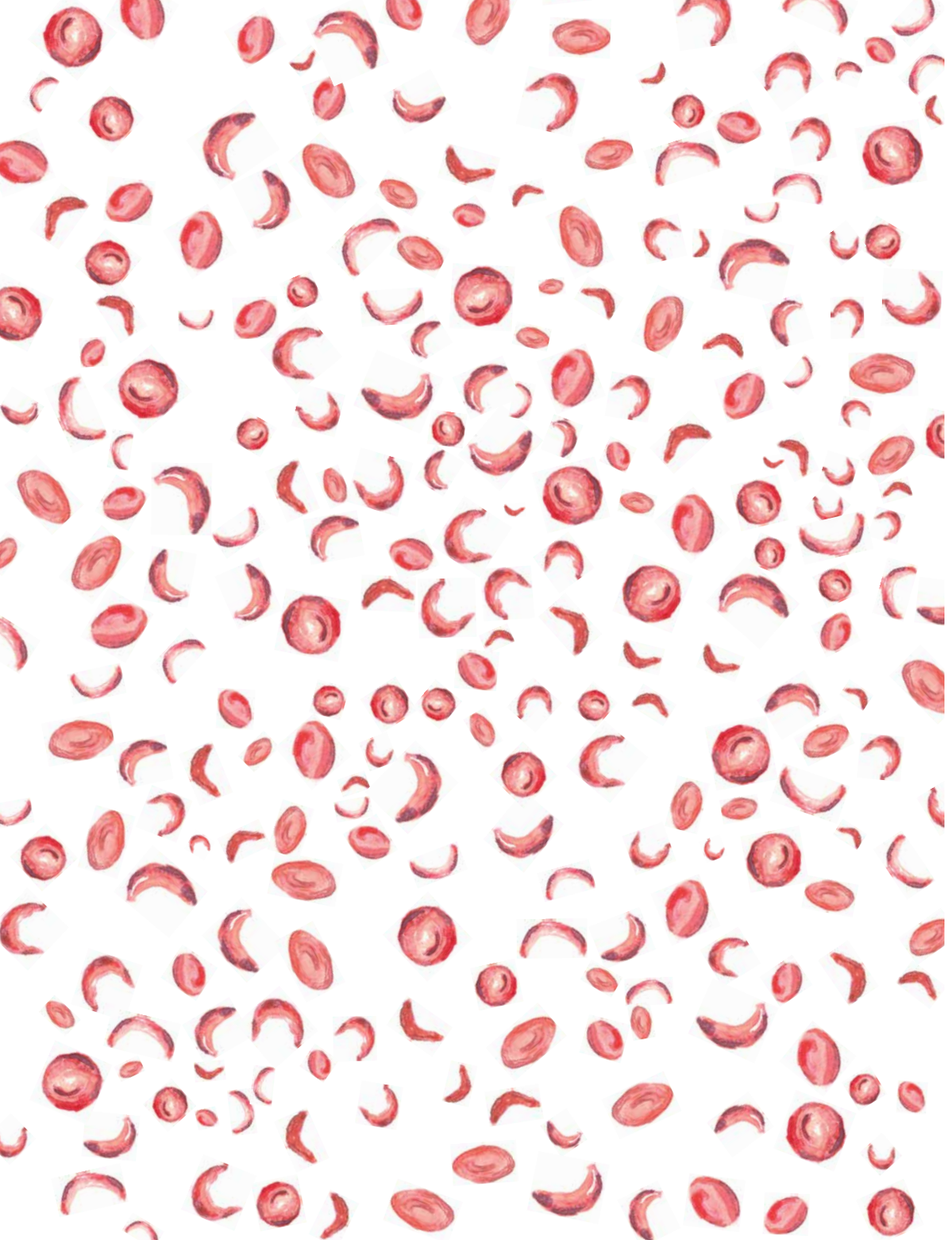

CHAPTER V

# Retinal oximetry and fractal analysis of capillary maps in sickle cell disease patients and matched healthy volunteers

*W.A.J. Birkhoff,[1,2,3*] L. van Manen,[2*] J. Dijkstr,[1,2] M.L. De Kam,[1] J.C. van Meurs,[3,4] A.F. Cohen[1,2]*

*1. Centre for Human Drug Research, Leiden, the Netherlands /2. Leiden University Medical Center, Leiden, the Netherlands / 3. Oogziekenhuis Rotterdam, Rotterdam, the Netherlands / 4. ErasmusMC, Rotterdam, the Netherlands / *WB and LVM contributed equally to this work*

**PURPOSE: Fractal analysis can be used to quantitatively analyze the retinal microvasculature and might be a suitable method to quantify retinal capillary changes in Sickle Cell Disease (SCD) patients. Retinal oximetry measurements might function as a proxy for the pathophysiology of cerebrovascular diseases. Moreover hypoxia has an important role in the pathophysiology of diabetic and other retinopathies. However little is known about the oximetry around the macula in SCD patients. With this study we explored the feasibility to perform these quantified measurements in SCD patients. METHODS: Retinal microvascular and oximetry measurements were performed in eight SCD patients and eight healthy matched controls. Oximetry pictures and non-invasive capillary perfusion maps (NCPM) were obtained by the Retinal Function Imager. Measurements were conducted twice on two different study days. Measured variables included monofractal dimension (DBOX), relative saturation, deoxygenated hemoglobin (deoxyHb) and oxygenated hemoglobin (oxyHb) concentration. RESULTS: No statistically significant differences in vessel density were found in the different annular zones (large vessels: p=0.66; small vessels: p=0.66) and anatomical quadrants (large vessels: p=0.74; small vessels: p=0.72). Furthermore, no significant between-group differences were found in the other different anatomical quadrants and annular zones around the fovea for relative saturation levels and deoxygenated HB. However, the oxyHb levels were significantly lower in SCD patients, compared to matched controls in the temporal quadrants (p=0.04; p=0.02) and the superior nasal quadrant (p=0.05). CONCLUSIONS: Our study demonstrated the feasibility of multispectral imaging to measure retinal changes in oxygenation in both SCD patients and matched volunteers. The results suggest that in SCD patients before any structural microvascular changes in the central retina are present functional abnormalities can be observed with abnormal oximetry measurements.**

**Sickle cell disease (SCD) is the most common inherited blood disorder in Europe and worldwide.**[1,2] Because of increasing immigration rates from Northern and sub-Saharan regions of Africa, SCD should be acknowledged as a major public health issue worldwide.[3] SCD is characterized by structural defects of the haemoglobin molecule, leading to acute or chronic anemia and vaso-occlusive crisis (VOC), which can lead to hospitalization and severe organ damage. Several organs might be affected including the kidneys, lungs, cerebrovascular damage, bones and the retina.[4] In general SCD is an inherited disease which may manifestate itself already at early childhood. Due to chronicity of the disorder patients may have intermittent live long symptoms and progressive organ failure due to multiple crises and insufficient oxygen perfusion.

Although SCD mostly manifests peripherally in the retina,[5] structural and functional abnormalities in the retinal vasculature around the macula have been observed.[6,7] Insights in these retinal microvascular changes allows for an optimal diagnosis and treatment of SCD patients. The retina is known for its high demand for oxygen and might therefore function as a proxy for the pathophysiology of cerebrovascular diseases in general, but also for SCD.

Retinal oximetry is a non-invasive imaging technique wherein fundus photography is combined with the use of multi-spectral filters to determine oxygen saturation in the retinal blood vessels.[8] As abnormal retinal saturation plays an important role in the pathophysiology of retinopathies in several conditions,[9] retinal oximetry imaging has been applied in several patient groups over the past decades.[10,11] Information about the retinal microvasculature can be obtained through the analysis of non-invasive capillary perfusion maps (NCPM) by means of fractal analysis. Fractal analysis provides a global index that quantifies the geometric complexity of the retinal vascular network, summarizing the entire branching pattern, and may be a more sensitive indicator of early microvascular disease compared to overt retinopathy signs.[12] This method has been applied in patients with Diabetes Mellitus,[13] Multiple Sclerosis,[14] and high myopia. [15]

Until now, knowledge about oximetry in retinal tissue around the macula in SCD patients is scarce. Oximetry images and NCPM can be obtained by the Retinal Function Imager (RFI). Previous studies performed with the RFI were only able to perform a qualitative analysis of the oximetry status of the retina,[10] whereas quantitative analysis can be more informative about the retinal status. The current study was the first to quantify retinal oximetry measurements obtained by the RFI in SCD patients and matched controls. With this study, we aimed to qualify new RFI-derived quantitative measures of retinal dysfunction in SCD.

## MATERIAL AND METHODS

### Study population

Details about the study population, study design, outcome measures and assessments were extensively described in the study protocol by Birkhoff et al.[7] In brief, retinal measurements were performed in SCD patients (self-reported) (n=8) aged 18-65 years and healthy controls matched for age, ethnicity, gender, and body mass index (n=8 for capillary maps imaging and n=9 for oximetry measurements). SCD patients were recruited through advertisements in local papers, or by referral from their treating specialist.

### Study design

This was an observational study conducted at the Centre for Human Drug Research (CHDR) in Leiden, the Netherlands. RFI was conducted twice on two study days separated by one week. The study protocol was approved by the ethics committee of Leiden University and performed according the Dutch law on medical research.

### Retinal capillary maps imaging

Retinal microcirculation was quantified using the RFI 3005 (Optical Imaging, Rehovot, Israel). Measurements were performed as described in the study protocol.[7] In brief, one pupil was dilated using tropicamide. The subject remained seated quietly with the head in a headrest, which allowed for the collection of 10-15 series of eight retinal images in 20 degrees field of view over a period of 25 minutes. Of the eight images per subject, eight were used for fractal analysis of the NCPM. The images were initially edited and exported using Odian browse software (Optical Imaging, Rehovot, Israel). Subsequently the best image series for each subject was manually selected based on the image quality (i.e. brightness and sharpness) and consequently analysed.

### Image processing

Fractal analysis of the NCPMs obtained by the RFI was performed with an Automated Matlab (The Mathworks, Inc., Natick, MA, USA) script, which was described elsewhere.[12] In brief, acquired capillary maps were processed to separate microvessels from the original image. Subsequently box-counting fractal analysis was performed on the processed images. Endpoints were defined as vessel density (DBOX) in different annular and quadrantal zones, which represents the counted small and large vessels at the capillary map. *Figure 3* demonstrates the image processing of NCPMs.

### Retinal oximetry

Retinal oximetry maps were acquired with use of the RFI by making series of eight retinal images in a field of view of 35 degrees, using a fast filter wheel with four different wavelengths, of which two oxygen insensitive wavelengths (548 nm and 586 nm) and two oxygen sensitive (575 nm and 600 nm). The eight images were aligned and were acquired at 55-100 Hz. Each series contained two images of four different wavelengths. Dark reference images, captured by keeping the camera shutter closed, were used to correct for non-uniformity. Due to the lack of a reference standard, only relative oxygenation could be calculated. To normalize the images taken at the oxygen sensitive wavelengths, we used the images taken at isosbestic points, i.e. a specific wavelength, at which the total absorbance of light of the oxygenated and deoxygenated HB is equal (*Figure 1*). The images taken at 600 nm were corrected with use of the images taken at 586 nm, thereby creating an image with deoxygenated HB (deoxyrel = 1600nm / 1586nm). The images taken at 575 nm were normalized with use of the images taken at 548 nm, thereby creating an image with oxygenated HB (oxyrel = 1575nm / 1548nm). Consequently, according to the modified Beer-Lambert law, a relative saturation map could be computed ($SO_2$ rel = - log (oxyrel / oxyrel + deoxyrel).[16] This relative saturation map was converted into a color-based map, to make interpretation of saturation easier (blue: low saturation; red: high saturation). For the analysis of the oximetry

**FIGURE 1 Schematic overview of oximetry measurements.** Images were taken using a fast filter wheel with four different wavelengths, of which two oxygen insensitive wavelengths (548 nm and 586 nm) and two oxygen sensitive (575 nm and 600 nm). The images from oxygen sensitive wavelengths were normalized with images from isosbestic points, thereby creating (de)oxygenated images. According to the modified Beer-Lambert law a relative saturation map was computed, of which different regions where analyzed.

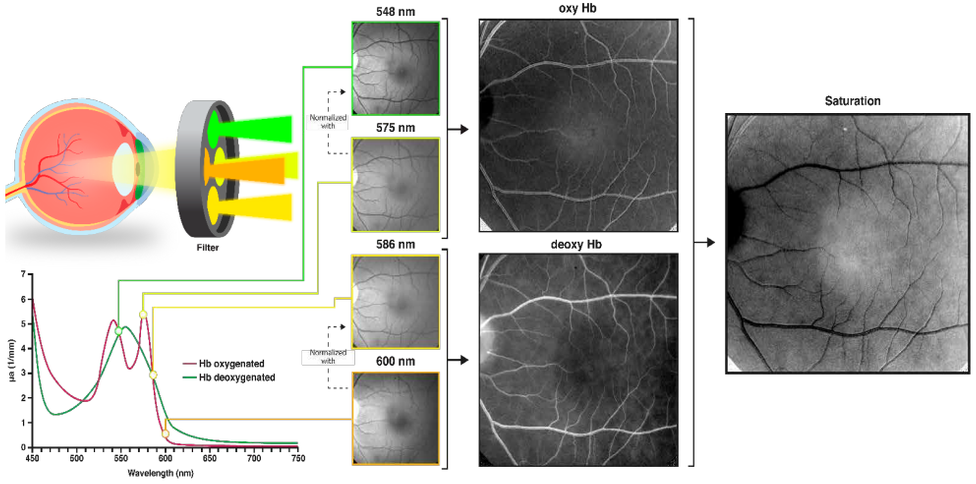

intensities, the best series were manualy chosen for each subject. We selected several regions of interest (ROIs), which were analyzed with use of MeVisLab, version 3.1 (MeVis Medical Solutions AG and Fraunhofer MEVIS, Germany). Circles were drawn showing four different diameters (10 mm, 25 mm, 50 mm and 75 mm) around the macula. Four quadrants (superior nasal, inferior nasal, superior temporal, inferior temporal) were defined. The side of each square, i.e. the size of the quadrants, was determined by taking the distance from the optic disk to the central part of the fovea. Outcomes indicative for the relative oxygen density were expressed per deoxygenated HB and oxygenated HB in arbitrary units (AU) and multiplied by 10,000 because analysis in our software (i.e. calculations based on histograms) required integer values. Saturation was calculated from deoxygenated HB and oxygenated HB according to the modified Beer-Lambert law (*Figure 1*).

### Statistical analysis

For repeatedly assessed endpoints (DBOX) of the capillary maps, contrasts between groups were estimated with a mixed model analysis of variance with fixed factors group (SCD patients and matched healthy subjects), day (day 1 and day 8), measurement (0 and 2 hour), group by day, group by measurement and group by day by measurement, and subject, subject by day and subject by time as random factors. By using the same Subject ID for the matched subjects, comparisons were pairwise. In both groups the intra subject variability, was calculated for DBOX, from the estimated variabilities within the statistical model.

For oxygenation determination, overall intensities (including minimum, maximum, mean, median, interquartile range (IQR) 25-75, peak intensity, standard deviation) were calculated for each ROI. Each parameter was analyzed using a unpaired Student's t-test comparing SCD patients and matched controls; p values < 0.05 were considered statistically significant. For oxygenation maps the minimal detectable effect size (MDES) was calculated, assuming a parallel comparison of two groups of eight subjects. All calculations were performed using SAS for windows V9.4 (SAS Institute, Inc., Cary, NC, USA).

## RESULTS

### Study population

Subject characteristics are summarized in *Table 1*. All included subjects were female.

Of all SCD patients, six had homozygous SCD (HBSS) and one heterozygous SCD (HBSE). One subject was uncertain about the SCD subtype. Patients received diverse medicaments, including folic acid, hydroxycarbamide, vitamin D, deferasirox, deferiprone, and acetaminophen. One SCD patient was on hydroxyurea therapy.

**TABLE 1 Demographics**

| | SCD patients (n=8) | Matched Controls (n=8) |
|---|---|---|
| Age (years) | 34 ± 7.5 | 31 ± 7.6 |
| BMI kg/m² | 25.4 ± 4.8 | 26.4 ± 4.2 |
| Male:female | 0:8 | 0:8 |
| Systolic blood pressure (mmHg) | 109 ± 8 | 116 ± 18 |
| Diastolic blood pressure (mmHg) | 65 ± 6 | 73 ± 12 |

*Demographics obtained during the first occasion for capillary maps measurements. Vital signs were acquired before any measurement had taken place, in both occasions.*

### Capillary maps

*Figure 2* summarizes the results from the fractal dimension analysis in SCD patients and matched controls, which was performed in the different anatomical quadrants and annular zones around the fovea. We found no significant difference between the SCD patients and the matched controls group with respect to vessel density (DBOX) in large vessels (estimate of the difference: 0.0096; 95%CI -0.0376, 0.0568; p=0.66) and small vessels (estimate of the difference 0.0033; 95%CI -0.0146, 0.0212; p=0.69) in the different annular zones around the fovea. In addition, we found no significant between-group difference with respect to vessel density in the different anatomical quadrants of large vessels (estimate of the difference 0.0086; 95%CI -0.0488, 0.0659; p=0.74) and small vessels (estimate of the difference 0.0188; 95%CI -0.1299, 0.0923; p=0.72).





**FIGURE 2 Vessel density expressed in DBOX values for all vessels (A), small vessels in different quadrantal zones (B) and annular zones (C)**

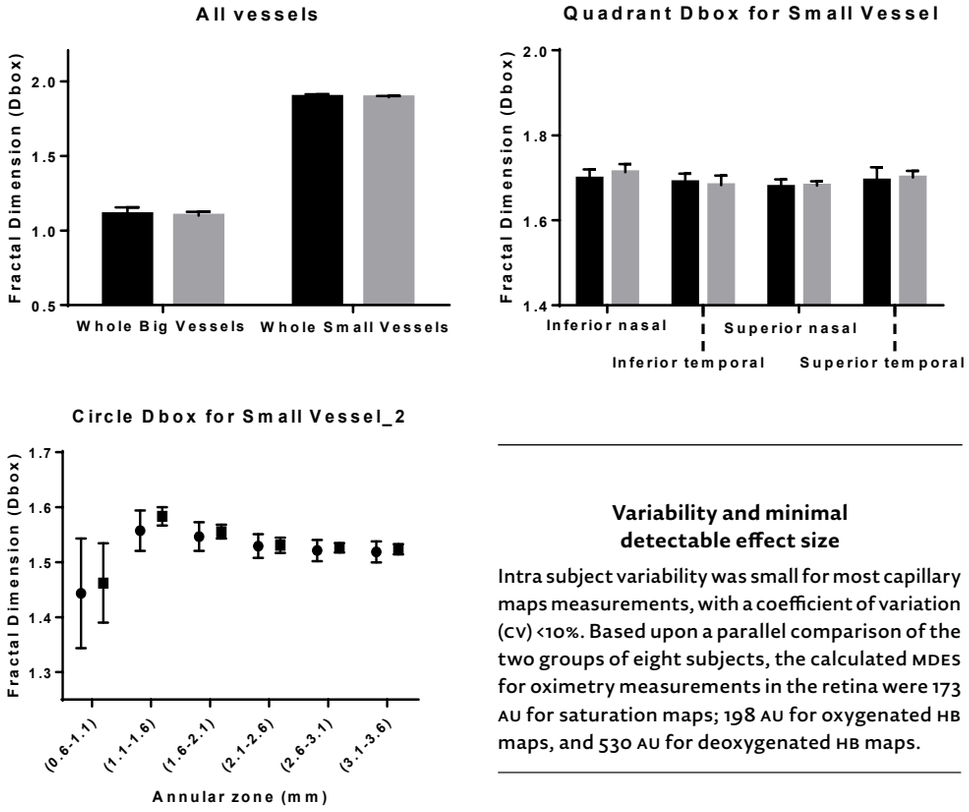


### Oximetry maps

We found no significant between-group difference in the different anatomical quadrants and annular zones around the fovea with respect to relative saturation levels and deoxygenated HB. Oxygenated HB levels were significantly lower in SCD patients compared to matched controls in the temporal quadrant 2 (Effect size (ES)=850.3; 95% CI 69.16, 1631; p=0.04), temporal quadrant 3 (ES=919.9; 95% CI 171.4, 1668; p=0.02) and in the superior nasal quadrant 1 (ES=763.8; 95% CI 16.03, 1512; p=0.05). *Table 2* provides an overview of all retinal oximetry outcomes in different quadrants and annular zones.

### Variability and minimal detectable effect size

Intra subject variability was small for most capillary maps measurements, with a coefficient of variation (CV) <10%. Based upon a parallel comparison of the two groups of eight subjects, the calculated MDES for oximetry measurements in the retina were 173 AU for saturation maps; 198 AU for oxygenated HB maps, and 530 AU for deoxygenated HB maps.

## DISCUSSION

In this study, we explored the performance of the RFI to study retinal oximetry measurements and to quantify capillary maps in SCD patients and matched healthy controls. A significant difference was observed for oxygenated HB maps in the peri-foveal quadrants. Oxygenated HB levels were significantly lower in SCD patients, compared to matched controls. We found no significant difference in vessel density, saturation and deoxygenated HB maps between SCD patients and matched controls in all anatomical quadrants and annular zones.

**FIGURE 3 A non-invasive capillary perfusion map (nCPM) (A) processed into an acquired capillary map (B) for box-counting fractal analysis of vessel density.**

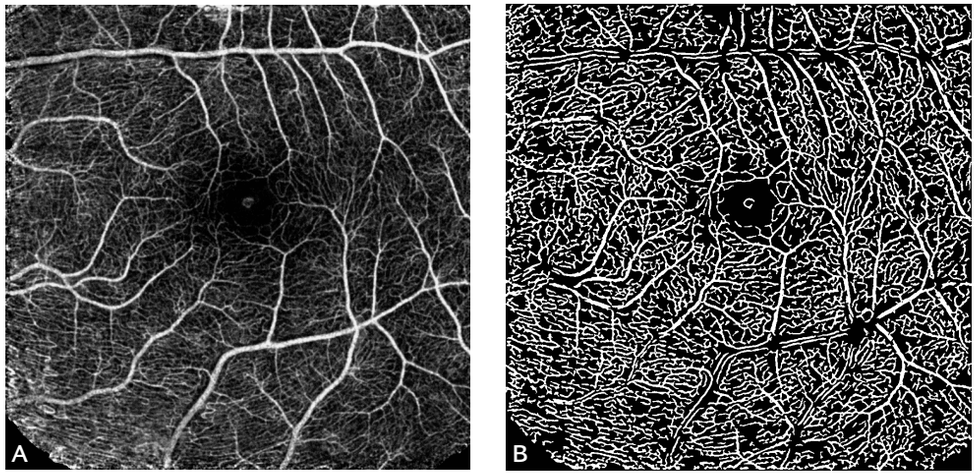


RFI is a validated methodology that was designed to directly and non-invasively image the capillary network of the retina in great detail. RFI has been able to measure functional microvascular abnormalities in different patient groups, including SCD patients.[7] Furthermore several studies have demonstrated the validity of fractal analysis of NCPM in different patients groups as Multiple Sclerosis patients and subjects with high myopia.[15,17] Our results, showing a low intra subject variability for most NCPM endpoints, support these findings,

Although previous studies using Optical Coherence Tomography -Angiography (OCT-A) in SCD patients found anatomical differences in capillary structure,[6,18] we were not able to repeat these results. This might be due to the fact that the sickle cell patients included in this study were relative healthy with no observed sickle cell retinopathy. This is also supported by a previous study which reported a strong correlation between vessel density around the fovea and retinal thickness, thereby confirming that the eyes of the patients included in this study were relatively unaffected by SCD.[6]

Also the limited sample size compared to previous studies[6,18] might be responsible for this observed difference. Although RFI measurements have been claimed to be equal and even more detailed compared to OCT- A,[19] the results might also have been distinct due to the use of different methodology (fractal analysis versus density analysis). Furthermore, the inclusion of more perifoveal regions and choroidal OCT-A measurements might have also induced more contrast compared to our study. Nevertheless this methodology was able to observe early retinal changes as expressed by differences in oxygenated HB.

Our measurements did not show a significant difference between the SCD group and the matched controls with respect to saturation measurements. This might be explained by the fact that the measured differences in endogenous contrast are probably too small for accurate detection. However we were able to observe a significant difference in oxygenated HB in the temporal quadrants of sickle cell patients, which is the location where the disease usually primarily manifestates.[20] It is unclear why the superior nasal quadrant also shows statistical difference. As expected, findings in the nasal quadrant however showed an smaller difference compared to the findings in the temporal area. The differences in oxygenation levels more peripheral from the macula might indicate early retinal damage. Furthermore in our analysis, we found a low inter subject variability, demonstrated by a low SD, which is in turn reflected by a low MDES. This demonstrates that in case of clinically relevant changes, they would have been observed.





The retina is one of the highest energy demanding tissues in the body, even surpassing the brain for metabolism, which leads to a high oxygen consumption.[21] Although decreased retinal vessel autoregulation has been reported in SCD patients,[22] SCD patients may compensate their lower HB and subsequently oxygen carrying capacity by vascular autoregulatory mechanisms, such as the dilation of the vessels. This is demonstrated by a higher retinal blood flow, previously measured in SCD patients.[7] Other techniques have also demonstrated an increased microvascular flow in other organs, thought to be a compensatory mechanism for the anemia.[23,24] The sickle cell patients in this study had an unimpaired microvasculature around the macula, as demonstrated by the NCPM measurements. Therefore the autoregulatory capacity of the retinal vessels might be sufficient in these patients, which in turn could lead to normal saturation levels when compared with controls. This theory is also confirmed in other studies.[25] Interestingly, our study demonstrates that even before microvascular changes are observed early retinal changes can already be seen by the reduced level of oxygenated hemoglobin. This is in line with findings from other studies in which differences in other organs such as cerebral oximetry have been reported.[26]

This is the first study to quantitatively analyze multispectral pictures obtained by the RFI, whereas previous studies had only qualitatively analyzed multispectral pictures.[10] In our current analysis we did not compensate for differences in path length, i.e. absorption and scattering, by the four wavelengths. The expected difference is negligible as the wavelengths are relatively close to each other. In contrast to other research we measured oximetry as an average in the retinal tissue not in the individual vessels. This is due to the fact that the current resolution of the RFI does not allow for the reliable quantification in individual vessels using our analysis technology.

A possible limitation of our study is that only females were included, therefore we cannot exclude gender effects. However, since all SCD patients were matched to a control subjects, this does not affect our main conclusions. Although this was a exploratory study the limited number of participants caused a wider confidence interval for most outcomes. However due to the low variability and subsequently the low MDES any clinically relevant contrast would have been picked up. Furthermore, our measurements were performed around the central macula, whereas in SCD retinal abnormalities are usually primarily observed peripheral. In this study NCPM measurements were performed around the macula, contrary to structural changes that are usually observed in peripheral areas in SCD. We cannot exclude that these patients have abnormalities outside the field of view, more temporal of the macula. Furthermore a common drawback of RFI, opposed to OCT-A, is that it only measures the retinal vasculature, not the choroidal vasculature. It should also be noted that the oximetry measurements were still relative, due to the lack of golden standards for retinal oximetry. Nevertheless our study demonstrated that small macular abnormalities expressed as subtle changes in oxygenated HB can already be picked up by this methodology.

In summary, our study demonstrated the feasibility of multispectral imaging to measure retinal changes in oxygenation in both SCD patients and matched volunteers and that even before a loss of vascular flow can be detected, a reduced level of oxygenated hemoglobin might affect retinal function. With the developed methodology, future studies could be performed in which retinal health is monitored by measuring changes in retinal oxygenation in diseases such as Central Retinal Venous Occlusions (CRVO), or retinal detachment.

*Compliance with Ethical Standards*

Funding: LM was funded by the European Union Horizon 2020 Program under grant agreement number 692470 (ASTONISH project) and funding for Topconsortia for Knowledge and Innovation (TKI's) from the Dutch Ministry of Economic Affairs.

Conflict of Interest: all AUTHors declare to have no conflict of interest

Ethical approval: All procedures performed in studies involving human participants were in accordance with the ethical standards of the (ethics committee of Leiden University and performed according the Dutch law on medical research) and with the 1964 Helsinki declaration and its later amendments or comparable ethical standards.

Informed consent: Informed consent was obtained from all individual participants included in the study before any measurement took place.

## *REFERENCES*


1 Ojodu J, Hulihan MM, Pope SN, Grant AM. Incidence of sickle cell trait – United States, 2010. MMWR Morbidity and mortality weekly report. 2014;63(49):1155-8.

2 Modell B, Darlison M. Global epidemiology of haemoglobin disorders and derived service indicators. Bulletin of the World Health Organization. 2008;86:480-7.

3 Weatherall DJ. The inherited diseases of hemoglobin are an emerging global health burden. Blood. 2010:blood-2010-01-251348.

4 Rees DC, Williams TN, Gladwin MT. Sickle-cell disease. The Lancet. 2010;376(9757):2018-31.

5 Fadugbagbe A, Gurgel R, Mendonça C, Cipolotti R, Dos Santos A, Cuevas L. Ocular manifestations of sickle cell disease. Annals of tropical paediatrics. 2010;30(1):19-26.

6 Han IC, Tadarati M, Pacheco KD, Scott AW. Evaluation of macular vascular abnormalities identified by optical coherence tomography angiography in sickle cell disease. American journal of ophthalmology. 2017;177:90-9.

7 Birkhoff W, de Vries J, Dent G, Verma A, Kerkhoffs JL, van Meurs AHF, et al. Retinal microcirculation imaging in sickle cell disease patients. Microvasc Res. 2018;116:1-5.

8 Beach J. Pathway to retinal oximetry. Translational vision science & technology. 2014;3(5):2-.

9 Stefánsson E, Olafsdottir OB, Einarsdottir AB, Eliasdottir TS, Eysteinsson T, Vehmeijer W, et al. Retinal oximetry discovers novel biomarkers in retinal and brain diseases. Investigative ophthalmology & visual science. 2017;58(6):BIO227-BIO33.

10 Jittpoonkuson T, Garcia PM, Landa G, Rosen RB. Retinal blood-flow velocity and oximetry status monitoring in a central retinal vein occlusion patient. Retinal Physician. 2009;6(3):50-2.

11 Einarsdottir AB, Hardarson SH, Kristjansdottir JV, Bragason DT, Snaedal J, Stefánsson E. Retinal oximetry imaging in Alzheimer's disease. Journal of Alzheimer's Disease. 2016;49(1):79-83.

12 Jiang H, DeBuc DC, Rundek T, Lam BL, Wright CB, Shen M, et al. Automated segmentation and fractal analysis of high-resolution non-invasive capillary perfusion maps of the human retina. Microvascular research. 2013;89:172-5.

13 Zahid S, Dolz-Marco R, Freund KB, Balaratnasingam C, Dansingani K, Gilani F, et al. Fractal dimensional analysis of optical coherence tomography angiography in eyes with diabetic retinopathy. Investigative ophthalmology & visual science. 2016;57(11):4940-7.

14 Jiang H, Delgado S, Tan J, Liu C, Rammohan KW, DeBuc DC, et al. Impaired retinal microcirculation in multiple sclerosis. Multiple Sclerosis Journal. 2016;22(14):1812-20.

15 Li M, Yang Y, Jiang H, Gregori G, Roisman L, Zheng F, et al. Retinal microvascular network and microcirculation assessments in high myopia. American journal of ophthalmology. 2017;174:56-67.

16 Lu G, Qin X, Wang D, Chen ZG, Fei B, editors. Estimation of tissue optical parameters with hyperspectral imaging and spectral unmixing. Medical Imaging 2015: Biomedical Applications in Molecular, Structural, and Functional Imaging; 2015: International Society for Optics and Photonics.

17 Jiang H, Delgado S, Liu C, Rammohan KW, DeBuc DC, Lam BL, et al. In vivo characterization of retinal microvascular network in multiple sclerosis. Ophthalmology. 2016;123(2):437.

18 Han IC, Tadarati M, Scott AW. Macular vascular abnormalities identified by optical coherence tomographic angiography in patients with sickle cell disease. JAMA ophthalmology. 2015;133(11):1337-40.

19 Wang L, Jiang H, Grinvald A, Jayadev C, Wang J. A mini review of clinical and research applications of the retinal function imager. Current eye research. 2018;43(3):273-88.

20 Stevens TS, Busse B, Lee C-B, Woolf MB, Galinos SO, Goldberg MF. Sickling hemoglobinopathies: macular and perimacular vascular abnormalities. Archives of Ophthalmology. 1974;92(6):455-63.

21 Wong-Riley M. Energy metabolism of the visual system. Eye and brain. 2010;2:99.

22 van Meurs JC, Schwoerer J, Schwartz B, Mulder PG, Meiselmann HJ, Johnson CS. Retinal vessel Autoregulation in sickle cell patients. Graefe's archive for clinical and experimental ophthalmology. 1992;230(5):442-5.

23 Shi PA, Manwani D, Olowokure O, Nandi V. Serial assessment of laser Doppler flow during acute pain crises in sickle cell disease. Blood Cells Mol Dis. 2014;53(4):277-82.

24 Minniti CP, Delaney KM, Gorbach AM, Xu D, Lee CC, Malik N, et al. Vasculopathy, inflammation, and blood flow in leg ulcers of patients with sickle cell anemia. American journal of hematology. 2014;89(1):1-6.

25 Shahidi M, Felder AE, Tan O, Blair NP, Huang D. Retinal Oxygen Delivery and Metabolism in Healthy and Sickle Cell Retinopathy Subjects. Investigative ophthalmology & visual science. 2018;59(5):1905-9.

26 Nahavandi M, Tavakkoli F, Hasan S, Wyche M, Castro O. Cerebral oximetry in patients with sickle cell disease. European journal of clinical investigation. 2004;34(2):143-8.




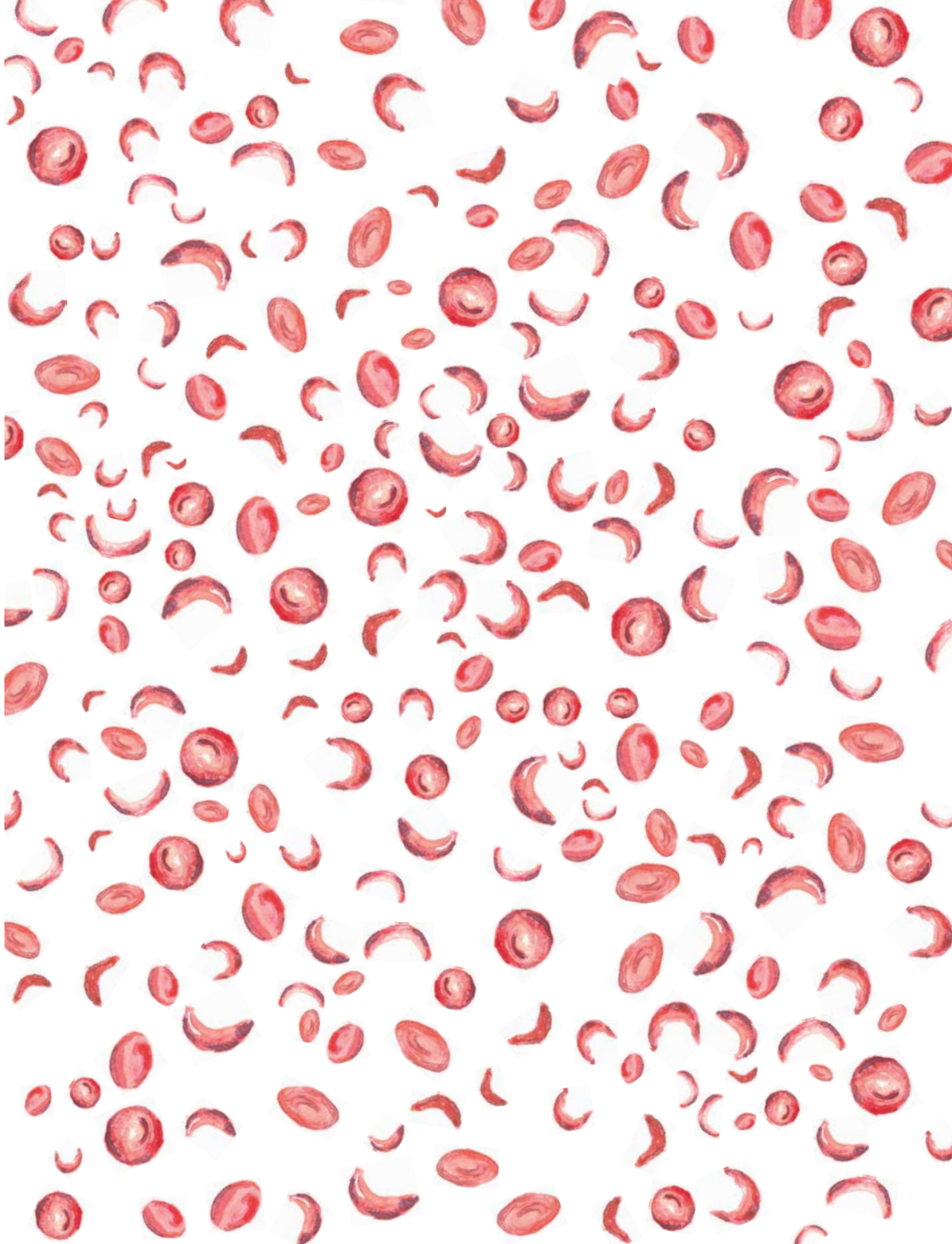

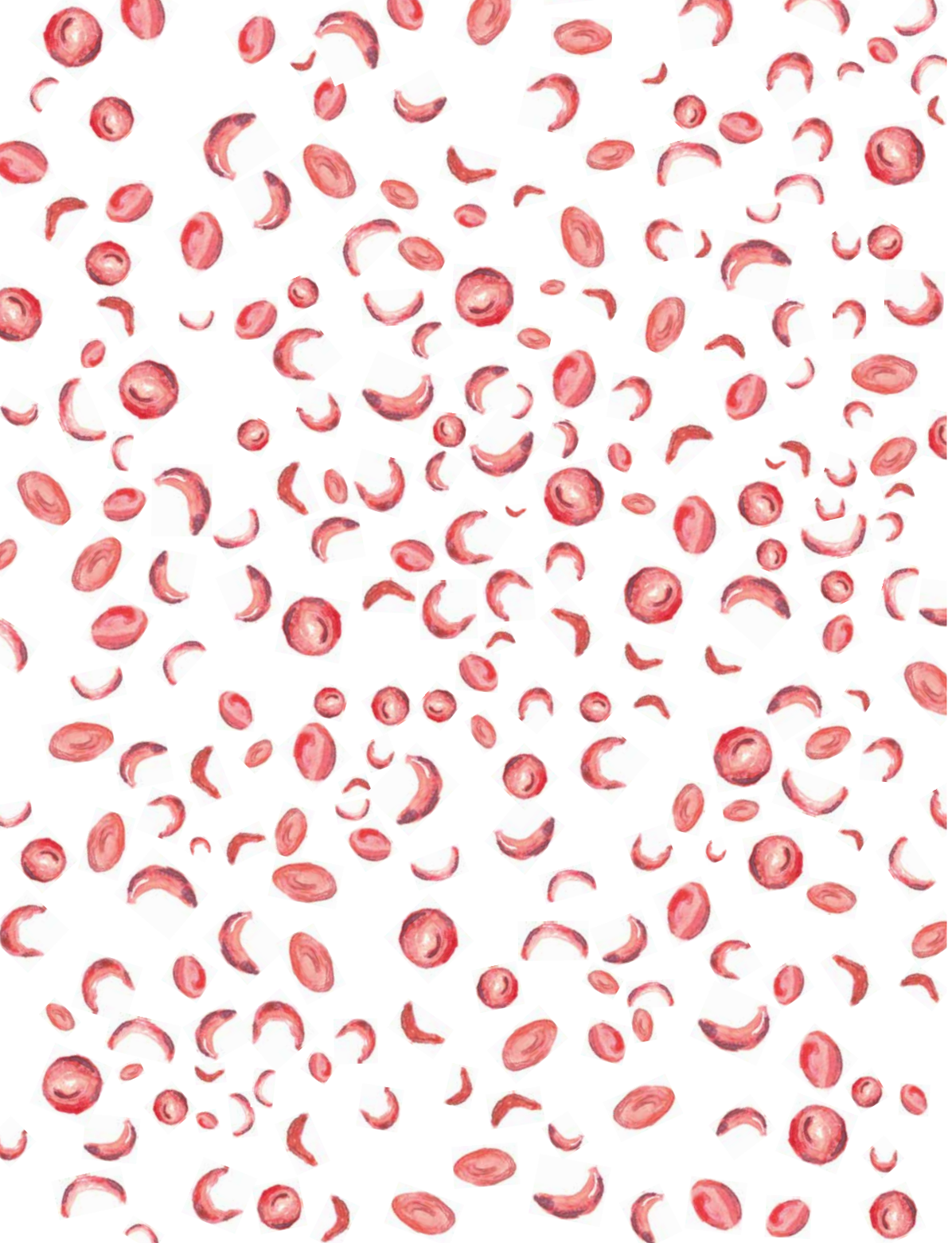

CHAPTER VI

# Validation of miniaturized dynamic light scattering in the evaluation of endothelial function, coagulation and rheology

*Willem A.J. Birkhoff[1,2], Frederik E. Stuurman[1], Dimitrios Ziagkos[1], Pim Gal[1,2], Matthijs Moerland[1,2], Jean L. Kerkhoffs[3], Ilya Fine[4], Adam F Cohen[1,2], Jacobus Burggraaf[1,2,5]*

*1. Centre for Human Drug Research, Leiden, the Netherlands / 2. Leiden University Medical Center, Leiden, The Netherlands / 3. HAGA Hospital, Den Haag, The Netherlands / 4. Elfi-Tech Ltd., Science Park, Rehovot, Israel / 5. Leiden Academic Center for Drug Research, Leiden, The Netherlands*

**BACKGROUND: Cutaneous microcirculation as a non-invasive measure for microvascular function is an interesting biomarker for use in the clinic. Miniaturized Dynamic Light Scattering (MDLS) is intended to non-invasively measure skin blood flow, rheological function and coagulation parameters. OBJECTIVE: We performed a validation study, comparing MDLS readouts between various populations, evaluate their intra-subject variability and correlation with laser speckle contrast imaging (LSCI). METHODS: Eight healthy volunteers (HV), sixteen patients using vitamin-K antagonists (VKA) and eight sickle cell disease (SCD) patients were included. MDLS and LCSI measurements were performed twice on two different study days to evaluate endothelial function, coagulation and rheology. Furthermore blood samples were taken to evaluate hematological, endothelial and rheological function. RESULTS: Intrasubject variability ranged from a coefficient of variation of 4.1% to 180% for MDLS parameters. MDLS endothelial function evaluation was not correlated with LSCI readouts., MDLS rheologic evaluation did not differentiate between HV and SCD and MDLS coagulation evaluation did not differentiate between HV and patients using VKA. MDLS readouts were not correlated with circulating biomarkers of coagulation or rheology. CONCLUSION: This validation study suggests that the MDLS device does not appear to be of added value for the evaluation of endothelial function, coagulation or rheologic status.**

**Cardiovascular disease is one of the leading causes of death and disability worldwide.[1,2]** Since microvasculature is often impaired and microvascular dysfunction might prelude cardiovascular events, microvascular measurements could be used as a predictor for clinical deterioration.[3–7] The cutaneous microcirculation as a non-invasive measure for microvascular

function[4,7] and is a candidate biomarker for use in in the clinic or in clinical trials.

A novel technique to measure microvascular function is miniaturized Dynamic Light Scattering (MDLS).[8] MDLS is an explorative non-invasive optical technology based on Dynamic Light Scattering. This novel technique has been designed to measure skin blood flow and as well as coagulation parameters and rheological function.[8–10] Due to its compactness, ease of use and broad spectrum of readouts it could be potentially an interesting device for microcirculation (home)monitoring.

We performed a validation study of the MDLS device, comprised of an evaluation of the intrasubject variability on different days and correlation to readouts from a validated device on endothelial function. In addition, the ability of the MDLS to differentiate patients using vitamin K antagonists from healthy volunteers on coagulation parameters were evaluated, as well as the ability of the MDLS to differentiate sickle cell disease patients from healthy volunteers on rheologic parameters.

## MATERIALS AND METHODS

The study protocol was approved by the ethics committee of Leiden University Medical Center (LUMC), executed at the Centre for Human Drug Research in Leiden, the Netherlands, and performed according the Dutch law on medical research. The trial was registered in the Dutch trial register (NTR) under number Trial NL5762 (old NTR ID NTR6004). The study consisted of a medical screening and two visits to the unit during which all measurements were executed. All study participants signed an informed consent form before study participation.

### Study population

In total, 32 participants were recruited for this study, consisting of healthy volunteers (HV; n=8), patients on Vitamin K antagonists (VKA; n=16) and sickle cell disease (SCD) patients (n=8). Eligibility was assessed during a medical screening, including a physical examination, detailed medical history, hematology, chemistry and coagulation blood panels and an electrocardiogram (ECG). In addition, for VKA patients, the target INR had to be ≥ 2.0. SCD patients were excluded when they underwent acute transfusion therapy within 3 weeks prior to the measurements and/or experienced a vaso-occlusive crisis within 1 week prior to the measurements. Patients continued their usual medication.

### mDLS

MDLS (Elfi-Tech, Rehovot, Israel) measurements were performed on the middle finger of the non-dominant hand. An occlusion ring was placed on the bottom of the middle finger with above a sensor on the ventral side of the middle finger (*Figure 1*). After two minutes of baseline measurements the occlusion ring automatically inflated to +/- 250 mm/Hg, effectively stopping the digital blood flow. The cuff automatically deflated after two minutes, after which measurements continued for two minutes. The data were analyzed by proprietary software (Elfi-Tech, Rehovot, Israel) using previously published underlying formulae.[11] Eleven parameters were identified for inclusion in the present analysis and were split up into three categories: four for endothelial function (MF pre and post, MDP1&2), five were for coagulation (Mdindex 1 through 4 and Mdparameter1) and two for rheologic evaluation (Mdparameter 2 and MDRBC), as also be observed in *Table 2*. The MDLS signal was also analysed using experimental algorithms for learning purposes. These exploratory analyses were omitted from the current manuscript as they did not reveal useful information, which may reflect the unvalidated nature of these analyses.

### LSCI

LSCI (PSI; Perimed, Järfälla, Sweden) was performed as previously described.[12] In short, the cutaneous blood flow was measured continuously on the ventral side of the non-dominant upper forearm, on a surface of 4 x 10 cm. A vacuum pillow was used to limit arm movements. For the endothelial function, a post-occlusive hyperemia (PORH) procedure was performed. This consisted of a 5-minute recording of the baseline flow, after which the brachial artery was occluded by inflating a pressure cuff placed around the upper arm to approximately 200 mmHg for 5 minutes. Subsequently, the cuff was deflated, inducing a hyperemic reaction in the lower forearm. Obtained data were analyzed using PIMsoft software (Perimed, Järfälla, Sweden). LSCI primary endpoints included basal flow (arbitrary units(AU)), maximal flow after occlusion (AU), ratio maximal flow/basal flow (%), time to maximal flow (seconds), time to return to basal flow after occlusion (seconds) and post-occlusive index as previously described [13] (AUC maximal flow/basal flow; %).





**FIGURE 1 Example of mDLS measurements**

### Statistical analysis

Data are presented as mean with their standard deviation. For each of the patient groups, the estimated intrasubject variability between days, describing the long-term repeatability, was calculated by parallel analysis. For repeatedly assessed endpoints, contrasts between groups were estimated with a mixed model analysis of variance with fixed factors group (healthy volunteer and patient groups), day (day 1 and day 16), and if applicable time (0 and 1 hour), and the interactions and subject, or if suitable, subject by day and subject by time as random factors.

LSCI time to maximum flow (sec), LSCI time to return to BF (sec) were log- transformed before analysis. All calculations were performed using SAS for windows V9.4 (SAS Institute, Inc., Cary, NC, USA), except for the correlations which were calculated using GraphPad Prism for Windows (GraphPad Software, La Jolla, CA, USA).

No formal power calculation was done for this exploratory study. The number of subjects included in this study is usual for this type of study.

**TABLE 1 Baseline measurements, including demographics, lab and LSCI measurements with LSM and (SD)**

| | HV | VKA* | SCD* |
|---|---|---|---|
| Age | 30.6 (17.0) | 62.6 (12.2) | 38.4 (13.5) |
| GENDER | | | |
| Male | 4 | 12 | 1 |
| Female | 4 | 4 | 7 |
| LSCI | | | |
| Basal flow (AU) | 26.8 (5.32) | 26.8 (6.78) | 34.23 (7.00) |
| Maximal flow after occlusion (AU) | 92 (5.1) | 80 (13.7) | 88 (15.6) |
| Ratio maximal/basal flow (%) | 342 (44.3) | 300 (62.3) | 257 (45.9) |
| Time to maximal flow (seconds) (contrast in%) | 13.8 (3.96) | 13.8 (3.76) | 21.4 (16.9) |
| Time to return to basal after maximal flow (seconds) | 1456 (15.7) | 168 (40.8) | 163 (39.6) |
| LABORATORY MEASUREMENTS AND VITAL SIGNS | | | |
| Systolic blood pressure (mmHg) | 116.63 (8.18) | 128.60 (18.25) | 117.33 (13.07) |
| Diastolic blood pressure (mmHg) | 73.78 (8.90) | 78.20 (10.94) | 62.38 (9.33) |
| Activated partial thromboplastin time (s) | 28.9 (2.45) | 37.2 (4.19) | 27.6 (3.53) |
| Prothrombin time (s) | 13.5 (0.77) | 35.2 (7.33) | 16.6 (7.51) |
| Platelet count (10E9/L) | 237 (56.5) | 248 (58.2) | 380 (144) |
| Fibrinogen | 2.69 (0.76) | 3.60 (0.78) | 2.84 (0.60) |
| ESR | 3.09 (8.25) | 7.85 (10.9) | 3.28 (2.87) |
| Erythrocytes (10E12/L) | 4.76 (0.32) | 4.59 (0.38) | 2.84 (0.78) |
| Hemoglobin | 8.69 (0.49) | 8.53 (1.03) | 5.19 (0.86) |
| Hematocrit (L/L) | 0.42 (0.02) | 0.42 (0.04) | 0.25 (0.04) |
| Cystatin-c | 341.41 (58.6) | 401.50 (104.41) | 464.81 (198.62) |
| Endothelin_1 | 1.03 (0.43) | 1.44 (0.49) | 1.07 (0.48) |

**patients*

**TABLE 2 MDLS parameters with LSM,(SD) and estimate of the difference between groups**

| Parameter name | Description | HV | Patients vitamin-k antagonists | SCD Patients | Estimate of the difference (95% CI) Patients using VKA VS HV | Estimate of the difference (95% CI) SCD patients VS HV |
|---|---|---|---|---|---|---|
| COAGULATION PARAMETERS | | | | | | |
| MD_index1 | Average mobility index over occlusion. Correlated with coagulability. | 0.64 (0.09) | 0.65 (0.09) | 0.66 (0.09) | 0.011 (-0.034, 0.055) p=0.62 | 0.015 (-0.037, 0.067) p=0.57 |
| MD_index2 | Average mobility index over occlusion. Correlated with INR (International Normalized Ratio) | 0.87 (0.13) | 0.88 (0.09) | 0.86 (0.11) | 0.003 (-0.053, 0.060) p=0.91 | -0.012 (-0.077, 0.054) p=0.72 |
| MD_index3 | EQV- Dynamic Coagulativity Response dynamic index of mobility. Associated with coagulability. Based on dynamical change during occlusion | 0.87 (0.10) | 0.88 (0.09) | 0.86 (0.11) | 0.005 (-0.052, 0.063) p=0.85 | -0.01 (-0.076, 0.057) p=0.77 |
| MD_index4 | EQV- Dynamic Coagulativity Response dynamic index of mobility. Associated with coagulability. Based on dynamical change during occlusion | 0.96 (0.15) | 0.94 (0.13) | 0.96 (0.14) | -0.022 (-0.099, 0.055) p=0.56 | -0.002 (-0.091, 0.087) p=0.97 |
| MD_Param1 | Indicative of dynamics of coagulabity | 2.67 (NA) | 2.4 (NA) | 2.9 (NA) | -0.272 (-0.794,0.25) p=0.30 | 0.232 (-0.374, 0.84) p=0.44 |
| FLOW DERIVED PARAMETERS | | | | | | |
| MD_MF_post | Mean Frequency- Equivalent to doppler flow-metry. Represents the mean frequency of blood flow velocity post occlusion. | 7.41 (0.63) | 7 (0.55) | 6.93 (0.64) | | -0.476 (-0.865, -0.088) p=0.02 |
| MD_MF_pre | Mean Frequency- Equivalent to doppler flow-metry. Represents the mean frequency of blood flow velocity pre occlusion. | 7.55 (0.70) | 7.22 (0.66) | 7 (0.70) | | -0.547 (-1.019, -0.075) p=0.02 |
| MD_P1 | Perfusion immediately after occlusion | 566.83 (71.5) | 562.46 (66.9) | 611.03 (47.4) | - | 44.201 (-13.37, 101.78) p=0.13 |
| MD_P2 | Perfusion at end of occlusion | 525.67 (73.0) | 517.43 (66.9) | 569.82 (47.2) | | 44.15 (-12.75, 101.05) p=0.12 |
| RBC PARAMETERS | | | | | | |
| MD_Param2 | Indicative of motion RBC | 0.29 (0.68) | 0.28 (0.55) | 0.24 (0.34) | | -16.80% (-58.2%, 65.6%) p=0.60 |
| MD_RBC_T1 | RBC diffusion time during occlusion | 0.25 (0.36) | 0.31 (0.33) | NA | 26.60% (-20.1%, 100.4%) p=0.30 | |





### Laboratory measurements

A broad panel of hematological, chemical and coagulation assessments were performed in the chemical and hematological laboratory of the LUMC. Furthermore analysis of endothelin-1 and Cystatin-c was performed batch wise upon study completion by enzyme-linked immunosorbent assay (R&D systems) at CHDR.

## RESULTS

### Demographics

Thirty-two participants were included and completed the study. *Table 1* displays the demographic data and baseline laboratory measurements. There was a notable difference in participant age between the three groups (30.6 ±17.0y for HVs, 62.6 ±12.2y for VKA patients and 38.4 ±13.5y for SCD patients). Six SCD patients had SCD type HbSS, one subject had HbSC, and one subject had HbS-B-thalassemia subtype.

### Variability

Intrasubject variability of MDLS readouts expressed as the coefficient of variation (CV) were 4.7 – 7.9% for endothelial readouts, 11.0 – 38.9% for coagulation readouts and 76.8 – 180% for rheologic readouts (*Table 3*). The intrasubject variability for cutaneous microcirculation by LSCI with a CV ranging between 6.1 -12.9% was low between days across all groups.

**TABLE 3 MDLS intrasubject CV% between days**

| Parameter name | HV | VKA | SCD patients |
|---|---|---|---|
| MD_index1 | 13.7% | 13.5% | 13.4% |
| MD_index2 | 11.1% | 11.0% | 11.2% |
| MD_index3 | (CV NA) | (CV NA) | (CV NA) |
| MD_index4 | (CV NA) | (CV NA) | (CV NA) |
| MD_Param1 | 35.0% | 38.9% | 32.0% |
| MD_MF_post | 6.2% | 6.6% | 6.7% |
| MD_MF_pre | 7.3% | 7.7% | 7.9% |
| MD_P1 | 5.1% | 5.1% | 4.7% |
| MD_P2 | 5.8% | 5.9% | 5.3% |
| MD_Param2 | 180% | 180% | 180% |
| MD_RBC_T1 | 76.8% | 76.8% | NA |

### Contrasts between populations

*mDLS*

Out of the 11 parameters, there were no significant differences between the patients on VKA and HV on coagulation parameters. There was a statistically significant difference for two of the endothelial function parameters between HVs and SCD patients: MD_MF_pre (7.41 (0.63) vs. 6.93 (0.64), p=0.02) and MD_MF_post (7.55 (0.70) vs. 7.00 (0.70), p=0.02), which represent the mean blood flow velocity pre and post occlusion. However, these parameters were not correlated with the gold standard for pre and post blood flow velocity measurements, LSCI. (*Table 4*)

**TABLE 4 Correlation of flow derived parameters in healthy volunteers, MDLS vs LSCI**

| | LSCI Basal flow | LSCI Maximal flow after occlusion | LSCI Ratio maximal/ basal flow | LSCI Time to maximal flow | LSCI Time to return to basal after maximal flow |
|---|---|---|---|---|---|
| MD_MFPpost | 0.23 | 0.35 | 0.07 | -0.10 | -0.02 |
| MD_MF_PRE | -0.06 | 0.05 | 0.15 | **-.424*** | 0.01 |
| MD_P1 | -0.17 | -0.07 | 0.14 | -0.13 | 0.30 |
| MD_P2 | -0.12 | -0.02 | 0.13 | -0.12 | 0.28 |

** Correlation is significant at the 0.05 level (2-tailed).*

### Correlations

In healthy volunteers there was a significant negative correlation between MDLS MF_pre and LSCI time to maximal flow (p=-0.424, P<0.05). For coagulation and rheologic parameters no significant correlation was found between lab measurements and MDLS measurements, as can be observed in *Table 5*.

## DISCUSSION

The present study aimed to validate the MDLS for the measurement of endothelial function, coagulation and rheologic status. Despite a limited intrasubject variability for several parameters, in particular endothelial indices, the results from this study suggest that the readouts from the MDLS device are not correlated with endothelial function. In addition, the technique was not capable to differentiate between HVs and patients using VKAs and SCD patients.

**TABLE 5 Correlation of flow derived parameters in healthy volunteers, MDLS vs LSCI**

| | LSCI Basal flow | LSCI Maximal flow after occlusion | LSCI Ratio maximal/ basal flow | LSCI Time to maximal flow | LSCI Time to return to basal after maximal flow |
|---|---|---|---|---|---|
| MD_MFPpost | 0.23 | 0.35 | 0.07 | -0.10 | -0.02 |
| MD_MF_PRE | -0.06 | 0.05 | 0.15 | **-.424*** | 0.01 |
| MD_P1 | -0.17 | -0.07 | 0.14 | -0.13 | 0.30 |
| MD_P2 | -0.12 | -0.02 | 0.13 | -0.12 | 0.28 |

** Correlation is significant at the 0.05 level (2-tailed).*

MDLS technique is based on dynamic light scattering, which has proven its use to detect particles in suspension and can be used for the characterization of nanoparticles.[14] Dynamic light scattering technique was able to detect an anticoagulated state in an earlier study, however this study was an ex vivo study and not performed in actual patients.[8] Additionally, there is not a physiological reason why anticoagulation would materially affect microvascular flow unless in the presence of appreciable vascular damage. However, dynamic light scattering is not used for the evaluation of microvascular function, which is why the MDLS was designed.

In a previous study, MDLS readouts were correlated to patient age.[11] In addition, this study also found that patients on either coumarin derivates or aspirin had a significantly different MDLS readout as compared to healthy controls.[11] Another study reported that the MDLS was capable of measuring the subject coagulation status.[15] In contrast to these findings, in the present analysis, the intrasubject variability of the MDLS parameters was limited for several parameters, in particular for parameters evaluating endothelial function although other parameters, in particular rheologic parameters, displayed large intrasubject variability. This also resulted in no clear differentiating ability of the MDLS on coagulation and rheologic status. As shown by these findings, the MDLS in the evaluated form does not appear to be a meaningful addition in either clinical practice or in research investigating microvascular function. This applies to the device as well as the software and algorithms. The MDLS technique nevertheless may be an appropriate device to measure vascular function, but updates to its design and algorithms must first be implemented.

**TABLE 6 Correlation coagulation parameters in healthy volunteers and VKA patients, MDLS vs lab and correlation RBC derived parameters in healthy volunteers and SCD patients, MDLS vs lab**

| Group | | aPTT | PT | Platelets | Fibrinogen |
|---|---|---|---|---|---|
| HV | MD_index1 | -0.329 | -0.060 | -0.111 | 0.404 |
| | MD_index2 | -0.288 | 0.055 | -0.232 | 0.246 |
| | MD_index3 | -0.492 | -0.234 | 0.061 | 0.343 |
| | MD_index4 | -0.111 | -0.230 | 0.250 | 0.396 |
| | MD_Param1 | 0.244 | 0.341 | 0.048 | -0.314 |
| VKA | MD_index1 | 0.207 | 0.141 | 0.287 | 0.250 |
| | MD_index2 | 0.247 | 0.275 | 0.338 | 0.339 |
| | MD_index3 | 0.239 | 0.234 | 0.248 | 0.165 |
| | MD_index4 | 0.134 | 0.173 | 0.001 | -0.012 |
| | MD_Param1 | -0.149 | -0.130 | 0.000 | 0.044 |
| | | ESR | Erythrocytes | Hb | Hematocrit |
| HV | MD_Param2 | 0.067 | 0.287 | 0.126 | 0.328 |
| | MD_RBC_T1 | 0.003 | 0.371 | 0.211 | 0.404 |
| SCD | MD_Param2 | -0.174 | 0.094 | 0.016 | 0.027 |
| | MD_RBC_T1 | B | B | B | B |

*** Correlation is significant at the 0.01 level (2-tailed)*
** Correlation is significant at the 0.05 level (2-tailed)*
*B Cannot be computed because at least one of the variables is constant*

## CONCLUSION

This validation study suggests that the MDLS device does not appear to be of added value for the evaluation of endothelial function, coagulation or rheologic status.





## *REFERENCES*


1 Kelly BB, Fuster V. Promoting cardiovascular health in the developing world: a critical challenge to achieve global health: National Academies Press; 2010.

2 WHO. Cardiovascular diseases (CVDs) Fact sheet May 2017 [updated May 2017. Available from: http://www.who.int/mediacentre/factsheets/fs317/en/.

3 Carpentier P, Maricq H. Microvasculature in systemic sclerosis. Rheumatic diseases clinics of North America. 1990;16(1):75-91.

4 Holowatz LA, Thompson-Torgerson CS, Kenney WL. The human cutaneous circulation as a model of generalized microvascular function. Journal of applied physiology. 2008;105(1):370-2.

5 Kang D-H, Kanellis J, Hugo C, Truong L, Anderson S, Kerjaschki D, et al. Role of the microvascular endothelium in progressive renal disease. Journal of the American Society of Nephrology. 2002;13(3):806-16.

6 Camici PG, Crea F. Coronary microvascular dysfunction. New England Journal of Medicine. 2007;356(8):830-40.

7 Shamim-Uzzaman QA, Pfenninger D, Kehrer C, Chakrabarti A, Kacirotti N, Rubenfire M, et al. Altered cutaneous microvascular responses to reactive hyperaemia in coronary artery disease: a comparative study with conduit vessel responses. Clinical Science. 2002;103(3):267-74.

8 Kalchenko V, Brill A, Bayewitch M, Fine I, Zharov V, Galanzha E, et al. In vivo dynamic light scattering imaging of blood coagulation. Journal of biomedical optics. 2007;12(5):052002-4.

9 Fine I, Kuznik BI, Kaminsky AV, Shenkman L, Kustovsjya EM, Maximova OG. New noninvasive index for evaluation of the vascular age of healthy and sick people. Journal of biomedical optics. 2012;17(8):0870021-7.

10 Wu Z, Boersema GS, Taha D, Fine I, Menon A, Kleinrensink G-J, et al. Postoperative hemodynamic index measurement with miniaturized dynamic light scattering predicts colorectal anastomotic healing. Surgical innovation. 2016;23(2):115-23.

11 Fine I, Kaminsky A, Kuznik B, Shenkman L. A non-invasive method for the assessment of hemostasis in vivo by using dynamic light scattering. Laser Physics. 2012;22(2):469-75.

12 Birkhoff W, de Vries J, Dent G, Verma A, Kerkhoffs JL, van Meurs AHF, et al. Retinal microcirculation imaging in sickle cell disease patients. Microvasc Res. 2018;116:1-5.

13 Yamamoto-Suganuma R, Aso Y. Relationship between post-occlusive forearm skin reactive hyperaemia and vascular disease in patients with Type 2 diabetes – a novel index for detecting micro- and macrovascular dysfunction using laser Doppler flowmetry. Diabetic Medicine. 2009;26(1):83-8.

14 Carvalho PM, Felício MR, Santos NC, Gonçalves S, Domingues MM. Application of light scattering techniques to nanoparticle characterization and development. Frontiers in chemistry. 2018;6:237.

15 Lerman Y, Werber MM, Fine I, Kemelman P. Preliminary clinical evaluation of a noninvasive device for the measurement of coagulability in the elderly. Journal of blood medicine. 2011;2:113.

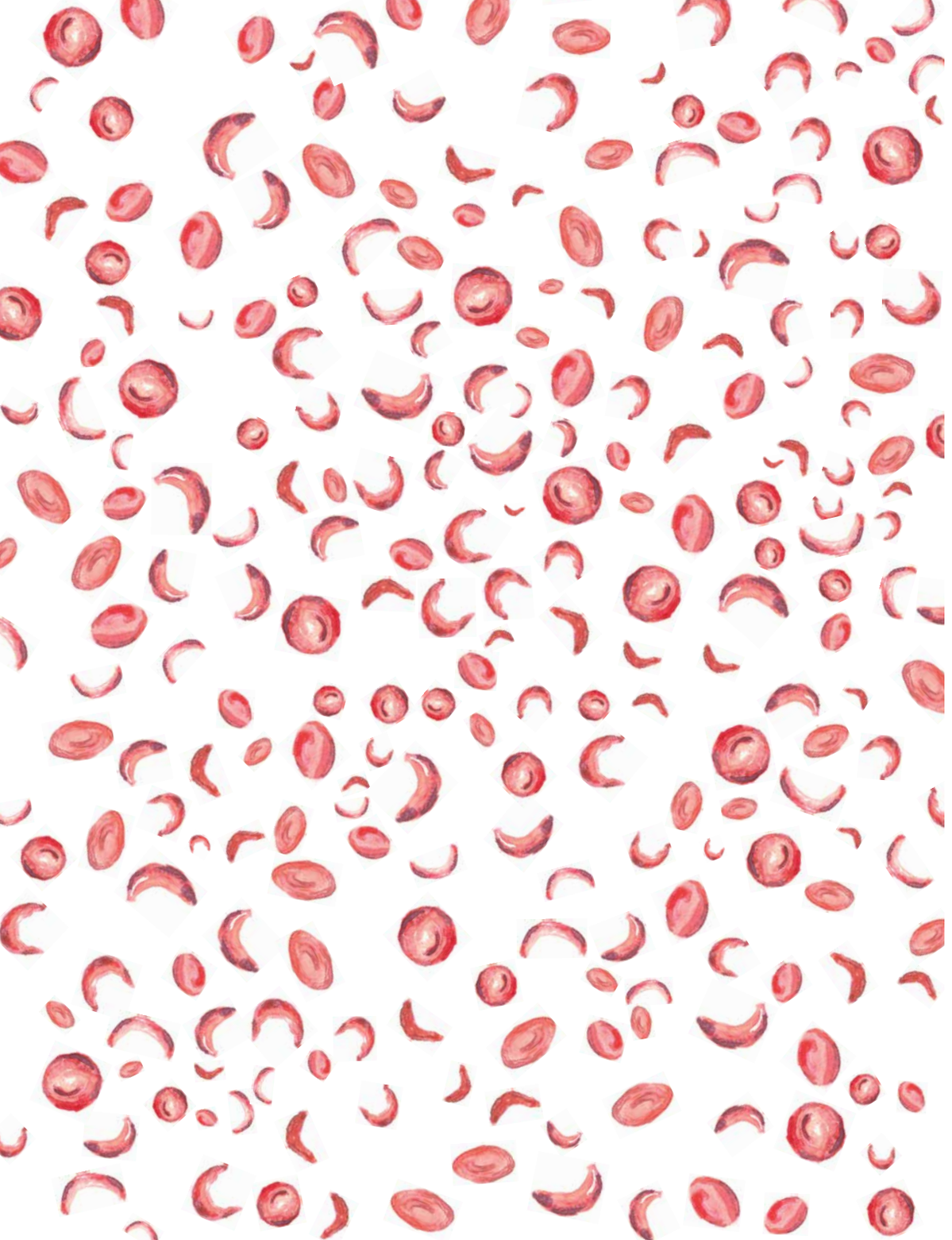

CHAPTER VII

# Recombinant human erythropoietin does not affect several microvascular parameters in well-trained cyclists

*Willem A.J. Birkhoff[1], Jules A.A.C. Heuberger[1], Titiaan E. Post[12], Pim Gal[1], Frederik. E. Stuurman[1], Jacobus Burggraaf[12], Adam F. Cohen[13]**

*1. Centre for Human Drug Research, Leiden, the Netherlands / 2. Leiden Academic Centre for Drug Research, Leiden, the Netherlands / 3. Leiden University Medical Center, Leiden, the Netherlands / *Corresponding author: Prof. Dr. A.F. Cohen*

**INTRODUCTION: Recombinant human erythropoietin (RHUEPO) has been used as a performance-enhancing agent by athletes in a variety of sports. The resulting increase in hematocrit levels leads to increased blood viscosity and can affect blood flow, potentially increasing the athlete's risk of developing health complications. However, the actual effects of using RHUEPO on microvascular blood flow and post-occlusive reactive hyperemia are currently unknown. We therefore evaluated the effect of RHUEPO on the cutaneous microcirculation in well-trained cyclists using laser speckle contrast imaging (LSCI). MATERIALS AND METHODS: This study was part of a randomized, double-blind, placebo-controlled, parallel trial designed to investigate the effects of RHUEPO in 47 well-trained adult cyclists age 18-50 years. Subjects received a weekly dose of either RHUEPO or placebo for 8 weeks, and LSCI was performed at baseline, after a maximal exercise test in week 6, and before maximal exercise in week 8. Endpoints included basal blood flux, maximum post-occlusion reperfusion, and time to return to baseline. RESULTS: Despite an increase in hematocrit levels in the RHUEPO-treated group, we found no statistically significant difference in microvascular function measured between the RHUEPO-treated group and the placebo. CONCLUSIONS: Our results suggest that the increased hematocrit levels in RHUEPO-treated well-trained cyclists are not associated with changes in microvascular blood flow or post-occlusive reactive hyperemia measured using LSCI.**

**The protein erythropoietin (EPO) is produced in the kidney and stimulates erythropoiesis in the bone marrow.** EPO production is often greatly reduced in patients with end-stage renal disease, leading to severe anemia. Recombinant human EPO (rHuEPO) is a biologically synthesized protein that helps maintain steady-state erythropoiesis;[6] in 1989, rHuEPO became available

for clinical use in patients with chronic renal failure.

Despite conflicting evidence with respect to its efficacy, RHUEPO has been used as a performance-enhancing agent by athletes in a variety of sports, including elite cycling. The use of RHUEPO by athletes is generally based on the notion that increasing hematocrit levels (i.e., increasing the ratio between the volume of red blood cells and total blood volume) increases the amount of oxygen available for the muscles, thereby increasing performance. However, there is currently no clear evidence to suggest that this is the case in elite cyclists.[8]

In addition, extensive 'doping' with RHUEPO has been reported with severe clinical outcomes in healthy athletes[11,19] Although the risks associated with RHUEPO use have been well studied in patients with kidney disease,[20] little research has been performed regarding possible health effects in athletes.

An increase in hematocrit levels causes increased blood viscosity, thereby decreasing blood flow.[18] This change in blood flow can in turn lead to thromboembolic events as is described by Virchows triad,[12] which can cause severe organ damage.[10] Furthermore, decreased blood flow can limit the ability of oxygen-transporting erythrocytes to reach the muscle tissue, thereby possibly – and paradoxically – reducing athletic performance.[7]

Administering RHUEPO to patients with kidney disease increases E-selectin and P-selectin and endothelin levels, suggesting that RHUEPO may affect the endothelium, platelet function and blood pressure.[3] However, whether RHUEPO causes a change in microcirculatory blood flow and/or post occlusive reactive hyperemia in athletes is currently unknown. Furthermore, if – and how – RHUEPO affects the ability of the microcirculation to adapt during and after maximal exercise is also unknown. Interestingly, a previous study found an impaired microvascular response in rowers after maximal exercise;[22] thus, the combination of exercise and use of RHUEPO might lead to increased health risk in athletes.

Changes in blood flow can be obtained by studying the microvasculature using a non-invasive technique such as laser speckle contrast imaging (LSCI). LSCI measures cutaneous microvascular blood flow by detecting the movement of laser-illuminated circulating red blood cells in dermal capillaries and has been used in numerous studies to assess microvascular function.[4,15,16] Importantly, LSCI measurements have low variability and high discriminating power, making LSCI a robust tool for use in clinical studies.[21,23]

Here, we used LSCI to measure the effect of RHUEPO on the cutaneous microcirculation in well-trained cyclists. This study was part of a larger randomized, double-blind, placebo-controlled, parallel clinical trial in which we studied the effect of RHUEPO on cycling performance in well-trained cyclists.[9]

The purpose of this study was to evaluate the effect of RHUEPO on basal and hyperemia induced cutaneous blood flow in resting state measured at week 0 and week 8. We also investigated post-maximal exercise responses between groups (performed at week 6).

## MATERIALS AND METHODS

### Study population

The complete study protocol was published previously by Heuberger et al..[9] In brief, the study included 47 well-trained cyclists with a maximum power output at baseline of ≥4 W/kg, a normal electrocardiogram (ECG) during exercise, a hemoglobin level of 8.0-9.8 mmol/L, and a hematocrit level <48%. Subjects who were taking any medication that could cause a possible interaction with the study medications and/or the study assessments were excluded from the study. The subjects were instructed to continue their weekly athletic training schedule during the study.

### Study design

This was a randomized, double-blind, placebo-controlled, parallel trial conducted at the Centre for Human Drug Research (CHDR) in Leiden, the Netherlands. The study protocol was approved by the Medical Review and Ethics Committee in Assen, the Netherlands and was performed in accordance with Dutch law regarding medical research. The trial was registered in the Dutch Trial Registry (number NTR5643).

Subjects received a weekly abdominal subcutaneous injection of RHUEPO (NeoRecormon, Roche, Basel, Switzerland) or placebo (0.9% NaCl) for 8 weeks. LSCI data were obtained at three time points. The first measurement was performed prior to the first dose while the subject was at rest (baseline). The second measurement was performed in after six weeks of RHUEPO treatment, 10-30 minutes after a maximal exercise test. The third measurement was performed in week 8 prior to injection of the 8th dose while the subject was at rest. Measurements in week 6 and 8 were planned, because a maximal increase in hematocrit was expected.

On each measurement day, the subjects were instructed to abstain from the use of alcohol for 24 hours prior to the visit and to abstain from using tobacco- or nicotine-containing products for at least 2 hours prior to the visit and until they were discharged from the clinical unit. All measurements were performed with the subject was in a seated position, in a climate-controlled room at 20–24°C following a 5-minute acclimatization period, at approximately the same time of day

### Laboratory assessment

Prior to each dose, the hematocrit level was measured using a Heamatokrit 200 centrifuge (Hettich Benelux BV, Geldermalsen, the Netherlands), and hemoglobin was measured using a HemoCue Hb 201+ analyzer (Radiometer Benelux BV, Zoetermeer, the Netherlands) at CHDR. In addition, samples were also collected at 2-week intervals and were assayed at the hematology laboratory at Leiden University Medical Center. All measurements took place prior to the administration of each dose, and the results of the measurements were accessible only to staff members who were not blinded to the study

### Dosing

The dosing regimen used in this study has been reported previously.[9] In brief, each subject received a weekly dose of either RHUEPO or placebo (saline). The RHUEPO group received a weekly injection of 5000-10000 international units (IU) of RHUEPO with the goal of achieving a hemoglobin level 110-115% above baseline without exceeding a hematocrit level of 52 L/L.

### Laser speckle contrast imaging (LSCI)

LSCI was performed using a PeriCam PSI imager (Perimed AB, Järfälla, Sweden). Measurements were performed on a patch of skin surface approximately 30 cm² on the ventral side of the subject's forearm. A beanbag was used to immobilize the arm in order to decrease movement artifacts. The laser was placed 15 cm above the skin surface, and cutaneous microcirculatory blood flux was measured continuously with 22 images per second. Basal flux was recorded for 5 minutes, after which the brachial artery was occluded for 5 minutes by inflating a pressure cuff placed around the upper arm to approximately 200 mmHg, which was above the systolic blood pressure for all subjects. After 5 minutes, the cuff was fully deflated, inducing a hyperemic response. The following study endpoints were measured:

1 Basal flux, as an average over the last minute before occlusion (BF) in arbitrary units (AU)
2 Maximal flux, as an average over 10 seconds during the peak (MF) in AU
3 The ratio of MF to BF, yielding post-occlusion reactive hyperemia (PORH), expressed as a percentage (%)
4 The time to reach maximal flux (measured as the time elapsed between the end of occlusion and maximal blood flux) in seconds
5 The time to return to baseline (measured as the time elapsed between maximal blood flux and the return to basal flux) in seconds.

The data were analyzed using the PIMsoft software program (Perimed AB, Järfälla, Sweden).

### Maximal exercise test

The protocol for this test has been described in detail.[9] In brief, subjects performed the maximal exercise test on a Monark LC4R ergometer (COSMED, Rome, Italy); during the test the workload was increased by 25 W every 5 minutes until the subject reached exhaustion. In week 6, LSCI measurements were performed approximately on average 15 minutes after the maximal exercise test, to avoid any movement artifacts during measurement. PORH was calculated 5 minutes after occlusion as described above.

### Statistical analysis

Repeated measures over the timepoints baseline, week 6 and week 8 were analyzed using a mixed model analysis of variance with treatment, time, and treatment by time as fixed factors, the participants as a random factor and – if available – the average pre-value as a covariate. The measures that

**TABLE 1 Summary of the subjects' demographics and clinical characteristics measured at baseline.**

| | Placebo group (n=24) | RHUEPO group (n=23) | P-value |
|---|---|---|---|
| Age in years | 33.5 (20-50.0) | 33.0 (22.0-48.0) | 0.8645 |
| Weight in kg | 76.9 (9.4) | 76.8 (9.0) | 0.9904 |
| Height in cm | 186 (7) | 186 (8) | 0.8738 |
| Mean arterial pressure in mmHg | 92.1 (7.1) | 94.7 (6.0) | 0.1657 |
| Hemoglobin in mmol/L | 8.9 (0.5) | 9.1 (0.5) | 0.3097 |
| Hematocrit in L/L | 0.435 (0.394-0.469) | 0.436 (0.387-0.469) | 0.5537 |
| Pmax W/kg | 4.34 (0.26) | 4.35 (0.37) | 0.65696 |
| $V_{O_2}$ max in ml/kg/min | 56.0 (4.1) | 55.4 (5.1) | 0.38772 |

*Data are expressed as the median (range) or mean (SD)*

were analyzed using the mixed model of analysis included basal flux, maximal flux, the time to return to baseline, and hematology values.
LSCI ratio maximal flux / basal flux and time to maximal flux were analyzed using a unpaired Student's t-test for the versus the placebo group.

For the placebo group, the estimated intra-subject variability of LSCI measurements between study days was calculated for the two at-rest measurements (i.e., baseline and week 8). For both the RHUEPO-treated group and the placebo group, the minimal detectable effect size (MDES) of the LSCI endpoints was calculated as a combined measure of the effect size and the estimated variability, assuming a parallel comparison of 24 subjects.

All calculations were performed using SAS for Windows V9.4 (SAS Institute, Inc., Cary, NC, USA), or Prism V6.05 (GraphPad Software, La Jolla, CA, USA).

## RESULTS

### Study population

Microvascular function was assessed in a total of 47 well-trained cyclists who received either RHUEPO (n=23) or placebo (saline; n=24). The demographics and characteristics of the two groups are summarized in *Table 1*. All subjects in the study were healthy males with resting blood pressure and heart rate values within the normal range.

### Hematocrit levels

*Figure 1* shows the hematocrit levels measured in the placebo and RHUEPO groups during the course of the study. As expected, the hematocrit levels increased significantly from 0.4334 l/l (95%CI 0.4240, 0.4428) at baseline to 0.4757 l/l (95%CI 0.4658, 0.4856) at week 7, in the subjects who received RHUEPO but was stable in the subjects who received placebo.

### Safety

Vital signs, including heart rate and blood pressure, were similar between the two groups.

### Variability and MDES

The intra-subject variability in subjects receiving placebo based on baseline and week 8 measurements of basal blood flow was (coefficient of variation (CV)) 14.4%, maximal flow 6.5% and PORH 11.4%. The variability for the time to return to baseline and time to maximal flow was larger (CV: 29.2% and 22.8%, respectively).

Based on the calculated variances in the placebo group, MDES were calculated for the main microvascular measures, assuming a parallel study design with 2 groups of 24 subjects The MDES for LSCI basal blood flow was 5.21 AU, for maximal flow after occlusion 7.91 AU and 50.97% for the effect of occlusion reperfusion. MDES for LSCI time to maximal flow was 3 sec, for time to return to baseline 23 sec

### Contrast between the two groups

*Figure 2* summarizes the LSCI measurements between the RHUEPO and placebo groups. We found no significant difference between the RHUEPO and placebo group with respect to basal blood flux (p=0.97), maximal blood flux following occlusion (p=0.41), or the ratio between peak flux and basal flux (p= 0.50). In addition, we found no significant





**TABLE 2 Summary of LSCI kinetics measured at the indicated time points in subjects who received placebo (n=24) or RHUEPO (n=23).**

| | Baseline (at rest) | | | 6 weeks (after max exercise) | | | 8 weeks (at rest) | | |
|---|---|---|---|---|---|---|---|---|---|
| LSCI parameter | Placebo | RHUEPO | P-value | Placebo | RHUEPO | P-value | Placebo | RHUEPO | P-value |
| Time to maximal flux (sec) | 11.92 (4.19) | 10.61 (3.43) | 0.2491 | 11.17 (6.34) | 10.00 (6.91) | 0.5494 | 11.63 (3.98) | 11.48 (5.41) | 0.9158 |
| Time to return to basal flux (sec) | 125.5 (32.6) | 112.2 (23.2) | 0.1158 | 135.7 (35.0) | 153.3 (47.4) | 0.1515 | 136.6 (28.7) | 127.5 (29.5) | 0.2913 |

*Data are expressed as the mean (SD).*

difference between the two groups with respect to the time to reach peak flux or the time to return to basal flux (*Table 2*).

## DISCUSSION

Here, we used LSCI to study the effect of RHUEPO injections and maximal exercise on the microvasculature and post-occlusive reactive hyperemia in well-trained cyclists. As expected, RHUEPO caused a significant increase in hematocrit levels; in contrast, however, we found no difference between the RHUEPO and placebo groups at 8 weeks with respect to blood flow in the cutaneous microvasculature. In addition, we found no difference between the two groups with respect to maximal flux in week 6 after the subjects performed the maximal exercise test.

LSCI is a highly sensitive method for measuring acute microvascular changes in response to various challenges such as an inspiratory breath hold, local thermal hyperemia, and post-occlusion hyperemia.[2,21] Previous studies using LSCI found that patients with sickle cell disease have increased basal microvascular blood flux possibly due to decreased hematocrit levels.[2,5] In contrast, patients with polycythemia vera have increased hematocrit levels and decreased microvascular blood flow;[10] this decreased blood flow in these patients can lead to pathological conditions such as hypertension, thromboembolism, stroke, and/or other severe clinical complications. However, the changes compared to healthy individuals in hematocrit levels measured in these patients were two to three fold larger than in the subjects in our study who received RHUEPO.

In our analysis, we found intermediate variability with respect to our LSCI measurements, with a coefficient of variation (CV) ranging from 7% to 14% (data not shown); this variability is slightly higher than previous reports (with CV values of 6-10%).[2,21] Importantly, the previous studies measured variation over a one-week period, compared to 8 weeks in our study; thus, the longer time frame in our study may have contributed to the slightly higher variability. An additional source of variability may be due the physiology of the well-trained cyclists in our study. However any clinically relevant changes would have been observed by LSCI measurements, which is shown by the calculated MDES of 5.21 AU for basal blood flux which was small and below relevant physiological changes.

Based on Poiseuille's law, the classic view is that a change in hematocrit levels can affect the blood's viscosity, thereby affecting blood flow.[1,17] However, recent studies suggest that a relatively small change in the hematocrit level of up to 13% may not directly affect microvascular blood flow[14] or cardiac output in healthy volunteers.[13] Thus, the effect of a change in the hematocrit level on blood flow may have a threshold and may only become evident with a relatively large change in hematocrit levels over a longer period of time. This notion is supported by our measurements of blood pressure, which were unaffected in the RHUEPO group. Accommodating a relatively small change in hematocrit levels over a short period can be compensated for by vascular autoregulatory mechanisms such as dilation of the vessels. However, this can only occur if there is sufficient autoregulatory capacity in the vessels,[1] which might not be the case for patients with sickle cell disease or polycythemia vera.

Although no difference was observed in LSCI PORH measurements due to RHUEPO, nor after

maximal exercise challenge, a possible effect on the endothelium was observed in other markers: P-selectin and E-selectin.[9] These findings can be indicative that short-term exposure to RHUEPO has an effect on platelets and/or the endothelium, but does not affect the reactive capability of the endothelium. However other factors, such as dehydration, exhaustion and extreme temperatures, might also influence the hematocrit levels due to fluid shifts or loss and thereby the microcirculatory flow and endothelial function in elite cyclists during races.[24]

This is the first reported placebo-controlled study of the effect of RHUEPO – and indirectly the accompanying changes in hematocrit levels – on microvascular blood flow in well-trained athletes. Although previous studies investigated the effect of exercise and RHUEPO on post-occlusion hyperemia in healthy volunteers, this is the first study to closely mimic the reported situation in professional cycling, in which RHUEPO is used as a doping agent. As we did not observe any difference in microvascular flow it is unlikely that the use of RHUEPO has negatively influenced the athletic performance by limiting the oxygen-transporting capabilities of the erythrocytes. This is also reflected in the exercise performance results published elsewhere.[9]

A possible limitation of our study is that the subjects in the RHUEPO group had a relatively small – albeit significant – increase in hematocrit levels. We therefore cannot exclude the possibility that a larger increase in hematocrit levels (for example, in professional cyclists who doped with RHUEPO in the past) may affect microvascular function. Because of the use of the Athletes Biological Passport and stringent doping controls, the increase in hematocrit levels observed in this study are most likely similar or even higher as what they would be in elite cyclist currently using RHUEPO as doping.

In summary, we report that weekly injections of RHUEPO increases hematocrit levels in well-trained cyclists, but does not appear to affect either pre-exercise or post-exercise microvascular blood flow measured using LSCI.

## *REFERENCES*


1 Baskurt OK, and Meiselman HJ. Blood rheology and hemodynamics. In: Seminars in thrombosis and hemostasisCopyright© 2003 by Thieme Medical Publishers, Inc., 333 Seventh Avenue, New York, NY 10001, USA. Tel.:+ 1 (212) 584-4662, 2003, p. 435-450.

2 Birkhoff W, de Vries J, Dent G, Verma A, Kerkhoffs J, van Meurs A, de Kam M, Moerland M, and Burggraaf J. Retinal microcirculation imaging in sickle cell disease patients. Microvascular Research 2017.

3 Carlini RG, Dusso AS, Obialo CI, Alvarez UM, and Rothstein M. Recombinant human erythropoietin (rHuEPO) increases endothelin-1 release by endothelial cells. Kidney international 43: 1010-1014, 1993.

4 Cracowski JL, and Roustit M. Current Methods to Assess Human Cutaneous Blood Flow: An Updated Focus on Laser-Based-Techniques. Microcirculation 23: 337-344, 2016.

5 Currier NV, Dent G, Swerdlow PS, Birkhoff W, Burggraaf J, de Vries J, Neelavalli J, Shahid M, Yadav BK, and Hobbs WE. Skin Blood Flow Measured By LSCI Demonstrates Treatment Effect of Chronic Transfusion Protocol in Sickle Cell Disease. American Society of Hematology, 2016.

6 Eschbach JW, Abdulhadi MH, Browne JK, Delano BG, Downing MR, Egrie JC, Evans RW, Friedman EA, Graber SE, and Haley NR. Recombinant human erythropoietin in anemic patients with end-stage renal disease: results of a phase III multicenter clinical trial. Annals of Internal Medicine 111: 992-1000, 1989.

7 Hardeman M, Alexy T, Brouwer B, Connes P, Jung F, Kuipers H, and Baskurt OK. EPO or PlacEPO? Science versus Practical Experience. Biorheology 51: 83-90, 2014.

8 Heuberger JA, Cohen Tervaert JM, Schepers FM, Vliegenthart AD, Rotmans JI, Daniels J, Burggraaf J, and Cohen AF. Erythropoietin doping in cycling: lack of evidence for efficacy and a negative risk–benefit. British journal of clinical pharmacology 75: 1406-1421, 2013.

9 Heuberger JA, Rotmans JI, Gal P, Stuurman FE, van't Westende J, Post TE, Daniels JM, Moerland M, van Veldhoven PL, and de Kam ML. Effects of erythropoietin on cycling performance of well trained cyclists: a double-blind, randomised, placebo-controlled trial. The Lancet Haematology 4: e374-e386, 2017.

10 Kwaan HC, and Wang J. Hyperviscosity in polycythemia vera and other red cell abnormalities. In: Seminars in thrombosis and hemostasisCopyright© 2003 by Thieme Medical Publishers, Inc., 333 Seventh Avenue, New York, NY 10001, USA. Tel.:+ 1 (212) 584-4662, 2003, p. 451-458.

11 Lage JMM, Panizo C, Masdeu J, and Rocha E. Cyclist's doping associated with cerebral sinus thrombosis. Neurology 58: 665-665, 2002.

12 Lowe GD. Virchow's triad revisited: abnormal flow.







Pathophysiology of haemostasis and thrombosis 33: 455-457, 2003.

13 Lundby C, Robach P, Boushel R, Thomsen JJ, Rasmussen P, Koskolou M, and Calbet JA. Does recombinant human Epo increase exercise capacity by means other than augmenting oxygen transport? Journal of applied physiology 105: 581-587, 2008.

14 Martini J, Carpentier B, Negrete AC, Frangos JA, and Intaglietta M. Paradoxical hypotension following increased hematocrit and blood viscosity. American Journal of Physiology-Heart and Circulatory Physiology 289: H2136-H2143, 2005.

15 Matheus ASdM, Clemente ELS, Rodrigues MdLG, Valença DCT, and Gomes MB. Assessment of microvascular endothelial function in type 1 diabetes using laser speckle contrast imaging. Journal of diabetes and its complications 31: 753-757, 2017.

16 Pauling JD, Shipley JA, Hart DJ, McGrogan A, and McHugh NJ. Use of laser speckle contrast imaging to assess digital microvascular function in primary Raynaud phenomenon and systemic sclerosis: A comparison using the Raynaud condition score diary. The Journal of rheumatology 42: 1163-1168, 2015.

17 Pirofsky B. The determination of blood viscosity in man by a method based on Poiseuille's law. The Journal of clinical investigation 32: 292-298, 1953.

18 Pries A, Neuhaus D, and Gaehtgens P. Blood viscosity in tube flow: dependence on diameter and hematocrit. American Journal of Physiology-Heart and Circulatory Physiology 263: H1770-H1778, 1992.

19 Ramotar J. Cyclists deaths linked to erythropoietin. McGraw Hill Healthcare Publications 4530 west 77th st, minneapolis, mn 55435-5000, 1990.

20 Robles NR. The Safety of Erythropoiesis-Stimulating Agents for the Treatment of Anemia Resulting from Chronic Kidney Disease. Clinical drug investigation 36: 421-431, 2016.

21 Roustit M, Millet C, Blaise S, Dufournet B, and Cracowski JL. Excellent reproducibility of laser speckle contrast imaging to assess skin microvascular reactivity. Microvascular research 80: 505-511, 2010.

22 Stupin M, Stupin A, Rasic L, Cosic A, Kolar L, Seric V, Lenasi H, Izakovic K, and Drenjancevic I. Acute exhaustive rowing exercise reduces skin microvascular dilator function in young adult rowing athletes. European journal of applied physiology 118: 461-474, 2018.

23 Tew G, Klonizakis M, Crank H, Briers JD, and Hodges GJ. Comparison of laser speckle contrast imaging with laser Doppler for assessing microvascular function. Microvascular research 82: 326-332, 2011.

24 Trangmar SJ, and González-Alonso J. New insights into the impact of dehydration on blood flow and metabolism during exercise. Exercise and sport sciences reviews 45: 146-153, 2017.

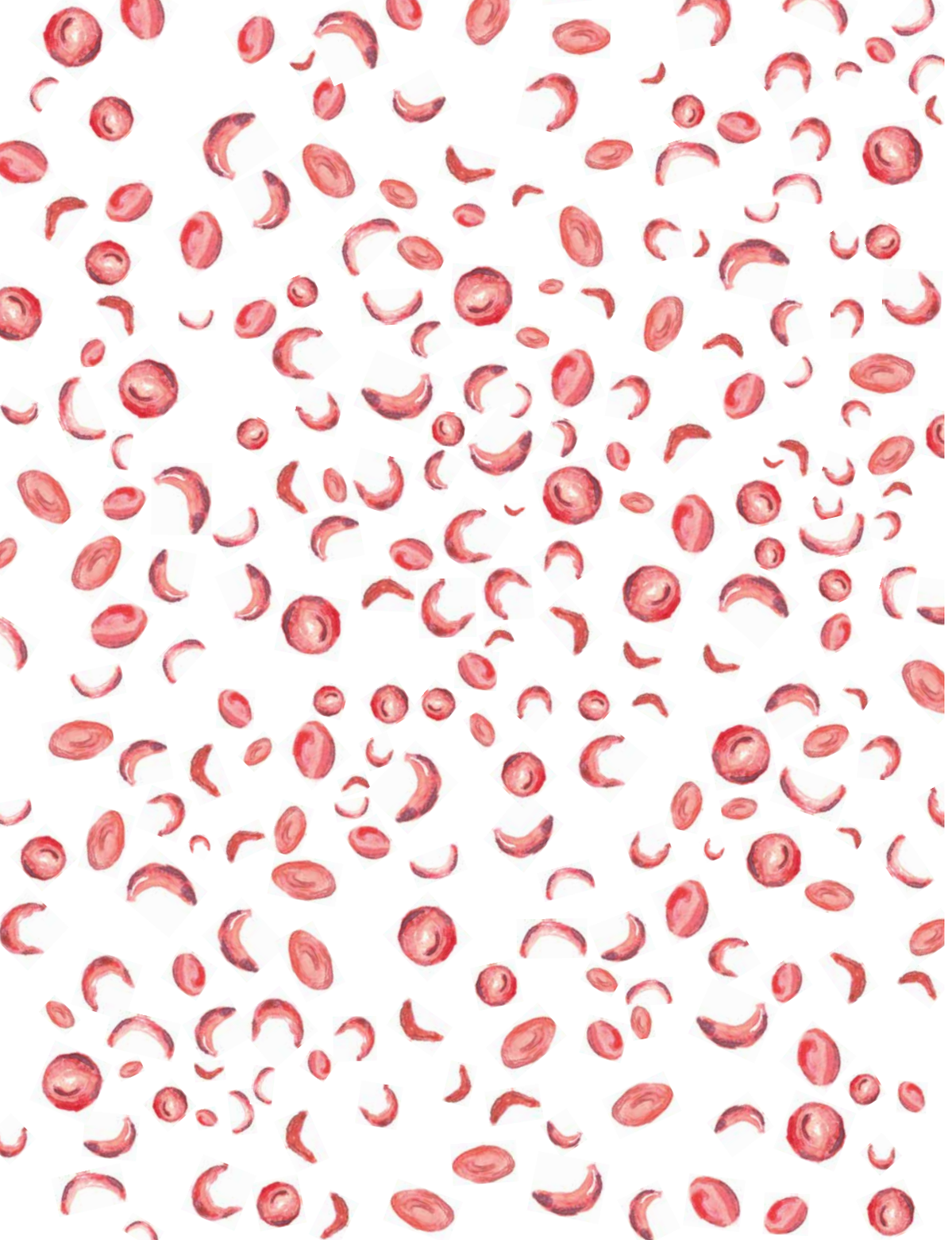

CHAPTER VIII

# Detection of cutaneous oxygen saturation using a novel snapshot hyperspectral camera: a feasibility study

*Labrinus van Manen[1]*, Willem A.J. Birkhoff[2]*, Jeroen Eggermont[3], Richelle J. Hoveling[4], Philip Nicklin[5], Jacobus Burggraaf[1,2], Roger Wilson[6], J. Sven D. Mieog[1], Dominic J. Robinson[7], Alexander L. Vahrmeijer[1], Michelle S. Bradbury[5,8,9]*, Jouke Dijkstra*[3] (*contributed equally)*

*1. Leiden University Medical Center, Department of Surgery, Leiden, NL/2. Centre for Human Drug Research, Leiden, NL/3. Leiden University Medical Center, Division of Image Processing, Department of Radiology, Leiden, NL/4. Quest Medical Imaging BV, Middenmeer, NL 5. Department of Radiology, Memorial Sloan Kettering Cancer Center, New York, USA 6. Department of Anesthesiology, Critical Care Medicine, and Surgery, Memorial Sloan Kettering Cancer Center Research, New York, USA/7. Erasmus Medical Center, Center for Optical Diagnostics and Therapy, Department of Otorhinolaryngology and Head and Neck Surgery, Rotterdam, NL/8. MSK-Cornell Center for Translation of Cancer Nanomedicines, Memorial Sloan Kettering Cancer Center, New York, USA/9. Molecular Pharmacology Program, Sloan Kettering Institute for Cancer Research, New York, USA*

**BACKGROUND: Tissue necrosis, a consequence of inadequate tissue oxygenation, is a common post-operative complication. As current surgical assessments are often limited to visual and tactile feedback, additional techniques that can aid in the interrogation of tissue viability are needed to improve patient outcomes. In this bi-institutional pilot study, the performance of a novel snapshot hyperspectral imaging camera to detect superficial cutaneous oxygen saturation ($StO_2$) was evaluated. METHODS: Healthy human volunteers were recruited at two participating centers. Cutaneous $StO_2$ of the forearm was determined by a snapshot hyperspectral camera on two separate study days during occlusion-reperfusion of the brachial artery and after induction of local vasodilation. To calculate the blood $StO_2$ at each pixel in the multispectral image, spectra were selected, and fitting was performed over wavelengths ranging from 470 to 950 nm. RESULTS: Quantitative detection of physiological changes in cutaneous $StO_2$ levels was feasible in all sixteen volunteers. A significant ($P<0.001$) decrease in cutaneous $StO_2$ levels from 78.3% (SD:15.3) at baseline to 60.6% (SD:19.8)**

**at the end of occlusion phase was observed, although $StO_2$ levels returned to baseline after five minutes. Mean cutaneous $StO_2$ values were similar in the same subjects on separate study days (Pearson $R^2$: 0.92 and 0.77, respectively) at both centers. Local vasodilation did not yield significant changes in cutaneous $StO_2$ values. CONCLUSIONS: This pilot study demonstrated the feasibility of a snapshot hyperspectral camera for detecting quantitative physiological changes in cutaneous $StO_2$ in normal human volunteers, and serves as a precursor for further validation in perioperative studies.**

## INTRODUCTION

The restoration of normal tissue function and wound healing following surgery is critically dependent on tissue oxygen saturation ($StO_2$) and perfusion, among other factors. Tissue ischemia and soft tissue necrosis, caused by inadequate tissue oxygenation, commonly occurs in patients with (micro)vascular diseases requiring surgical interventions. However, in the post-operative period, wound complications can arise, such as tissue necrosis that necessitates a second surgical procedure. Traditionally, surgeons use tactile and visual feedback, sometimes in combination with handheld Doppler ultrasound, for intraoperatively evaluating tissue perfusion. Nevertheless, healing complications can occur, for instance, in up to 8 and 15% of patients undergoing breast reconstructive surgery or surgical amputations (i.e., below-the-knee), respectively.[1,2] Therefore, additional techniques that can reliably monitor perfusion and oxygenation status in post-operative settings and accurately predict and stratify patients at-risk for delayed surgical wound healing are essential for timely surgical management and for improved quality of life.

Although, transcutaneous oxygen saturation mapping ($TcPO_2$) and optical coherence tomography (OCT) are techniques that could be used for $StO_2$ monitoring, only $TcPO_2$ is currently used as a standard of care procedure. Both techniques can measure $StO_2$ levels in vivo by detecting optical absorption coefficient differences between oxygenated and deoxygenated haemoglobin.[1,3] However, these techniques have a limited field of view and require contact with the tissue for accurate assessments. Therefore, handheld cameras with a larger field of view, but not requiring direct skin contact, may serve as a practical alternative, in addition to being readily implemented in the perioperative setting. One emerging technique is hyperspectral imaging, which has been used for biomedical applications, including the assessment of tumour margins and detection of tissue $StO_2$ in pathologic conditions.[4–6] This device detects the skin diffuse reflectance spectrum of light reflected from tissues after it has been scattered and absorbed by tissue chromophores, such as haemoglobin, fat, or water illuminated with a full spectrum light source.[4] Current available camera systems are mostly push-broom or band sequential scanners, which are limited by the long acquisition times needed to sequentially acquire spectral wavelength bands, precluding real-time imaging evaluations. Therefore, snapshot hyperspectral cameras have recently evolved to address this drawback. The first in vivo application of such a snapshot hyperspectral camera system was demonstrated by Gao et al. for the detection of retinal $StO_2$ levels.[7,8]

We have developed a novel snapshot hyperspectral imaging camera with a large field of view as a prototype system for non-invasively interrogating superficial anatomic structures and for monitoring changes in microvascular perfusion and oxygenation. This feasibility study herein aims to explore the novel capabilities of this hyperspectral snapshot camera system for detecting quantitative physiological changes in cutaneous $StO_2$ in healthy human volunteers under ambient light conditions, and without the need for direct skin contact.

## MATERIAL AND METHODS

### Study design

This study was an open observational multicenter feasibility study at the Leiden University Medical Center (LUMC), The Netherlands, and Memorial Sloan Kettering Cancer Center (MSKCC), USA. Healthy human volunteers, equally divided between these Centers, were recruited for participation in this study. Informed consent was obtained from all patients. All patients had a normal Body Mass Index (between 18.5 and 29,9 kg/m$^2$)[9], were not taking medications, and had no past medical history. The study exclusion criteria were hypertension, regular tobacco use, and any confirmed allergies to medications. Furthermore, alcohol and caffeine consumption were prohibited within 12 hours of initiating each imaging session.[10,11] Approval for conducting the clinical trial was obtained at both Centers from their Institutional Review/Regulatory Boards. This trial was registered at the Dutch Trial Register (NL6381).

#### *Study population*

Sixteen human volunteers, equally divided between trial sites, were included in this feasibility study. Subject demographics are provided in *Table 1*. Age, vital signs (basal blood pressure, heart rate), and the BMI, were in the range of those measured in normal healthy adults, and were similar in both patient cohorts. Skin temperatures between cohorts showed statistically significant differences (32.2 [1.1] versus 36.0 [0.5] °C; P<0.001). Skin types, assessed according to the Flitzpatrick scale, were similar between the two groups (P=0.637).

#### *Hyperspectral imaging system*

A snapshot hyperspectral camera system (Hyperea, Quest Medical Imaging B.V., Middenmeer, The Netherlands), which acquires 41 spectral bands across the visual (VIS) and near-infrared (NIR) spectrum, ranging between 470 and 950 nm, was used for image acquisition.[12] The camera system consists of three sensors (RGB, VIS and NIR), which are combined to facilitate simultaneous colour and spectral imaging. The effective sensor resolution is 2048 x 1080 pixels. The spectral bands are acquired using two mosaic sensors, one (4×4 filter pattern) having a spectral range of 470-630 nm, and one sensor (5×5 filter pattern) having a spectral range of 600-950 nm (*Figure 1*). This hyperspectral camera system is based on a tiled-filter approach where pixels are individually filtered with narrow Fabry-Pérot bandpass filters (bandwidth ≈ 12 nm each). The camera sensors are pixel aligned on the prism, with a maximum deviation of 1/3 pixel. In this study a camera lens of 35 mm with an aperture size of f/2.8 was used. The camera allows real-time imaging at video frame rates (max. frame rate: 16 frames per second) without the need to scan in either the x- or y- direction. The camera lens was 35 mm. The field of view of the camera is 5 by 10 cm using a 40 cm working distance, which makes this system suitable for clinical use. A signal to noise ratio of maximum 14 could be achieved. The hyperspectral imaging set-up used for this study has four 50 Watt halogen light sources (Philips Lighting B.V., Eindhoven, The Netherlands), which were mounted on the top of a black box, for optimal control of the lighting conditions (*Figure 1*).

#### *Laser speckle contrast imager*

For superficial skin perfusion analysis, a Laser Speckle Contrast Imager (LSCI) (PSI; Perimed, Järfälla, Sweden) was used at one participating center (LUMC). This non-invasive technique is capable of detecting the subcutaneous movement of light-scattering particles.[13,14] The measurement depth of the LSCI device is approximately 0.5 mm. The system uses a divergent laser beam with a wavelength of 785 nm. Measurements were performed on an area of 3×3 cm, with a frequency of 22 images per second (averaged for capsaicin snapshots). Point density was normal (resolution 0.45 mm). The LSCI data obtained were analysed using PIMsoft software (Perimed, Järfälla, Sweden).

#### *Imaging procedure*

To assess the imaging characteristics of the hyperspectral camera, its output was compared with contact measurements obtained using a fiber optic probe and multi-diameter reflectance spectroscopy.[15,16] During each measurement, the reflectance spectra are collected at effective diameters of 200, 600, and 1000 µm; $StO_2$, and blood volume fraction, was determined using the largest effective single fiber diameter with an interrogation depth of approximately 500 µm.[17]) The pathlength of light in the interrogated volume for the point spectroscopy is fixed by the fiber (equal to approximately ½ the fiber diameter). For hyperspectral imaging, the illumination spot size is similar to that of the spectroscopy measurements but longer pathlength light from other points elsewhere are present in the illuminated field of the snapshot camera. Occlusion-reperfusion experiments were performed to characterize tissue optical properties.

**TABLE 1 Demographics of study population and overall results of cutaneous oxygen saturation measurements.**

| | LUMC cohort (N=8) | MSKCC validation cohort (N=8) | P-value |
|---|---|---|---|
| Sex, male (%) | 4 (50) | 2 (25) | 0.302 |
| Age (year), median (IQR) | 23.5 (22.3-24.0) | 23.5 (21.3-38.0) | 0.798 |
| BMI (kg/m$^2$), mean (SD) | 24.6 (2.7) | 23.3 (2.4) | 0.348 |
| Blood pressure, mean (SD) | | | |
| Systolic | 120 (6.1) | 119 (9.9) | 0.834 |
| Diastolic | 77 (7.7) | 73 (5.3) | 0.309 |
| Skin temperature (°C), mean (SD) | 32.3 (1.1) | 36.0 (0.5) | <0.001 |
| Heart rate (BPM), mean (SD) | 77 (16.5) | 81 (11.8) | 0.497 |
| Skin type Flitzpatrick (N, %) | | | |
| I | 3 (37.5) | 2 (25.0) | 0.637 |
| II | 3 (37.5) | 5 (62.5) | |
| III | 1 (12.5) | 1 (12.5) | |
| IV | 1 (12.5) | - | |
| V | - | - | |
| VI | - | - | |
| Cutaneous $StO_2$, mean (SD) | | | |
| Basal phase | 69.9 (15.3) | 86.6 (10.0) | |
| Max. occlusion | 49.6 (16.5) | 72.3 (15.9) | <0.001 |
| Reperfusion | 70.4 (16.4) | 85.5 (9.9) | |

*IQR: interquartile range; SD: standard deviation; BMI: body mass index; BPM: beats per minute; $StO_2$: oxygen saturation.*

In each human volunteer, baseline skin $StO_2$ measurements were made of the right forearm over a two-minute interval. After acquiring these measurements, $StO_2$ of the right forearm was monitored for five minutes following occlusion of the right brachial artery; this procedure was repeated during the subsequent reperfusion period. In total, the arms of the included subjects did stay for 12 minutes in front of the camera and lamps during the occlusion-reperfusion experiments. Both snapshot images and spectroscopy measurements were taken every 30 seconds, except for the first minute after reperfusion, during which phase images and measurements were taken every second.

To validate this technique, human volunteers were recruited to undergo occlusion-reperfusion at two separate times, separated by more than three days. The patients' vital signs were obtained, namely their blood pressure, heart rate, basal finger oxygenation, and skin temperature, at the start of the measurements. Occlusion-reperfusion experiments were performed, as described above. Hereafter, capsaicin cream, a vasodilator, was applied on the right forearm. It works by activating the vanilloid type-1 receptor that, in turn, results in cutaneous vasodilation.[18] Capsaicin was administered on the same arm over an area of 3 by 3 cm, with an average distance of 5 cm under the radiocarpal joint, after the occlusion-reperfusion measurement. However, this was done only after the subject had rested for approximately 15 minutes, thereby restoring normal cutaneous blood flow. Subsequently, and before the capsaicin challenge, surgical tape was placed about the region of interest (ROI) to prevent spillage of capsaicin beyond the region of application. Thirty minutes after application of the crème, it was removed from the skin, and a superficial skin $StO_2$ measurement was acquired over a 30-minute time interval, with snapshots taken every 5 minutes. Results were compared with those of control regions located on the same forearm. In the LUMC cohort, blood flow was imaged simultaneously using LSCI.

### *Data processing*

Due to the configuration of the 4×4 and 5×5 mosaic in the sensors and the different offsets that are applied for the placement of this mosaic pattern on the sensor pixels, specific demosaicing of the sensor information into the different spectral datacube components was required. By comparing the differences between the different planes in the spectral datacube, the alignment, cropping and scaling of the sensor data could be optimized. Based on the filter characteristics of both the sensors and the filters in the camera system, a camera-specific correction matrix could be generated for the correction of the spectral artifacts that occur due to the configuration of the filters on the sensor pixels and the nature of the interference filters, e.g. crosstalk and higher-order transmission. The correction matrix for the spectral data was validated with reference spectra. (*Figure 1*). Next, acquired images were normalized using white and dark reference images, as previously described by Lu et al.[4] Furthermore, a correction for the second-order light effect due to light diffraction,[19] provided by the manufacturer, was performed after the normalization of images. Lastly, in order to calculate the blood $StO_2$ at each pixel in the hyperspectral images, all spectral bands (N=41) were selected in the full range of 470-950 nm to enable





fitting using a method described previously, although implemented for hyperspectral imaging.[17,20,21]

As previously described, reflectance spectra were analyzed using an analytical model developed to characterize the wavelength-dependent optical properties in order to extract physiological and morphological characteristics from the tissue of interest.[17] Briefly, attenuation caused by tissue absorption, is modeled using a modified Beer–Lambert law and is a function of both the tissue absorption coefficient ($\mu_a$) and the single fiber photon path length. The scattering properties of the tissue influence both the reflectance amplitude and the single fiber photon path length, with a dependency on the reduced scattering coefficient ($\mu'_s$) and the angular distribution of scattering (phase function). The preliminary model assumed that tissue absorption was attributable to oxygenated and deoxygenated hemoglobin confined within the local microvasculature.

Minimizing the chi-squared metric between the measured reflectance data and predictions of our model was achieved by using a Levenberg–Marquardt algorithm in order to estimate the parameter values for the microvascular hemoglobin $StO_2$, the blood volume fraction and average blood vessel diameter.[17] To estimate the confidence intervals of the parameters, the square root of the diagonal covariance matrix was used.[9] These values were averaged over repeated measurements, weighted by the confidence interval of individual spectral fits, and also reported with the associated weighted standard deviation.

This fitting method assumed that blood is the dominant absorber in the field-of-view, and that each wavelength travels an equal pathlength in the tissue with scattering losses approximately equal across the wavelength range of interest. The wavelength dependence of the penetration depth is not a confounding factor for the spectroscopy meas-

**FIGURE 1 Overview of the hyperspectral snapshot camera system and its specifications.** Images of the forearm of human volunteers were acquired by the hyperspectral snapshot camera, which was mounted in a black box containing four halogen light (broad band illumination) spots on top of each corner (A). The spectral response covers the wavelength range of 470-630 nm for the VIS sensor and 600-950 nm for the NIR sensor (B). The experimental prototype of the camera consists of three camera sensors (RGB-VIS-NIR) which are pixel aligned on the prism (37,38) and a 35 mm lens with a f/2.8 aperture (C). The camera is based on a tiled filter approach where pixels are individually filtered with narrow Fabry-Pérot bandpass filters (bandwidth ≈ 12 nm each). Each image acquisition leads to a hypercube with a spatial resolution of 2048 x 1080 pixels and 41 spectral bands after processing (D).

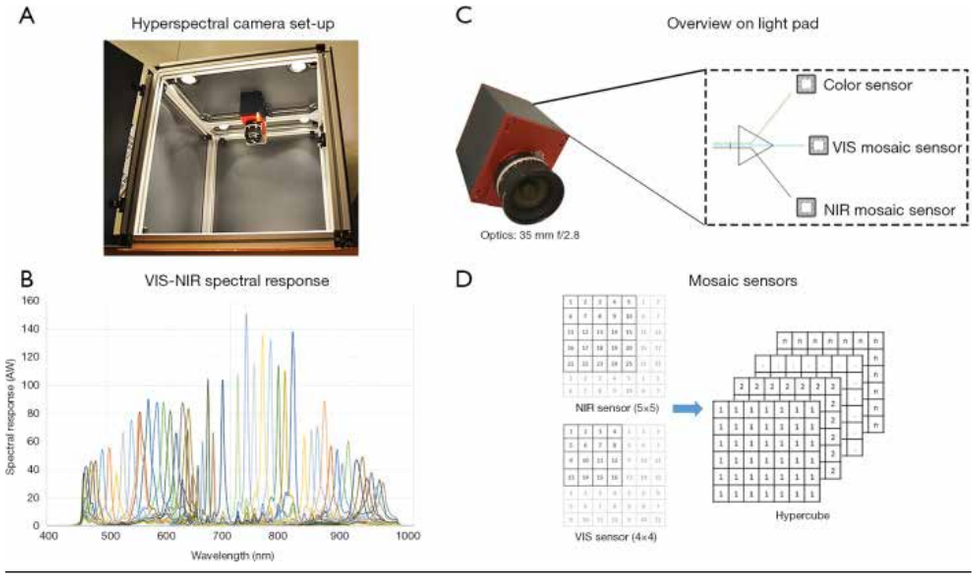

urements because the fiber (probe) determines the penetration depth and is approximately equal over the wavelength range measured. This is not the case for the hyperspectral camera where longer wavelength photons also contribute to the acquired signal. We determined the effective light collection area of the camera system to be approximately 320 by 320 microns per pixel. $StO_2$ fitting was performed using software developed in-house, written in C++ programming language. It has been shown that the recovery of blood $StO_2$ in patients with skin types 1-3 is not affected by skin type.[15] Hyperspectral data were not corrected for skin type. Saturation maps were converted to color-based maps for improved interpretation (blue: low $StO_2$; red: high $StO_2$). The fitted $StO_2$ was not allowed to be greater than 100%, nor lower than 0%, for both spectroscopy and the hyperspectral camera system. The $StO_2$ maps were imported into MeVisLab (MeVis Medical Solutions AG, Bremen, Germany), and skin $StO_2$ subsequently calculated based on selecting corresponding ROI, which were located on a planar surface of the forearm and marked with a dermatological marker at the beginning of each measurement procedure. For all analyses, the marked area on the volar side of the forearm was chosen as the ROI. Care was taken during the repeated measurements to choose an ROI as close as possible to the previous used ROI, using the LSCI and hyperspectral images as reference. In the analysis software, the ROI was manually selected using the dermatological markers as reference point.

### Statistical analysis

Continuous variables were presented as mean values + standard deviations ([SD]) in normal distributed data or as median values (interquartile range [IQR]) in non-normal distributed data, respectively. The Mann-Whitney U-test, independent t-test, paired t-test and ANOVA test were used for comparison of continuous variables. For categorical variables, a Chi-Squared test was used to compare groups. Correlations were calculated by using the mean correlation coefficient (Pearson $R^2$). Correlation coefficients were interpreted according to Schober et al.[22] A P-value below 0.05 (two-sided) was considered statistically significant. SPSS Statistics for Windows, version 23.0 (IBM Corp., Armonk, N.Y., USA) was used for the statistical analysis. Graphs were created using Graphpad 8.0 (GraphPad Software, Inc., San Diego, CA).

## RESULTS

### Spectral fitting

*Figure 2* shows the variation in the percentage (%) of $StO_2$ measured using single fiber reflectance and hyperspectral imaging. The baseline $StO_2$ measured before occlusion using the fiber optic reflectance technique is significantly lower than that using hyperspectral imaging, but is consistent with previous measurements in the skin of the inner forearm.[15] During occlusion, the skin blood volume fraction is reduced (data not shown); consequently, there are large confidence intervals on these data points. Upon reperfusion, blood volume increases and subsequently returns to near baseline levels; in this regime, no significant differences in $StO_2$ levels were found using these measurement techniques. However, it is important to note that there are substantial uncertainties in both measurements of $StO_2$ due to the relatively low blood volume in the interrogated region, as we have described previously.[9]

*Occlusion-reperfusion experiments*

Measurement of $StO_2$ levels using a linear fitting algorithm was feasible in all volunteers during all phases of occlusion and reperfusion. General analysis showed a statistically significant (P<0.001) decrease in cutaneous $StO_2$ levels from 78.3% (SD: 15.3) at baseline to 60.6% (SD: 19.8) at the end of occlusion phase (*Figure 3*). Subgroup analysis showed that baseline $StO_2$ differed significantly between the subjects recruited at LUMC and MSKCC (mean $StO_2$: 69.9 versus 86.6 %, P<0.001), with a decrease in $StO_2$ of 20.3 and 14.3 %, respectively. Overall $StO_2$ levels returned to baseline at the end of the reperfusion phase, which was after 12 minutes (mean $StO_2$: 70.4 versus 85.1 %, for the two cohorts respectively). An additional perfusion analysis was performed in the LUMC cohort using LSCI and showed a strong correlation (Pearson $R^2$: 0.86) of blood flow with $StO_2$ levels during occlusion-reperfusion phases (*Figure 4*).

Moreover, $StO_2$ correlations between the two measurement days were analysed, resulting in an overall Pearson $R^2$ of 0.85, although a higher correlation was observed in the LUMC cohort (Pearson $R^2$: 0.92) compared to the MSKCC cohort (Pearson $R^2$: 0.77). Individual analyses of all patients showed





**FIGURE 2 Comparison of single fiber reflectance spectroscopy with hyperspectral imaging for blood oxygen saturation ($StO_2$) detection.** It shows the variation in the percentage (%) of $StO_2$ measured using single fiber reflectance and hyperspectral imaging. The baseline $StO_2$ measured before occlusion using the fiber optic reflectance technique is significantly lower than that using hyperspectral imaging. During occlusion, the skin blood volume fraction is reduced. Upon reperfusion, blood volume increases and subsequently returns to near baseline levels. It is important to note that there are substantial uncertainties in both measurements of $StO_2$ due to the relatively low blood volume in the interrogated region.
*StO2: oxygen saturation.*

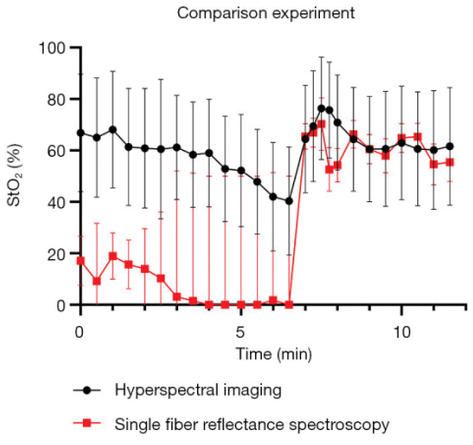


**FIGURE 4 Correlation of cutaneous blood oxygen saturation with vascular perfusion during occlusion-reperfusion experiments in the LUMC cohort.** Average of separate measurements of cutaneous blood oxygen saturation on measurement day 1 and 2 show a strong correlation with corresponding perfusion assessments by laser speckle imaging during occlusion-reperfusion experiments. Occlusion was performed after two minutes baseline measurements for a total of five minutes. Both oxygen saturation and blood flow levels returned to baseline after 12 minutes.
*AU: arbitrary units; StO2: oxygen saturation.Effect of local vasodilatation*

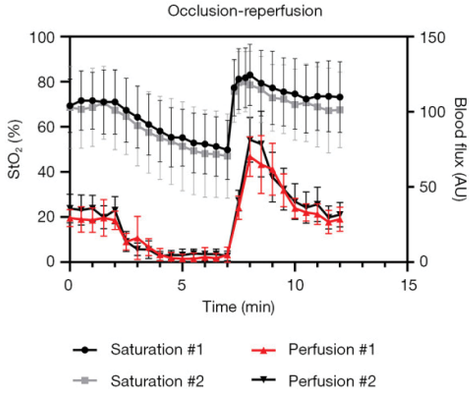


**FIGURE 3 A typical example of the effect of vascular occlusion on superficial cutaneous oxygen saturation determined using hyperspectral imaging (color, saturation and saturation overlay maps) and perfusion determined by Laser Speckle Contrast Imaging (LSCI, perfusion maps).**

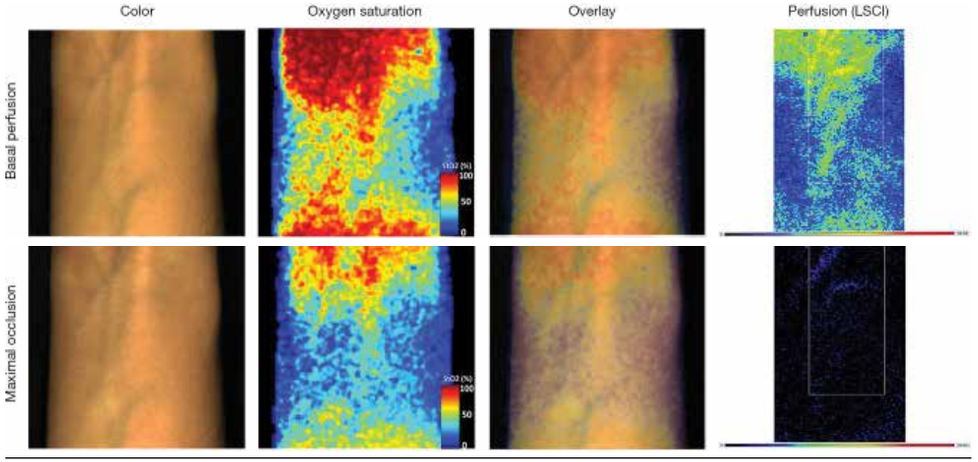

an excellent correlation in 13 (81%), a strong correlation in 2 (13%) and a fair correlation in 1 (6%) subject.

*Effect of local vasodilatation*

After application of capsaicin cream, statistically significant increases in blood flow due to vasodilatation (P<0.001) were measured (with LSCI) within the most superficial layers of the skin; blood flow increased from 76.7 (SD:11.1) to 146.9 (SD: 38.4) arbitrary units (AU). However, cutaneous $StO_2$ did not change significantly (P=0.927) after application of capsaicin in the most superficial layers (*Figure 5*). Nevertheless, mean $StO_2$ levels in the MSKCC cohort were significantly (P<0.001) higher compared to the LUMC cohort.

## DISCUSSION

In this multicenter study, we explored the feasibility of a novel snapshot hyperspectral camera system for non-invasive detection of superficial cutaneous $StO_2$ under different physiological conditions in normal, healthy human volunteers. Strong correlations were found between the $StO_2$ measurements acquired during occlusion-reperfusion experiments. Furthermore, local vasodilation did result in an increased cutaneous vascular flux, but not in a significantly higher tissue $StO_2$ level in the most superficial layers of the skin.

In general, non-invasive imaging using endogenous contrast for the detection and monitoring of cutaneous $StO_2$ levels is advantageous, and may offer distinct benefits over methods requiring injection of exogenous contrast agents for specific indications. In the perioperative setting, there is a general lack of real-time non-invasive imaging tools for reliably monitoring alterations in perfusion and oxygenation status. In the future, such tools could potentially improve patient care outcomes by their ability to detect decreased $StO_2$ about surgical margins, wound sites, and sites of graft placement, for instance, in addition to guiding clinical management. Moreover, direct skin contact is not needed for such measurements. To our knowledge, this is the first study implementing an existing and validated algorithm for quantitatively analysing cutaneous $StO_2$ by utilizing a snapshot hyperspectral camera system in human subjects.

**FIGURE 5 Tissue oxygen saturation levels after application of capsaicin cream, including subgroup analysis per cohort (LUMC vs MSKCC validation cohort).** Cutaneous $StO_2$ levels did not change significantly after application of capsaicin in the most superficial layers.
*MSKCC: Memorial Sloan Kettering Cancer Center; LUMC: Leiden University Medical Center; StO2: oxygen saturation.*

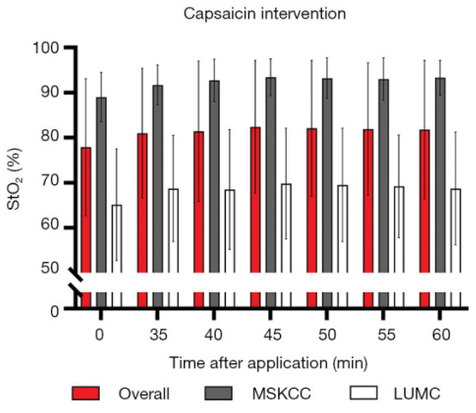


Recently, more systems have been introduced into the clinic for $StO_2$ monitoring of the bowel, skin and cerebral cortex.[23–27] Current available hyperspectral camera systems have longer acquisition times than those used by this snapshot hyperspectral camera system, precluding the types of evaluations performed herein. Moreover, other camera systems lack the ability to quantitatively monitor changes in tissue $StO_2$ by using relative oxyhemoglobin or deoxyhemoglobin measurements as surrogate markers for tissue $StO_2$. Our data supports the hypothesis that quantitative cutaneous $StO_2$ imaging is feasible and reproducible with good correlations in human volunteers. This is also underlined by the fact that the performance of this system was independently evaluated at two different centers.

However, a few limitations are noteworthy. First, as the study recruited a relatively small number of normal, healthy human volunteers, the results may not be representative of larger patient populations, who may exhibit a variety of baseline characteristics. Second, the hyperspectral camera system has 41 wavelength bands divided over two mosaic sensors, which implies a lower spatial resolution (i.e., either 2 or 2.5 times) that of the original resolution, noted earlier, although this was found not to be a limiting factor in the current study. Furthermore, we decided to use contact point optical spectroscopy as a reference for comparing the $StO_2$ of the most superficial layers of tissue. Based on these comparisons, a fitting algorithm was proposed, in order to quantify $StO_2$, which has been validated in other clinical studies.[21] Nevertheless, we acknowledge that other reference hyperspectral imaging devices suitable for $StO_2$ detection could have also been used to supplement the perfusion data obtained by LSCI, which was unfortunately only performed one center. Moreover, a general drawback of hyperspectral imaging is that penetration depths of only several hundred micrometres to a maximum of multiple millimetres can be interrogated, which are wavelength-dependent, limiting the applicability of this optical tool to assessments of the most superficial layers of the target tissue of interest (up to the dermis at the red end of the spectrum).[28] Nevertheless, compared to contact point spectroscopy, it seems that the sampling depth is greater for the hyperspectral camera, resulting in higher $StO_2$ values (*Figure 2*). The simple linear model of light transport in tissue we have used in the present study is based on assumptions that the scattering remains constant, and that the pathlength traveled is equal for all photons over the wavelength range of interest. The reduced scattering coefficient is known to vary across the visible spectrum. This means that the calculated absorbance of the tissue may be overestimated at the red end of the spectrum. Furthermore, the algorithm did not account for the effect of melanin, as it is very difficult to separate the influence of scattering and the absorption due to melanin without measuring in the blue-green portion of the visible spectrum. Finally, alterations in penetration depth and sampling volume may occur during occlusion, given that the distribution of absorbers changes. While these changes were not accounted for in our analysis, it was felt that the scattering properties of tissues in the forearm would not be significantly affected by occlusion remote from that site.

A high inter-patient variability in cutaneous $StO_2$ values was observed in this study, both within and across patient cohorts, however the differences in $StO_2$ values were not significant between the two measurement days in both cohorts, which was also demonstrated by a Pearson $R^2$ value of 0.85. Controversial data has been published for baseline cutaneous $StO_2$ values in the range of 50-96%, depending on the camera system used and region of interest in which the measurement was taken.[27,29–32] One explanation for the differences in $StO_2$ within cohorts may be attributed to gender differences. For example, in the LUMC cohort, females tended to have a higher baseline $StO_2$ or more subcutaneous fat. It has been demonstrated that fatty tissues are relatively poorly oxygenated, although the BMI included for all volunteers was within the normal range.[9,33] A high inter-patient variability may also be attributed to known wavelength-dependent and depth-dependent variations in cutaneous $StO_2$ values, that is, superficial skin layers exhibit lower $StO_2$ values than those found for the well-perfused deeper tissue layers. Another possible explanation is that skin temperature might have led to differences in cutaneous $StO_2$ between the two cohorts, as this parameter was significantly different at baseline. The large differences in baseline $StO_2$ between both cohorts could probably be explained by the room temperature, which was significantly higher at MSKCC, leading to increased vasodilatation with subsequent higher $StO_2$ levels, as previously demonstrated.[31] Moreover, the skin temperature could have been affected by the heat of the light sources, although $StO_2$ levels in both groups were similar at the beginning and at the end of the measurement period. Interestingly, capsaicin interventions did not result in significantly higher $StO_2$ levels for either patient cohort. Through activation of the TLPRV1 receptor, capsaicin is known to cause an increased neurogenic vasodilation (amongst other responses, such as flare, pain, heat, and cutaneous hypersensitivity). This challenge showed that a flare and increased vasodilation did not significantly influence $StO_2$ measurements, which might be explained by the fact that healthy volunteers are already well oxygenated under normal circumstances and consequently the effect of local vasodilation is minimal. Nevertheless, there is still a trend towards higher saturation levels after application of capsaicin, however due to the expected limited effect on the $StO_2$ and the small sample size of our study, the detected $StO_2$ values are not changed significantly.

Besides hyperspectral imaging, other non-invasive techniques for $StO_2$ mapping, such as optical coherence tomography (near-infrared) spectroscopy, or photoacoustic imaging can be

used, although these techniques have significant shortcomings, including the offering of only a limited field of view and/or an inability to acquire imaging data, respectively.[3,34] Recently, another imaging technique termed Single Snapshot of Optical Properties (SSOP), which is based on the Spatial Frequency Domain Imaging (SFDI) principle, allows real-time quantitative imaging of tissue oxygenation.[35,36]

Future work will focus on developing a more user-friendly system and evaluating other sources for better controlled light conditions. Furthermore, data analysis steps and software will be improved to enable real-time intraoperative $StO_2$ mapping, as current frame rate settings are only about 16 frames per second. Additional refinements, such as mounting the camera head, including light sources, on a stable arm, are needed to efficiently translate and implement such a prototype system into a variety of clinical settings. Importantly, $StO_2$ measurements are expected to be similar for both elderly adults and younger individuals.[21] In this proof-of-concept study, we focused on the assessment of cutaneous oxygenation status. For intraoperative applications, however, additional technical issues that may limit accuracy e.g., variations in skin thickness, would need to be addressed. In the present work, we attempted to minimize such contributions by imaging the inner aspect of the arm. Different applications and clinical conditions may necessitate specific mechanical solutions to be advanced, which will need to be evaluated and tested. These additional capabilities, however, would also enable high-resolution, full-field $StO_2$ imaging to be combined, in the same setting, with other real-time imaging strategies, such as fluorescence imaging that utilizes near-infrared wavelengths for the visualisation of multiple fluorophores. Such a hybrid system could also potentially allow for the simultaneous assessment of tissue $StO_2$ and perfusion. As this camera system has only been evaluated in healthy volunteers, it will be necessary to validate its clinical utility in a more heterogenous patient population. Future implementation will therefore focus on assessing feasibility under clinical circumstances such as patients with vascular conditions arising from, for example, diabetes mellitus, or during reconstructive surgical procedures.

## CONCLUSIONS

In conclusion, this early-stage multicenter clinical trial demonstrated the feasibility of utilizing a novel snapshot hyperspectral camera system for the detection of cutaneous $StO_2$ in normal, healthy human volunteers. These findings are being used to inform next-stage camera system developments for monitoring oxygenation status in both non-surgical oncologic and peri-operative settings. In these settings, patients with vascular disease might potentially be risk-stratified for improving clinical decision-making and outcomes.

## *REFERENCES*


1. Arsenault KA, Al-Otaibi A, Devereaux PJ, Thorlund K, Tittley JG, Whitlock RP. The use of transcutaneous oximetry to predict healing complications of lower limb amputations: a systematic review and meta-analysis. Eur J Vasc Endovasc Surg 2012;43:329-36.
2. Wilkins EG, Hamill JB, Kim HM, Kim JY, Greco RJ, Qi J, Pusic AL. Complications in Postmastectomy Breast Reconstruction: One-year Outcomes of the Mastectomy Reconstruction Outcomes Consortium (MROC) Study. Ann Surg 2018;267:164-70.
3. Yi J, Chen S, Backman V, Zhang HF. In vivo functional microangiography by visible-light optical coherence tomography. Biomed Opt Express 2014;5:3603-12.
4 Lu G, Fei B. Medical hyperspectral imaging: a review. J Biomed Opt 2014;19:10901.
5 Zherebtsov E, Dremin V, Popov A, Doronin A, Kurakina D, Kirillin M, Meglinski I, Bykov A. Hyperspectral imaging of human skin aided by artificial neural networks. Biomed Opt Express 2019;10:3545-59.
6 Dremin V, Marcinkevics Z, Zherebtsov E, Popov A, Grabovskis A, Kronberga H, Geldnere K, Doronin A, Meglinski I, Bykov A. Skin complications of diabetes mellitus revealed by polarized hyperspectral imaging and machine learning. IEEE Trans Med Imaging 2021;Pp.
7 Kashani AH, Kirkman E, Martin G, Humayun MS. Hyperspectral computed tomographic imaging spectroscopy of vascular oxygen gradients in the rabbit retina in vivo. PLoS One 2011;6:e24482.
8 Gao L, Smith RT, Tkaczyk TS. Snapshot hyperspectral retinal camera with the Image Mapping Spectrometer (IMS). Biomed Opt Express 2012;3:48-54.
9 Amelink A, Robinson DJ, Sterenborg HJ. Confidence intervals on fit parameters derived from optical reflectance spectroscopy measurements. J Biomed Opt 2008;13:054044.
10 Noguchi K, Matsuzaki T, Sakanashi M, Hamadate N, Uchida T, Kina-Tanada M, Kubota H, Nakasone J, Sakanashi M, Ueda S, Masuzaki H, Ishiuchi S, Ohya Y, Tsutsui M. Effect of caffeine contained in a cup of coffee on microvascular function in healthy subjects. J Pharmacol Sci 2015;127:217-22.
11 Gillespie JA. Vasodilator properties of alcohol. Br Med J 1967;2:274-7.
12 Manni F, van der Sommen F, Zinger S, Shan C, Holthuizen R, Lai M, Buström G, Hoveling RJM, Edström E, Elmi-Terander A, de With PHN. Hyperspectral Imaging for Skin Feature Detection: Advances in Markerless Tracking for Spine Surgery. Applied Sciences 2020;10(12):4078.
13 Matheus ASM, da Matta MFB, Clemente ELS, Rodrigues MLG, Valenca DCT, Gomes MB. Sensibility and specificity of laser speckle contrast imaging according to Endo-PAT index in type 1 diabetes. Microvasc Res 2018;117:10-5.
14 Birkhoff WAJ, Heuberger J, Post TE, Gal P, Stuurman FE, Burggraaf J, Cohen AF. Recombinant human erythropoietin does not affect several microvascular parameters in well-trained cyclists. Physiol Rep 2018;6:e13924.
15 Brooks S, Hoy CL, Amelink A, Robinson DJ, Nijsten TE. Sources of variability in the quantification of tissue optical properties by multidiameter single-fiber reflectance and fluorescence spectroscopy. J Biomed Opt 2015;20:57002.
16 Hoy CL, Gamm UA, Sterenborg HJ, Robinson DJ, Amelink A. Method for rapid multidiameter single-fiber reflectance and fluorescence spectroscopy through a fiber bundle. J Biomed Opt 2013;18:107005.
17 Stegehuis PL, Boogerd LS, Inderson A, Veenendaal RA, van Gerven P, Bonsing BA, Sven Mieog J, Amelink A, Veselic M, Morreau H, van de Velde CJ, Lelieveldt BP, Dijkstra J, Robinson DJ, Vahrmeijer AL. Toward optical guidance during endoscopic ultrasound-guided fine needle aspirations of pancreatic masses using single fiber reflectance spectroscopy: a feasibility study. J Biomed Opt 2017;22:24001.
18 Buntinx L, Vermeersch S, de Hoon J. Development of anti-migraine therapeutics using the capsaicin-induced dermal blood flow model. Br J Clin Pharmacol 2015;80:992-1000.
19 Toivonen ME, Rajani C, Klami A. Snapshot hyperspectral imaging using wide dilation networks. Machine Vision and Applications 2020;32:9.
20 Amelink A, Bard MP, Burgers SA, Sterenborg HJ. Single-scattering spectroscopy for the endoscopic analysis of particle size in superficial layers of turbid media. Appl Opt 2003;42:4095-101.
21 Middelburg TA, Kanick SC, de Haas ER, Sterenborg HJ, Amelink A, Neumann MH, Robinson DJ. Monitoring blood volume and saturation using superficial fibre optic reflectance spectroscopy during PDT of actinic keratosis. J Biophotonics 2011;4:721-30.
22 Schober P, Boer C, Schwarte LA. Correlation Coefficients: Appropriate Use and Interpretation. Anesth Analg 2018;126:1763-8.
23 Barberio M, Longo F, Fiorillo C, Seeliger B, Mascagni P, Agnus V, Lindner V, Geny B, Charles AL, Gockel I, Worreth M, Saadi A, Marescaux J, Diana M. HYPerspectral Enhanced Reality (HYPER): a physiology-based surgical guidance tool. Surg Endosc 2020;34:1736-44.
24 Giannoni L, Lange F, Davies AL, Dua A, Gustavson B, Smith KJ, Tachtsidis I. Hyperspectral Imaging of the Hemodynamic and Metabolic States of the Exposed Cortex: Investigating a Commercial Snapshot Solution. Adv Exp Med Biol 2018;1072:13-20.
25 He Q, Liu T, Wang RK. Enhanced spatial resolution for snapshot hyperspectral imaging of blood perfusion and melanin information within human tissue. J Biophotonics 2020;13:e202000019.
26 Rubins U, Marcinkevics Z, Cimurs J, Saknite I, Kviesis-Kipge E, Grabovskis A. Multimodal Device for Real-Time Monitoring of Skin Oxygen Saturation and Microcirculation Function. Biosensors (Basel) 2019;9.
27 Nkengne A, Robic J, Seroul P, Gueheunneux S, Jomier M, Vie K. SpectraCam(®) : A new polarized hyperspectral imaging system for repeatable and reproducible in vivo skin quantification of melanin, total hemoglobin, and oxygen saturation. Skin Res Technol 2018;24:99-107.
28 Zhang R, Verkruysse W, Choi B, Viator JA, Jung B, Svaasand LO, Aguilar G, Nelson JS. Determination of human skin optical properties from spectrophotometric measurements based on optimization by genetic algorithms. J Biomed Opt 2005;10:024030.
29 Yudovsky D, Pilon L. Retrieving skin properties from in vivo spectral reflectance measurements. J Biophotonics 2011;4:305-14.
30 Vyas S, Banerjee A, Burlina P. Estimating physiological skin parameters from hyperspectral signatures. J Biomed Opt 2013;18:57008.
31 Jafari-Saraf L, Wilson SE, Gordon IL. Hyperspectral image measurements of skin hemoglobin compared with transcutaneous PO2 measurements. Ann Vasc Surg 2012;26:537-48.
32 Chin MS, Freniere BB, Lo YC, Saleeby JH, Baker SP, Strom HM, Ignotz RA, Lalikos JF, Fitzgerald TJ. Hyperspectral imaging for early detection of oxygenation and perfusion changes in irradiated skin. J Biomed Opt 2012;17:026010.
33 Kabon B, Nagele A, Reddy D, Eagon C, Fleshman JW, Sessler DI, Kurz A. Obesity decreases perioperative tissue oxygenation. Anesthesiology 2004;100:274-80.
34 Li M, Tang Y, Yao J. Photoacoustic tomography of blood oxygenation: A mini review. Photoacoustics 2018;10:65-73.
35 Ghijsen M, Lentsch GR, Gioux S, Brenner M, Durkin AJ, Choi B, Tromberg BJ. Quantitative real-time optical imaging of the tissue metabolic rate of oxygen consumption. J Biomed Opt 2018;23:1-12.
36 Ghijsen M, Choi B, Durkin AJ, Gioux S, Tromberg BJ. Real-time simultaneous single snapshot of optical properties and blood flow using coherent spatial frequency domain imaging (cSFDI). Biomed Opt Express 2016;7:870-82.
37 IMEC (2021, April 2) https://www.imec-int.com/en/hyperspectral-imaging.
38 Geelen B, Tack N, Lambrechts A. A compact snapshot multispectral imager with a monolithically integrated per-pixel filter mosaic. SPIE MOEMS-MEMS. SPIE; 2014.

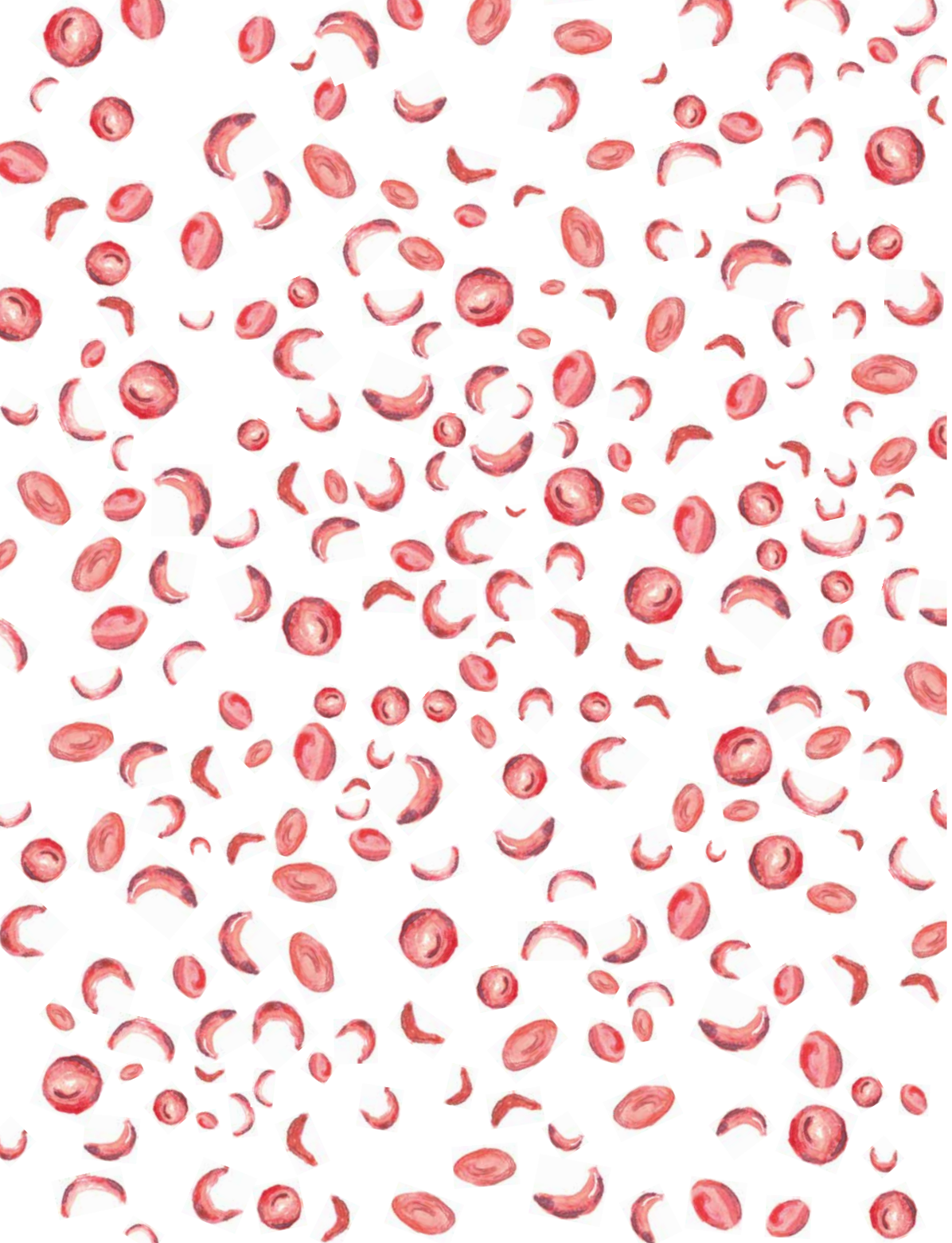



# SUMMARY

In this thesis, we have discussed the ability and inability of the microvasculature to be valuable in measuring the pharmacodynamic effects of compounds. This was done in seven chapters, using various angles to evaluate the microvasculature.

**Chapter two** provides an overview on the application of microcirculation measurements in current practice. Emphasis was put on the clinical utility of the minimal-invasive microvascular imaging techniques that are currently commercially available for skin and retinal microcirculation assessments. Included in this review are the most common used cutaneous and retinal microvascular measurements devices and promising new techniques alongside with challenges and description of minimal invasive biochemical tests to provide guidance when investigating the microcirculation.

In **chapter three**, microvascular functionality was explored in 8 sickle cell disease patients and matched healthy volunteers with two new devices: the laser speckle contrast imager (LSCI) and the retinal function imager. Both devices showed excellent repeatability (CVC of 8.5% 9.5%, 7.6% and 7.7% respectively) and between measurements on one day (CVC of 7.0%, 7.7%, 7.6% and 4.7% respectively) and were able to measure a difference in microvascular functionality between the patients and healthy volunteers, making these devices feasible for further use in clinical microvascular research. Although the retinal function imager showed great potential, acquisition of the images had a steep learning curve.

**Chapter four**: The results of the study in chapter three were used to set up a larger study in which microvascular measurements were compared with cerebral hemodynamics using MRI. A total of 17 sickle cell patients and 6 healthy volunteers were included. An increased cerebral and skin blood flow was found in sickle cell patients compared to controls. Furthermore microvascular skin measurements (basal flow) were strongly correlated [ASL vs. LSCI: r = 0.70; PC-MRI vs. LSCI: r = 0.75] with MRI measurements. This suggests that cutaneous microvascular measurements might be a low cost, non-invasive alternative method to obtain details on the hemodynamic state of sickle cell patients.

**Chapter five**: Retinal microcirculation and retinal oximetry were quantitatively analyzed using fractal analysis in 8 sickle cell patients and matched healthy volunteers. Oximetry pictures and non-invasive capillary perfusion maps (nCPM) were obtained by the retinal function imager. No significant difference was observed for the fractal analysis between the patients and healthy controls, however significantly lower oxygenated Hb levels (Effect size (ES)=850.3; 95% CI 69.16, 1631; p=0.04), and (ES=919.9; 95% CI 171.4, 1668; p=0.02). were detected in sickle cell patients as compared to the healthy controls in the temporal quadrants, suggesting that in sickle cell patients before any structural microvascular changes are present, functional abnormalities could be observed in oximetry measurements.

**Chapter six** provides an exploration of a new tool the miniaturized Dynamic Light Scattering (MDLS). The MDLS was evaluated in 16 patients with different vascular abnormalities for which they used vitamin K antaganost (amongst them cardiac dysfunction, protein c deficiency pulmonary thrombosis), 8 sickle cell disease patients and 8 unmatched healthy volunteers, by having two measurements on two different days and was benchmarked against LSCI measurements and several biochemical and hematological measurements. There was a large intra-subject variability in MDLS (depending on the type of measurement up to CV> 150%) and none of the endpoints discriminated between the patients and the healthy controls. LSCI and laboratory measurements were stable over time and were able to measure difference between the groups, suggesting that the MDLS device is not suitable for measuring pharmacologically induced changes in microcirculation.

**Chapter seven**: In this study, we evaluated the effect of recombinant human erythropoietin (RHUEPO) on the cutaneous microvascular function in well-trained cyclists using LSCI. Forty-eight subjects received a weekly dose of either RHUEPO or placebo (1:1 ratio) for 8 weeks, and LSCI was performed

at baseline, after a maximal exercise test in week 6, and before maximal exercise in week 8. Despite an increase in hematocrit levels in the RHUEPO- treated group, we found no statistically significant difference in microvascular function measured between the RHUEPO-treated group and the placebo group. The results of this study suggest that the increased hematocrit levels in RHUEPO-treated well-trained cyclists are not associated with changes in microvascular measurements using LSCI.

**Chapter eight:** In this study, hyperspectral imaging was evaluated by using a snapshot hyperspectral camera that can measure tissue oxygenation non-invasively using relevant wavelengths in the VIS-NIR region (450-950 nm) and benchmarked the outcomes against LSCI. Several challenges were explored in 16 healthy volunteers including occlusion-reperfusion of the brachial artery and measurements of local changes in skin oxygenation and blood flow after applying a local vasodilator (capsaicin-based cream) and a local vasoconstrictor (brimonidine gel) and outcomes were compared to measurements of an untreated area of the skin. Hyperspectral results (cutaneous $StO_2$ levels) were correlated to the haemoglobin oxygen saturation measured by an oximeter, furthermore a strong correlation (Pearson $R^2$: 0.86) of blood flow with $StO_2$ levels during occlusion-reperfusion phases was observerd. The results of this pilot study showed that the snapshot hyperspectral camera was able to detect different levels of cutaneous $StO_2$ in human volunteers.

## DISCUSSION

Due to technological advances in the last decades the possibilities for microvascular measurements have taken a flight. In this thesis, we have investigated several new devices that have been developed or are that are currently under development and we investigated the applicability of several novel microcirculation measurement devices for their utility in the clinic or in a clinical research setting.

As outlined in chapters one and two, new devices must be validated before the can be used in clinical research. This validation process consists of several steps that allows the investigators to determine how precise the measurements are, what the variability of the endpoints is and if the device can pick up diseases or pharmacodynamic effects of compounds. In this thesis, we have attempted to validate several devices, and there are several points that can be discussed. First, the measurements should be fairly easy to perform and operator dependency should be limited. This is applicable for the LSCI, however for other devices such as the RFI or MDLS, there is a steep learning curve and large operator dependency, hampering the possibility of these devices to provide the researchers with quality data during the course of a study. Therefore for experimental devices such as the hyperspectral camera, it is essential that findings on the applicability and validity are taken into account.

The nature of the microvasculature and in particular its accessibility make it a potentially valuable biomarker, although this does require the devices used to evaluate the microvasculature to be as minimally invasive as possible, which is certainly the case for most devices investigated in this thesis. And finally, although most imaging devices require a large initial investment (see chapter 2), the devices have in general low maintenance and low operational costs.

The role of microvascular dysfunction in the pathophysiology of several diseases is well known, and is not only limited to vascular disease but also in ischemic nerve damage, kidney disease and retinal dysfunction. Moreover recent research provides us the insight that microvascular alterations might be an early predictor for onset of certain disease. This has been well studied in ophthalmology with relation to stroke[1], kidney damage and cardiovascular disease.[2,3] Besides the traditional risk factors for cardiovascular diseases such as smoking, hypertension and obesity a substantial proportion of cardiovascular disease is not explained by these risk factors. Therefore more extensive investigation into the mechanisms behind microvascular dysfunction might provide novel insights into the biomarkers that can be used as key endpoints for which devices can then be developed.

In the current global health crisis due to the SARS-CoV-2 virus, evidence is emerging for a key role of the microvasculature in critically ill patients. In COVID-19 severe organ damage has been observed related to a hypercoagulable state.[4] The underlying cause might be microvascular endothelial dysfunction leading to this hypercoagulable state.[5,6] Further research is warranted to evaluate if microvascular assessment can improve risk stratification of patients, or if the microvasculature is a target in the prevention or treatment of the hypercoagulable state.





## FUTURE DIRECTIONS

There are plenty novel devices claiming to enable non-invasive measurements of the microcirculation, however for successful wide implementation of microvascular measurements, it is essential that implementation of these devices in clinical studies is regulated in such a way that the outcome of the studies can be relied upon. The new EMA guidelines foresee in this problem and must be adhered to when implementing novel devices in clinical studies.

We foresee a broader implementation of microvascular measurements, not only in the clinic but also in the home situation. For example, PPG measurements are integrated in wearables or mobile devices more and more. As microcirculation might play a dominant role as predictor for certain disease, home monitoring using mobile devices may allow early detection of, for example, myocardial infarction or acute heart failure and provide a time window for cardiologists to take action, preventing hospital admission or worse. Furthermore, microvascular measurements might be more often used as a method to obtain more information about the pharmacodynamics in (early phase) pharmacological research, certainly considering the key role for nitric oxide, also in immune activation and metabolic disease. Currently microvascular measurements are not frequently applied in studies, however due to the relatively low cost, low burden for patients and useful insights this could be valuable add on in pharmacological trials.

Although there have been decades with microvascular measurements it is not only until the last two decades that microvascular research has taken a flight. New imaging techniques, more advanced algorithms for analysis and better computing processing have established microvascular research methods. However before wide implementation these methods should be tested for their validity an integrity. Microvascular research has already brought us interesting new insight in the pathophysiology of diseases and we are only at the beginning of a new era of microvascular research. In this thesis we hope to have contributed with our validation studies of new and existing microcirculation measurement tools to a wider implementation of microvascular measurements in current clinical and research practice.

### *REFERENCES*


1 Wong TY, Klein R, Couper DJ, Cooper LS, Shahar E, Hubbard LD, et al. Retinal microvascular abnormalities and incident stroke: the Atherosclerosis Risk in Communities Study. The Lancet. 2001;358(9288):1134-40.

2 Wong TY, Coresh J, Klein R, Muntner P, Couper DJ, Sharrett AR, et al. Retinal microvascular abnormalities and renal dysfunction: the atherosclerosis risk in communities study. Journal of the American Society of Nephrology. 2004;15(9):2469-76.

3 Wong TY, Klein R, Klein BE, Tielsch JM, Hubbard L, Nieto FJ. Retinal microvascular abnormalities and their relationship with hypertension, cardiovascular disease, and mortality. Survey of ophthalmology. 2001;46(1):59-80.

4 Wadman M, Couzin-Frankel J, Kaiser J, Matacic C. How does coronavirus kill. Clinicians trace a ferocious rampage through the body, from brain to toes. 2020:1502-3.

5 Green SJ. Covid-19 accelerates endothelial dysfunction and nitric oxide deficiency. Microbes Infect. 2020;22(4-5):149-50.

6 Colantuoni A, Martini R, Caprari P, Ballestri M, Capecchi PL, Gnasso A, et al. COVID-19 Sepsis and Microcirculation Dysfunction. Frontiers in Physiology. 2020;11(747).

# NEDERLANDSE SAMENVATTING

Cardiovasculaire ziekten zijn een van de belangrijkste oorzaken van overlijden, met 17,7 miljoen sterfgevallen in 2015, hoewel dit de laatste decennia aanzienlijk is gedaald. Momenteel is er voor de meeste macrovasculaire ziekten een behandelingsoptie beschikbaar. Interventies gericht op de microcirculatie zijn echter schaars. De evaluatie van behandelingen die de microcirculatie beïnvloeden is moeilijk vanwege het ontbreken van gestandaardiseerde geaccepteerde technieken. Recente studies hebben echter aangetoond dat grote macrovasculaire ziekten vooraf worden gegaan door microvasculaire afwijkingen en dat microvasculaire metingen sterke voorspellers zijn van langdurige cardiovasculaire ziekte en overleving. Vroege interventies gericht op microvasculaire afwijkingen kan daarom latere cardiovasculaire problemen uitstellen.

De microcirculatie speelt een cruciale rol in weefselperfusie, de uitwisseling van voedingsstoffen, zuurstof en koolstofdioxide tussen bloed en interstitieel vocht, en in vasculaire homeostase. Endotheelweefsel is een belangrijke regulator van de microcirculatie. Fysiologische meting van de microcirculatie is uitdagend vanwege de ruimtelijk heterogene structuur en variabiliteit in perfusie over tijd en onder verschillende omstandigheden, zoals temperatuur.

De microcirculatie is het gedeelte van het bloed en lymfestelsel wat de arteriolen, capillairen, venules en lymfatische capillairen omvat. De hoeveelheid bloedstroom in de (micro)circulatie wordt voornamelijk gereguleerd door de arteriolen. De endotheliale weefsels in de bloedvaten reageren op verschillende stimuli, waaronder neuropeptiden, neurotransmitters, verschillende hormonen en distensie van de vaten als gevolg van een verhoogde bloeddruk. De belangrijkste hormonen die door de endotheelweefsels worden afgescheiden, zijn stikstofmonoxide (NO) en endotheline-1 (ET-1).

Endotheliale disfunctie speelt een rol in de pathofysiologie van atherosclerose en is een sterke voorspeller van atherosclerotische cardiovasculaire ziekte. Endotheliale disfunctie is geassocieerd met cardiovasculaire risicofactoren zoals diabetes, dyslipidemie, hypertensie, roken en veroudering. Klinische studies hebben aangetoond dat de endotheliale functie kan worden verbeterd door behandeling met angiotensineconverterende enzym (ACE) -remmers, antioxidanten, bètablokkers, calciumkanaalblokkers, fosfodiësterase (PDE) 5-remmers en statines. Deze interventies hebben indirecte antioxidantische effecten en verbeteren de functie van het endotheel door hun ontstekingsremmende werking. Daarnaast is er toenemend bewijs dat microvasculaire disfunctie niet alleen een gevolg is van atherosclerose, maar ook een onafhankelijke risicofactor is voor vasculaire gebeurtenissen.

Hoewel bovenstaande behandelingen wijdverspreid beschikbaar zijn en hebben aangetoond dat ze cardiovasculaire risico's verminderen, is er behoefte aan evaluatie van het effect van deze en nieuwe farmacologische therapieën gericht op microvasculaire (endotheliale) disfunctie. Beoordeling van de microcirculatie is moeilijk vanwege het ontbreken van gestandaardiseerde technieken en daarom zijn er momenteel weinig interventies gericht op de microcirculatie. Vroege detectie en behandeling van endotheliale disfunctie kan echter een belangrijke rol spelen in het voorkomen van (onomkeerbare) aandoeningen. Verder onderzoek is nodig om de mechanismen te begrijpen en effectieve interventies te ontwikkelen om de microvasculaire disfunctie te behandelen en zo de cardiovasculaire gezondheid te verbeteren. Omdat er momenteel weinig behandelingsopties zijn specifiek gericht op microvasculaire afwijkingen, is er een grote behoefte aan verder onderzoek om effectieve interventies te ontwikkelen die gericht zijn op de microcirculatie, zoals geneesmiddelen die de NO-productie verhogen of de activiteit van ET-1 remmen..

Een belangrijk aspect van dit proefschrift is de evaluatie van gestandaardiseerde technieken voor het onderzoeken van de microcirculatie. Momenteel worden er verschillende technieken gebruikt om de microvasculatuur te beoordelen, waaronder flow-gemedieerde vasodilatatie (FMD), laser Doppler fluxmetrie en videomicroscopie. Er is echter geen consensus over welke techniek het meest geschikt is voor het evalueren van de microcirculatie.

Er zijn verschillende manieren om de microcirculatie te evalueren. Hoewel de invloed van het endotheel- variabel is in vasculaire bedden van verschillende organen, zijn de pathologische veranderingen in signaalroutes opmerkelijk vergelijkbaar. De huid is een uitstekende locatie om farmacologische effecten op de microcirculatie te onderzoeken, vanwege de gemakkelijke toegankelijkheid. Verscheidene simulatie modellen zijn ontwikkeld voor gezonde vrijwilligersstudies. Buiten de huid is het netvlies ook een locatie waar de microcirculatie gemakkelijk kan worden gevisualiseerd en gemonitord. Retinale microvasculaire afwijkingen zijn in verband gebracht met verschillende cerebrovasculaire, cardiovasculaire, renale en metabole ziekten.

Er zijn weinig overzichten gepubliceerd over de toepasbaarheid van microvasculaire metingen, en deze richtten zich vaak op een beperkt aantal beeldvormingstechnieken of op metingen in één orgaansysteem. Er zijn echter nieuwe ontwikkelingen geweest en er is behoefte aan een bijgewerkt overzicht. De meeste microcirculatiemetingen zijn indirect en geven beperkte informatie over de microvasculaire functie over het volledige scala. Daarom worden deze metingen meestal gecombineerd met interventies om het regelgevende systeem naar een extremere toestand te brengen. In de loop der jaren zijn verschillende interventies ontwikkeld die inzicht kunnen geven in verschillende aspecten van de microcirculatoire functie, hoewel de meeste zich richten op de endotheel- functie.

Samenvattend is de microcirculatie cruciaal voor de uitwisseling van voedingsstoffen en gassen, en vasculaire homeostase. Er zijn diverse methoden om microcirculatie te evalueren en ontwikkelingen in technologie hebben bijgedragen aan verbeterde beeldverwerking. Dit proefschrijft heeft tot doel de meest geschikte microvasculaire beeldvormingstechnieken voor klinische toepassing en onderzoek te identificeren, met nadruk op huid- en netvliesmicrocirculatiebeoordelingen. Bovendien worden in dit overzicht de meest gebruikte interventies besproken, die helpen bij het verkrijgen van meer inzicht in de microcirculatie.

In dit proefschrift onderzoeken we de mogelijkheden en onmogelijkheden van het meten van de microvasculatuur voor farmacodynamische uitkomstmaten van nieuwe interventies en geneesmiddelen. Dit werd gedaan in zeven hoofdstukken, waarbij verschillende invalshoeken werden gebruikt om de microvasculatuur te evalueren.

**Hoofdstuk twee** heeft een overzicht gegeven van microcirculatiemetingen in de huidige kliniek. De nadruk van dit overzicht lag op de klinische bruikbaarheid van microvasculaire beeldvormingstechnieken die momenteel commercieel beschikbaar zijn voor metingen va de huid- en retina. In dit overzicht werden de meest gebruikte cutane en retinale microvasculaire meetapparaten alsmede veelbelovende nieuwe technieken geevalueerd. Daarnaast werd een overzicht gegeven van minimaal-invasieve (biochemische) interventies die kunnen helpen bij het onderzoeken van de microcirculatie.

In **hoofdstuk drie** werd de microvasculaire functionaliteit onderzocht bij acht patiënten met sikkelcelziekte en gematchte gezonde vrijwilligers met twee nieuwe apparaten: de laser speckle contrast imager (LSCI) en de retinal function imager. Beide apparaten toonden een uitstekende herhaalbaarheid (CVC van respectievelijk 8,5% 9,5%, 7,6% en 7,7%) en tussen metingen op één dag (CVC van respectievelijk 7,0%, 7,7%, 7,6% en 4,7%) en waren in staat om een verschil in microvasculaire functionaliteit te meten tussen de patiënten en gezonde vrijwilligers. Dit maakt deze apparaten geschikt maakt voor verder gebruik in klinisch microvasculair onderzoek. Hoewel de retinale functie -imager veel potentieel liet zien, was het verkrijgen van goede kwaliteit beelden een uitdaging.

**Hoofdstuk vier**: De resultaten van de studie in hoofdstuk drie werden gebruikt om een grotere studie op te zetten waarin microvasculaire metingen werden vergeleken met cerebrale hemodynamica gemeten door de MRI. In totaal werden 17 patiënten met sikkelcelanemie en 6 gezonde vrijwilligers onderzocht. Er werd een verhoogde cerebrale- en huidbloedstroom gevonden bij patiënten met sikkelcelanemie in vergelijking met controles. Bovendien waren de huidmetingen (basale bloedstroom) sterk gecorreleerd [ASL vs. LSCI: r = 0,70; PC-MRI vs. LSCI: r = 0,75] met MRI-metingen. Dit suggereert dat cutane microvasculaire metingen een goedkope, niet-invasieve alternatieve methode zou kunnen zijn om details over de hemodynamische toestand van patiënten met sikkelcelanemie te verkrijgen.

**Hoofdstuk vijf**: Retinale microcirculatie en retinale oximetrie werden kwantitatief geanalyseerd met behulp van fractalanalyse bij 8 patiënten met sikkelcelanemie en evenveel gematchte gezonde vrijwilligers. Oximetrie-afbeeldingen en niet-invasieve capillaire perfusiemaps (nCPM) werden verkregen met behulp van de RFI. Er werd geen significant verschil waargenomen voor de fractalanalyse tussen de patiënten en gezonde controles. Bij de oximetrie metingen werden significant lagere geoxideerde Hb-niveaus werden gedetecteerd bij patiënten met met name in de temporale kwadranten. Dit suggereert dat functionele afwijkingen in oximetriemetingen bij patiënten met sikkelcelanemie kunnen worden waargenomen voordat structurele microvasculaire veranderingen optreden.

**Hoofdstuk zes** werd een nieuw meetapparaat: de miniaturized Dynamic Light Scattering (mDLS). geëvalueerd in verschillende patiënten populaties met vaatafwijkingen. Deze metingen werden vergeleken met LSCI-metingen en verschillende bloedmetingen. Er was een grote intra-subject-variabiliteit in de mDLS metingen en geen van de eindpunten kan onderscheid maken tussen patiënten groepen en gezonde vrijwilligers. LSCI- en laboratoriummetingen waren wel in staat om verschillen te meten. Deze resultaten suggereren dat het mDLS-apparaat (nog) niet geschikt is voor het meten van veranderingen in de microcirculatie.

**Hoofdstuk zeven**: In deze studie hebben we het effect geëvalueerd van recombinant humaan erytropoëtine (rHuEPO) op de cutane microvasculaire functie bij goed getrainde wielrenners met behulp van LSCI. Achtenveertig proefpersonen kregen gedurende 8 weken wekelijks een dosis rHuEPO of placebo (1:1 verhouding). LSCI metingen werden uitgevoerd op drie tijdstrippen:

1 Bij het begin van de studie;
2 Na een maximale inspanningstest in week 6;
3 Voor maximale inspanning in week 8.

Ondanks een toename van hematocrietwaarden in de rHuEPO-groep werd er geen statistisch significante verschil gevonden in de microvasculaire functie tussen de rHuEPO-groep en de placebogroep. De resultaten van deze studie suggereren dat de verhoogde hematocrietwaarden bij rHuEPO-behandelde goed getrainde wielrenners niet geassocieerd zijn met veranderingen in microvasculaire metingen met behulp van LSCI.

**Hoofdstuk acht**: In deze studie werd hyperspectrale beeldvorming geëvalueerd met behulp van een snapshot hyperspectrale camera die weefseloxygenatie non-invasief kan meten met relevante golflengtes in het VIS-NIR-gebied (450-950 nm) en de resultaten werden vergeleken met LSCI. Verschillende interventies werden onderzocht bij 16 gezonde vrijwilligers, waaronder occlusie-reperfusie van de brachiale slagader en metingen van lokale veranderingen in huidoxygenatie en bloedstroom na toediening van een lokale vasodilatator (capsaïcinecrème) en een lokale vasoconstrictor (brimonidinegel). Hyperspectrale metingen (cutane $StO_2$-niveaus) waren gecorreleerd aan de hemoglobinezuurstofsaturatie gemeten door een oximeter. Daarnaast werd een sterke correlatie (Pearson R2: 0,86) van de bloedstroom met $StO_2$-niveaus tijdens occlusie-reperfusiefases waargenomen. De resultaten van deze pilotstudie toonden aan dat de snapshot hyperspectrale camera verschillende niveaus van cutane $StO_2$ kon detecteren bij menselijke vrijwilligers.

## DISCUSSIE

Als gevolg van technologische vooruitgang in de afgelopen decennia zijn de mogelijkheden voor microvasculaire metingen sterk toegenomen. In dit proefschrift hebben we verschillende nieuwe apparaten onderzocht die al beschikbaar zijn of momenteel in ontwikkeling zijn, en we hebben de toepasbaarheid van verschillende nieuwe microcirculatie meetmethodes onderzocht voor hun nut in de kliniek of in een klinische onderzoek setting.

Zoals uiteengezet in hoofdstukken één en twee, moeten nieuwe apparaten worden gevalideerd voordat ze kunnen worden gebruikt in klinisch onderzoek. Dit validatieproces bestaat uit verschillende stappen die onderzoekers in staat stellen om te bepalen hoe nauwkeurig de metingen zijn, wat de variabiliteit van de eindpunten is en of het apparaat ziekten of farmacodynamische effecten van nieuwe interventies kan detecteren. In dit proefschrift hebben we verschillende apparaten geprobeerd te valideren, en hierover willen wij het volgende stellen.

Ten eerste moeten de metingen redelijk eenvoudig uit te voeren zijn en moet de afhankelijkheid van de diegene die de metingen uitvoert beperkt zijn. Dit is van toepassing op de LSCI, maar voor andere apparaten zoals de RFI of mDLS is er een steile leercurve en grote afhankelijkheid van de operateur van de apparaten

De fysiologie van de microvasculatuur en in het bijzonder de toegankelijkheid om het te meten maken het een potentieel waardevolle biomarker. Hoewel de meeste beeldvormingsapparaten een grote initiële investering vereisen (zie hoofdstuk 2), hebben de apparaten over het algemeen lage onderhouds- en operationele kosten.

De rol van microvasculaire disfunctie in de pathofysiologie van verschillende ziekten is bekend en is niet alleen beperkt tot vaatziekten, maar ook tot ischemische zenuwschade, nieraandoeningen en retinale disfunctie. Bovendien biedt recent onderzoek ons het inzicht dat microvasculaire veranderingen een vroege voorspeller kunnen zijn voor het ontstaan van bepaalde ziekten. Dit is goed bestudeerd in de oogheelkunde met betrekking tot beroerte , nierschade en hart- en vaatziekten. Een aanzienlijk deel van de hart- en vaatziekten niet verklaard door de traditionele risicofactoren voor hart- en vaatziekten zoals roken, hypertensie en obesitas. Daarom kan een uitgebreider onderzoek naar de mechanismen achter microvasculaire disfunctie nieuwe inzichten bieden in deze ziektebeelden en mogelijk worden ingezet als biomarkers voor vroege interventies.

### Toekomstige richtingen

Er zijn tal van nieuwe apparaten die claimen niet-invasieve metingen van de microcirculatie mogelijk te maken. Echter voor een succesvolle implementatie van microvasculaire metingen is het essentieel dat de implementatie van deze apparaten in klinische onderzoeken op een zodanige manier wordt gereguleerd dat de uitkomst van de metingen betrouwbaar is. De nieuwe EMA-richtlijnen voorzien in dit probleem.

We voorzien een bredere implementatie van microvasculaire metingen, niet alleen in de kliniek, maar ook in de thuissituatie. Bijvoorbeeld, PPG-metingen worden steeds vaker geïntegreerd in wearables. Aangezien de microcirculatie mogelijk een dominante rol speelt als voorspeller voor bepaalde ziekten, kan thuismonitoring met wearables vroege detectie van bijvoorbeeld een myocardinfarct mogelijk maken en cardiologen een tijdsvenster bieden om actie te ondernemen. Verder kunnen microvasculaire metingen vaker worden gebruikt als een methode om meer informatie te verkrijgen over de farmacodynamiek in (vroege fase) farmacologisch onderzoek, zeker gezien de sleutelrol van stikstofoxide in immuunactivatie en metabole ziekten. Momenteel worden microvasculaire metingen niet vaak toegepast in onderzoeken, maar vanwege de relatief lage kosten, lage belasting voor patiënten en nuttige inzichten kan dit een waardevolle aanvulling zijn in (farmacologisch) onderzoeken.

Hoewel er decennia zijn geweest met microvasculaire metingen, is het pas in de laatste twee decennia dat microvascular onderzoek een vlucht heeft genomen. Nieuwe beeldvormingstechnieken, geavanceerdere algoritmen voor analyse en betere computerprocessen hebben microvasculaire onderzoeksmethoden gevestigd. Voordat deze methoden echter op grote schaal geïmplementeerd worden, moeten ze worden getest op hun validiteit en integriteit. Microvasculair onderzoek heeft ons al interessante nieuwe inzichten gebracht in de pathofysiologie van ziekten en we staan pas aan het begin van een nieuw tijdperk van microvasculair onderzoek. In dit proefschrift hopen we met onze validatiestudies van nieuwe en bestaande microcirculatie meetinstrumenten bij te dragen aan een bredere implementatie van microcirculatie metingen in de huidige klinische en onderzoekspraktijk.

## LIST OF PUBLICATIONS


**Birkhoff, W.A.J.**, Jaac Heuberger, T.E. Post, P. Gal, F.E. Stuurman, J. Burggraaf, and A.F. Cohen. 2018. 'Recombinant human erythropoietin does not affect several microvascular parameters in well-trained cyclists', *Physiol Rep, 6: e13924.*

**Birkhoff, W.A.J.**, L. van Manen, J. Dijkstra, M.L. De Kam, J.C. van Meurs, and A.F. Cohen. 2020. 'Retinal oximetry and fractal analysis of capillary maps in sickle cell disease patients and matched healthy volunteers', *Graefes Arch Clin Exp Ophthalmol, 258: 9-15.*

**Birkhoff, W**., J. de Vries, G. Dent, A. Verma, J.L. Kerkhoffs, A.H.F. van Meurs, M. de Kam, M. Moerland, and J. Burggraaf. 2018. 'Retinal microcirculation imaging in sickle cell disease patients', *Microvasc Res, 116: 1-5.*

Dijkmans, A.C., E.B. Wilms, I.M. Kamerling, **W. Birkhoff**, N.V. Ortiz-Zacarías, C. van Nieuwkoop, H.A. Verbrugh, and D.J. Touw. 2015. 'Colistin: Revival of an Old Polymyxin Antibiotic', *Ther Drug Monit, 37: 419-27.*

Dijkmans, A.C., E.B. Wilms, I.M. Kamerling, **W. Birkhoff**, C. van Nieuwkoop, H.A. Verbrugh, and D.J. Touw. 2014. '[Practical guideline for the use of colistin]', *Ned Tijdschr Geneeskd, 158: A7445.*

Grievink, H.W., Jaac Heuberger, F. Huang, R. Chaudhary, **W.A.J. Birkhoff**, G.R. Tonn, S. Mosesova, R. Erickson, M. Moerland, P.C.G. Haddick, K. Scearce-Levie, C. Ho, and G.J. Groeneveld. 2020. 'DNL104, a Centrally Penetrant RIPK1 Inhibitor, Inhibits RIP1 Kinase Phosphorylation in a Randomized Phase I Ascending Dose Study in Healthy Volunteers', *Clin Pharmacol Ther, 107: 406-14.*

Kervezee, L., V. Gotta, J. Stevens, **W. Birkhoff**, I. Kamerling, M. Danhof, J.H. Meijer, and J. Burggraaf. 2016. 'Levofloxacin-Induced QTc Prolongation Depends on the Time of Drug Administration', *CPT Pharmacometrics Syst Pharmacol, 5: 466-74.*

Kervezee, Laura, Jasper Stevens, **Willem Birkhoff**, Ingrid MC Kamerling, Theo de Boer, Melloney Dröge, Johanna H Meijer, and Jacobus Burggraaf. 2016. 'Identifying 24 h variation in the pharmacokinetics of levofloxacin: a population pharmacokinetic approach', *British Journal of Clinical Pharmacology, 81: 256-68.*

Kletzl, H., A. Marquet, A. Günther, W. Tang, J. Heuberger, G.J. Groeneveld, **W. Birkhoff**, E. Mercuri, H. Lochmüller, C. Wood, D. Fischer, I. Gerlach, K. Heinig, T. Bugawan, S. Dziadek, R. Kinch, C. Czech, and O. Khwaja. 2019. 'The oral splicing modifier RG7800 increases full length survival of motor neuron 2 mRNA and survival of motor neuron protein: Results from trials in healthy adults and patients with spinal muscular atrophy', *Neuromuscul Disord, 29: 21-29.*

Kruizinga, M.D., **W.A.J. Birkhoff**, M.J. van Esdonk, N.B. Klarenbeek, T. Cholewinski, T. Nelemans, M.J. Dröge, A.F. Cohen, and R.G.J.A. Zuiker. 2020. 'Pharmacokinetics of intravenous and inhaled salbutamol and tobramycin: An exploratory study to investigate the potential of exhaled breath condensate as a matrix for pharmacokinetic analysis', *Br J Clin Pharmacol, 86: 175-81.*

Street, Jonathan M, **Willem Birkhoff**, Robert I Menzies, David J Webb, Matthew A Bailey, and James W Dear. 2011. 'Exosomal transmission of functional aquaporin 2 in kidney cortical collecting duct cells', *The Journal of physiology, 589: 6119-27.*

van Manen, L., **W.A.J. Birkhoff**, J. Eggermont, R.J.M. Hoveling, P. Nicklin, J. Burggraaf, R. Wilson, J.S.D. Mieog, D.J. Robinson, A.L. Vahrmeijer, M.S. Bradbury, and J. Dijkstra. 2021. 'Detection of cutaneous oxygen saturation using a novel snapshot hyperspectral camera: a feasibility study', *Quant Imaging Med Surg, 11: 3966-77.*

## CURRICULUM VITAE

Willem A.J. Birkhoff was born in the eldest city of the county of Holland (Dordrecht) on the 9th of november 1985. After completing secondary school at the Johan van Oldebarnevelt Gymnasium in Amersfoort, he studied medicine at Leiden university from 2005 to 2013. Thereafter he worked at Centre for Human Drug Research in Leiden, where all the research described in this thesis was performed under the supervision of prof. dr. A.F. Cohen. In 2019 he started in the clinic in the st Elisabeth hospital in Curacao as a non training resident neurology for a year after which he started his current training as an ophthalmologist in het Oogziekenhuis Rotterdam. Willem lives together with his spouse Jacolien.